The role of CD38 expression on NAD levels and cell physiology in a leukaemia model

by

Zainab Nejim Al-Abady

A thesis submitted to Plymouth University in partial fulfilment for the degree of

DOCTOR OF PHILOSOPHY

School of Biomedical and Biological Sciences

Faculty of Science and Technology

2013

Copyright Statement

Dedication

I dedicate this thesis to my beloved mother and to my beloved family:

My husband, Abbas Al-Shabany

My lovely daughter, Ayiat

My sons, Haider and Abdu-Allah

The role of CD38 expression on NAD levels and cell physiology in a leukaemia model

Zainab Nejim Al-Abady

Abstract

CD38 is a transmembrane glycoprotein with both ADP-ribosyl cyclase/cyclic ADP-ribose hydrolase activities; it is also known as a cell surface receptor. CD38 utilizes NAD(P) as a substrate to produce the second messengers, Nicotinic acid adenine dinucleotide phosphate (NAADP) and Cyclic adenosine diphosphate ribose (cADPR). CD38 has been implicated in several diseases. For instance, in chronic lymphocytic leukemia (CLL), it is known as a poor prognostic marker and as a disease modifier. Also, abundant data are available on the receptor functions of CD38 in CLL. However, the aim of the work described in this thesis was to investigate the enzymatic functions of CD38 in leukemia. The work also addresses the question of why $CD38^+$ subset leukemia patients are characterised by poor outcome.

It has been postulated that CD38 is the major NADase in cells, and that knocking it down increases NAD levels significantly. Thus, it was hypothesized that NAD levels might be depleted and result in detrimental consequences on cell physiology when CD38 is significantly expressed. Also, it was suggested that a similar linkage might be also present in leukemia, contributing to poor outcome. To test this hypothesis, a human leukaemia cell line (HL60) was used as a convenient model that differentiates into $CD38^+$ cells when stimulated using all-*trans* retinoic acid (ATRA). It is shown that CD38 is expressed extracellularly and intracellularly in the differentiated cells, as evaluated by qPCR, FACS, Western blotting and the NGD cyclization assay. However, one of the major consequences of the early expression of CD38 (at 3 h) was a substantial depletion of intracellular NAD^+ levels that was apparent by 4 h after treatment with ATRA. These novel data suggest a major role for CD38 as a main regulator of

NAD during the differentiation. The main role of CD38 in degradation of NAD was confirmed by using a CD38 inhibitor (kuromanin). Interestingly, the drop in NAD^+ levels during the differentiation was reversed after treatment with kuromanin. Furthermore, the CD38 homologue, CD157, and other NAD-consuming enzymes (PARP and SIRT) were all investigated, and it was found that there are no substantial roles of all these enzymes on the NAD^+ degradation during the differentiation. In contrast, qPCR results for NAD-biosynthesis enzymes during the differentiation process showed a significant rise in indolamine 2,3-dioxygenase (IDO) mRNA expression, with lesser increases in nicotinamide nucleotide adenyltransferase (NMNAT) and nicotinamide phosphoribosyl transferase (NAMPT) mRNA levels.

The consequences of low NAD levels on cell metabolism were also assessed; the results show a reduction in lactate production and glutathione levels with an elevation of TBARS levels. However, the NAD^+:NADH ratio remained relatively constant. Moreover, the effects of low NAD levels on DNA repair and cell death were also investigated in response to DNA damage caused by UVB. Preliminary findings show that, in $CD38^+$ cells, there is a resistance to apoptotic cell death. Additionally, CD38 expression was also investigated in leukaemia cells, and was found to be regulated in response to hypoxic environment, or the change in NAD^+ levels following FK866, kuromanin and NAD^+ application. Altogether, these studies raise the possibility that the impact of CD38 enzymatic function on NAD levels and the negative consequences on NAD(P)-dependent processes might play an important role in the poor prognosis in $CD38^+$ leukemia patients.

Table of Contents

List of Figures

Chapter 1

Chapter 3

Chapter 4

Chapter 5

Chapter 6

Chapter 7

List of Tables

Abbreviations

Abbreviation	*Glossary*
9-cis RA	9-cis retinoic acid
ADH	Alcohol Dehydrogenase
ADPR	Adenosine diphosphate ribose
ADPRP	ADP-ribose 2'- phosphate
ALDH	Aldehyde dehydrogenase
AML	Acute myeloblastic leukaemia
ANOVA	Analysis of variance
APL	Acute promyelocytic leukaemia
ARTs	ADP-ribose transferases
ATL	Adult T-cell leukemia-lymphoma
ATO	Arsenic trioxide
ATP	Adenosine triphosphate
ATRA	All *trans* retinoic acid
BCR	B-cell–receptor
BER	Base excision repair
BM	Bone marrow

BSA	Bovine serum albumin
BST-1	Bone marrow stromal cell antigen 1
cADPR	Cyclic adenosine diphosphate ribose
CAMs	Coronary arterial myocytes
CCD	Charge-coupled device
CCL19	CC ligand 19
cGDPR	Cyclic guanosine diphosphate ribose
CICR	Ca^{2+}-induced Ca^{2+} release
cIDPR	Cyclic inosine diphosphate ribose
CLL	Chronic lymphocyte leukaemia
CNT	Concentrative nucleoside transporters
CPD	Cyclobutane pyrimidine dimer
CtBP	C-terminal binding protein
CX43	Connexin-43
CXCL12	CXC ligand 12
CXCR4	CXC receptor 4
DC	Dendritic cells
DMSO	Dimethylsulfoxide

ECL	Electro generated chemiluminescence
ECCAC	European collection of cell culture
eNAMPT	Extracellular NAMPT
ENT	Equilibrative nucleoside transporters
ER	Endoplasmic reticulum
ETC	Electron transport chain
FACS	Fluorescence-activated cell sorter
FCS	Fetal Calf Serum
FDC	Follicular dendritic cells
FKBP	FK506-binding protein
FSC	Forward scatter
G6P-DH	Glucose 6-phosphate dehydrogenase
GM-CSF	Granulocyte-macrophage colony-stimulating factor
GSH	Reduced glutathione
HAE	4-hydroxyalkenals
HASM	Human airway smooth muscle
HEB	Hypertonic extraction buffer
HIF	Hypoxia inducible factors

HL60	Human leukaemia cells
HLA	Human leukocyte antigen
HLB	Hypotonic lysis buffer
HMW	High molecular weight
HPV	Hypoxic pulmonary vasoconstriction
HRP	Horseradish Peroxidase
IDO	Indoleamine 2, 3-dioxygenase
IDP	Isocitrate dehydrogenase
IFN	Interferons
IgV	Immunoglobulin variable
IL	Interleukin
IP3	Inositol trisphosphate
KO	Knock out
LDH	Lactate dehydrogenase
LN	Lymphoid nodes
LPS	Lipopolysaccharide
mAbs	Monoclonal antibodies
MAPK	Mitogen-activated protein kinase

MDA	Malondialdehyde
ME	Malic enzyme
MFI	Mean fluorescence index
MMPs	Matrix metalloproteinases
MPT	Mitochondrial permeability transition
MTT	3-(4, 5-dimethylthiazole-2-yl)-2, 5-diphenyl tetrazolium bromide
NA	Nicotinic acid
NAADP	Nicotinic acid adenine dinucleotide phosphate
NAD	Nicotinamide adeninedinucleotide
NADase	NAD glycohydrolase
NADK	NAD kinase
NADP	Nicotinamide adeninedinucleotide phosphate
NADs	NAD synthetase
Nam	Nicotinamide
NaMN	Nicotinic acid mononucleotide
NAMPT	Nicotinamide phosphoribosyltransferase
NAPRT	Nicotinic acid phosphoribosyl transferase
NBT	Nitroblue tetrazolium

NER	Nucleotide excision repair
NGD	Nicotinamide guanine dinucleotide
NHD	Nicotinamide hypoxanthine dinucleotide
NIDDM	Non-insulin dependent diabetes
NK	Natural killer cells
NLC	Nurse-like cells
NMNAT	Nicotinamide mononucleotide adenylyltransferase
NOD	Non-obese diabetic
NOX4	NAD(P)H oxidase
NRK	Nicotinamide riboside kinase
NuT	Nucleoside transporter
PAGE	Polyacrylamide gel electrophoresis
PAR	Poly ADP-ribose
PARPs	Poly-ADP-ribose-polymerases
PBS	Phosphate buffered saline
PCs	Proliferation centre
PE	Phycoerythrin
PECAM-1	Platelet endothelial cell adhesion molecule-1

PES	Phenazine ethosulfate
PGC-1α	Peroxisome proliferator-activated receptor δ co-activator-1α
PI3-K	Phosphoinositide 3-kinase
PMA	Phorbol 12-myristate 13-acetate
PML	Promyelocytic leukemia
PVDF	Polyvinylidine difluoride
QPCR	Quantitative polymerase chain reaction
RAR	Retinoic acid receptor
RARE	Retinoic acid response element
RAS	Retinoic acid syndrome
ROS	Reactive oxygen species
RPMI	Roswell Park Memorial Institute
RXR	Retinoid x receptor
RyR	Ryanodine receptor
SAP	Saponin and PBS
SDS	Sodium dodecyl sulphate
SSBR	Single strand break repair
SSC	Side scatter

TBA	Thiobarbituric acid
TBARS	Thiobarbituric acid reactive substances
TBS	Tris-buffered saline
TCA	Tricarboxylic acid cycle
TCR	T-cell receptor
TGase	Transglutaminase
TLR	Toll-like receptors
TNB	5-thio-2-nitrobenzoate
TNF-α	Tumor necrosis factor-α
TPCs	Two-pore channels
TRPM2	Transient receptor potential cation channel member 2
TTBS	TBS-Tween
ZAP-70	Zeta1-associated protein of 70 kDa

Author's Declaration

At no time during the registration for the degree of Doctor of Philosophy has the author been registered for any other University award without prior agreement of the Graduate Committee. This study was financed with the aid of Ministry of the Higher Education and Scientific Research/Iraq. Relevant scientific seminars and conferences were attended at which work was presented and papers have been prepared for publication:

Publications

Z.N. Al-Abady *et al.,* Large changes in NAD levels associated with CD38 expression during HL-60 cell differentiation, Biochem. Biophys. Res. Commun. (2013), http://dx.doi.org/10.1016/j.bbrc.2013.10.170 (published)

Platform presentations

Role of CD38 in disease. University of Plymouth, Plymouth, UK, March 2010

CD38 in human leukaemia cells. University of Plymouth, Plymouth, UK, March 2012

Poster presentations

Enzymatic activity of CD38 comparative to NAD levels in leukemia cells. Centre for Research in Translational Biomedicine, research day. University of Plymouth, Plymouth, UK, Aprill, 2011

CD38 expression regulates NAD(H) levels during HL-60 differentiation. The Postgraduate Society Annual Conference, University of Plymouth, Plymouth, UK, June, 2012. Also were presented by colleagues at FASEB Summer Research Conference, Lucca, Italy, September, 2011.

The forgotten role of CD38: is enzymatic activity important in CLL pathophysiology. Centre for Research in Translational Biomedicine, research day. University of Plymouth, Plymouth, UK, July, 2012.

CD38 Expression Regulates NAD(H) Levels in Human Leukemia Cells. International conference, 16th BIENNIAL meeting. London, UK, September 2012.

Workshop

Practical Techniques in molecular biology workshop, 16-19 July, 2012, Plymouth University.

Word count of main body of thesis: (42,266 words)

Signed ----------

Date ----------

Acknowledgements

The work presented here would not have been possible were it not for the support of a number of people. Firstly, I would like to express my sincere gratitude to my supervisors, Dr. Richard Billington for his kind support and advice throughout the duration of this research even in his very busy time and Dr. John Moody; for his contributions of time, ideas, and support during these studies.

Besides my supervisors, I would also like to extend my thanks to all my colleagues in the School of Biomedical and Biological Sciences, who answered my request for help especially Dr. Wondwossen Abate. Appreciation also goes out to technical colleagues, especially William Vevers and Michele Kierman. Further, I am grateful to the Ministry of the Higher Education and Scientific Research, Republic of Iraq for giving me this opportunity for graduate studies and for their financial support.

Above all, I must acknowledge my husband Abass Al-Shabany without his love, encouragement and editing assistance, I would not have finished this thesis. I cannot forget also to express my loving thanks to my daughter Ayiat and my sons; Haider and Abdu-Allah; they have missed and lost a lot due to my research. My Mum, Dad, Sisters and Brothers were all behind me throughout this journey. Their prayers and emotional support were with me especially during the difficult times.

CHAPTER 1

GENERAL INTRODUCTION

1. GENERAL INTRODUCTION

1.1 Nicotinamide adenine dinucleotide (NAD)

Nicotinamide adenine dinucleotide (NAD) and its phosphorylated form, NADP (Fig 1.1) were first discovered by Harden and Young (1906); NAD and NADP have long been known to be essential co-enzymes in some of the most fundamental redox reactions of basic metabolism, such as glycolysis, the tricarboxylic acid (TCA/Krebs') cycle and the pentose phosphate pathway (Mathew *et al*., 2000; Ziegler, 2000). The oxidized and reduced forms of NAD (NAD^+ and NADH, respectively) regulate glycolysis by acting as cofactors for the glycolytic enzyme glyceraldehyde-3-phosphate dehydrogenase. NAD(H) also mediates important energy metabolism-related reactions, such as the lactate dehydrogenase-catalyzed lactate-pyruvate conversion in the cytosol (Stryer, 1995; Berger *et al.*, 2004). Generally, NADH is the substrate of over 300 cellular dehydrogenases, including those located in the inner mitochondrial membrane that catalyzes the transfer of electrons from NADH to coenzyme Q during oxidative phosphorylation (Li and Chen, 2002). Hence NAD(H) is essential for the synthesis of ATP (Stryer, 1995; Berger *et al.*, 2004). Moreover, beyond the function of NAD in energy metabolism, its phosphorylated form ($NADP^+$) has important functions in the cellular antioxidant capacity through its role as a precursor for synthesizing the major reducing molecule NADPH; the latter provides several cell protective functions (Stryer, 1995; Pollak *et al.*, 2007).

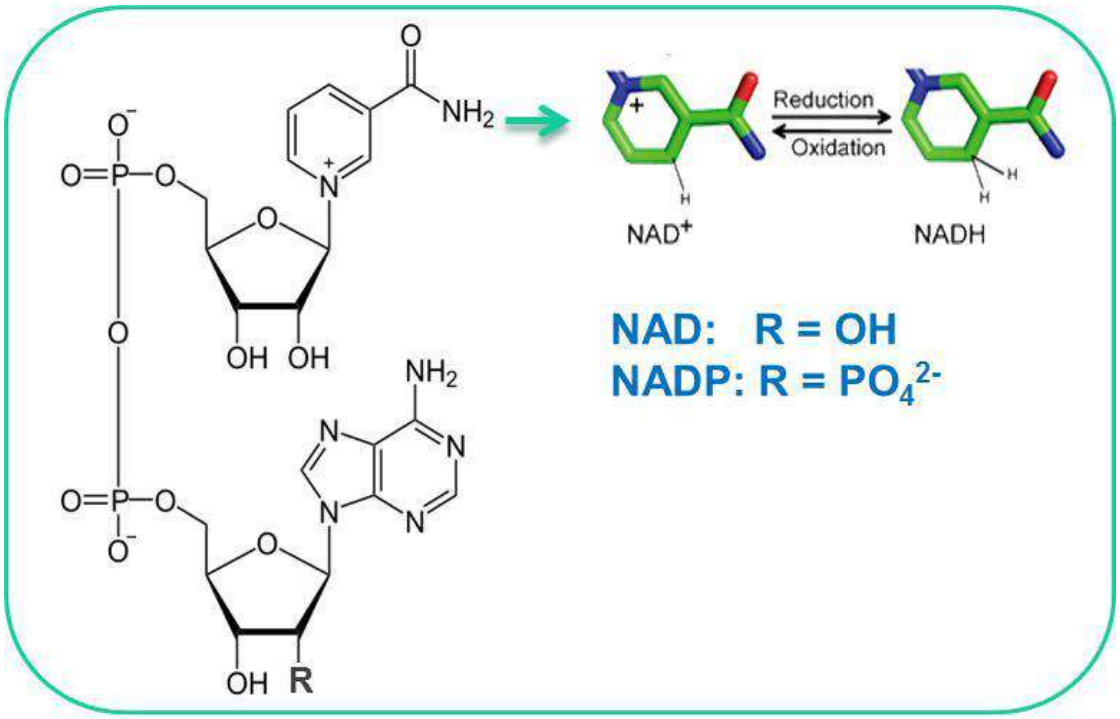

Figure 1.1 The structures of the nicotinamide nucleotides, NAD, NADP and NADH.

Interestingly, NAD has other important functions, as a signalling molecule, via acting as substrate for several NAD-consuming enzymes. These enzymes are represented by the CD38/CD157 system, poly-ADP-ribose-polymerases (PARPs), mono-ADP-ribose transferases (ARTs) and sirtuins (NAD-dependent protein deacetylases) in cells. NAD mediates post-translational protein modification by serving as substrate for the ADP-ribosylation reaction (via ARTs; Koch-Nolte *et al.*, 2008). It also controls DNA repair (via PARP; Kim *et al.*, 2005). This group of enzymes uses NAD as a substrate to catalyze the addition of a polymer of ADP-ribose to the protein. Further, NAD mediates gene silencing and longevity (via sirtuins; Michan and Sinclair, 2007). These enzymes catalyse the deacylation of proteins, in which the acetyl group is transferred from the protein to the ADP-ribose portion of NAD, releasing the nicotinamide group from NAD in the process. Additionally, in the late 1980s, NAD(P) was discovered to be a key substrate in producing two novel Ca^{2+} messengers; cADPR and NAADP (Lee *et al.*, 1989; Lee

and Aarhus, 1995). These messengers are involved in a wide range of biological functions. Thus, NAD mediates Ca^{2+}-signalling (via CD38/CD157; Malavasi *et al.,* 2008). In fact, extracellular and intracellular NAD levels may be regulated by CD38; EC 3.2.2.6 (Adebanjo *et al.,* 1999), which has been defined both as an ectoenzyme and as a receptor molecule (Howard *et al.,* 1993; Malavasi *et al.,* 1994).

Extracellular NAD^+ as a signalling molecule for CD38 and ARTs has additional functions. It may work like a cytokine, deriving rapid and functional responses through binding to specific purinergic type 2 receptors. It may also induce cell proliferation, migration, chemotaxis and apoptosis. For example, NAD^+ activates the purinergic receptor P2Y11, which results in cell activation in human granulocytes (Moreschi *et al.,* 2006). In human monocytes, NAD^+ binds different receptors such as P2X1, P2X4, and P2X7, which trigger Ca^{2+} influx (Klein *et al.,* 2009). Furthermore, NAD^+ induces cell proliferation, migration and release of prostaglandin E2 and cytokines in mesenchymal stem cells (Fruscione *et al.,* 2011). NAD^+ is involved in immunoregulation through the extracellular enzymatic network that control NAD^+ levels, which may be responsible for providing an essential second signal for chemotaxis through the two intracellular Ca^{2+} mobilizers, cADPR and ADPR (Berridge, 1993; Meszaros *et al.,* 1993; Perraud *et al.,* 2001). Furthermore, the mechanism to control regulator T lymphocytes cells is mediated through the immunomodulatory functions of NAD^+ that are mainly linked to the activation of ART enzymes. This can be done by transferring the ADP moiety of NAD^+ to specific amino acids in target proteins; P2X7 receptor (Koch-Nolte *et al.,* 2008), which causes activation signalling, leading to apoptotic cell death (Adriouch *et al.,* 2001; Seman *et al.,* 2003).

In contrast, while several NAD-dependent enzymes catalyse consumption of NAD in cells, resynthesis of NAD is necessary to maintain the functions of a wide variety of these enzymes. Thus, cellular NAD is synthesized either via a *de novo* pathway from tryptophan or via one of two possible recycling pathways: from nicotinic acid (NAc) or nicotinamide (NAM); vitamin PP, or niacin (Fig. 1.2; Magni *et al.,* 2004), and from nicotinamide riboside (NR; Bieganowski and Brenner, 2004).

There are two important enzymes, nicotinamide phosphoribosyltransferase (NAMPT) and nicotinamide mononucleotide adenylyltransferase (NMNAT), that constitute an NAD salvage recycling pathway in mammalian cells (Rongvaux *et al.,* 2003). Specifically, NAMPT catalyzes the conversion of NAM to nicotinamide mononucleotide (NMN), and localizes to both the cytosol and nucleus (Rongvaux *et al.,* 2002). NMN produced from NAM (via NAMPT) or from NR (via nicotinamide riboside kinase (NRK)) is further converted into NAD by NMNAT. NAD can be also synthesized from NAc, by nicotinic acid phosphoribosyl transferase (NAPRT), in addition to other enzymes such as NAD synthetase (NADs) via the intermediate nicotinic acid mononucleotide (NaMN; Wilhelm and Hirrlinger, 2012). In the nucleus, NAMPT and NMNAT have been observed to produce NAD as a substrate for NAD-dependent enzymes, including SIRT1 and PARP1 (Zhang *et al.,* 2009a). On the other hand there are three different enzymes that catabolise tryptophan in the endogenous *de novo* pathway, including tryptophan dioxygenase (TDO), indoleamine 2,3-dioxygenase (IDO) and indoleamine 2,3-dioxygenase-2; IDO2 (Ball *et al.,* 2009). Specifically, IDO activity is inducible in multiple cell types (Mellor and Munn, 2004), and it is chronically activated in many cancer patients (Schroecksnadel *et al.,* 2007).

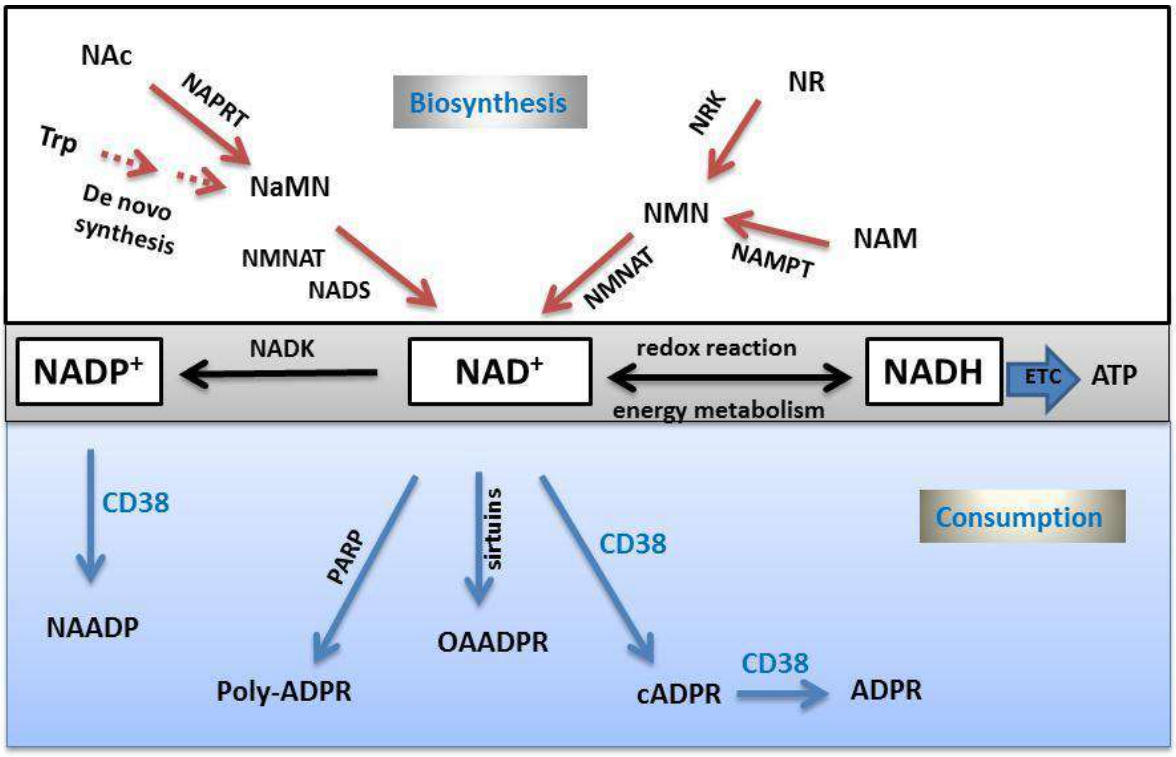

Figure 1.2 NAD metabolism represented by the biosynthesis pathways (the de novo pathway and salvage pathway), in addition to a network of NAD-consuming enzymes included (CD38, PARP, and sirtuins). NAD is shuttling between its oxidized form NAD^+ and the reduced form NADH. The electrons bound by NADH can be transferred to the electron transport chain (ETC) of mitochondria. The reaction catalyzed by NAD kinase (NADK) links NAD to the redox pair of $NADP^+$ and NADPH (adapted from Wilhelm and Hirrlinger, 2012).

In humans, the distribution of NAD^+ levels in plasma and tissue is different; the concentration of NAD^+ in human plasma ranges between 10 and 50 nM (De Flora *et al.*, 2004). NAD^+ levels may depend on the balance between the opposing processes of dinucleotide release from cells and its enzymatic degradation (De Flora *et al.*, 2004). However, NAD^+ levels in specific tissue regions may be significantly higher than those in plasma, such as during inflammation (Scheuplein *et al.*, 2009). Investigation of cellular NAD^+ and NADH levels in response to different environmental stimuli has been an important subject of several studies. For instance, the intracellular NAD^+/NADH ratio reflects the cellular metabolic status and redox state. It has been reported that under oxidative stress some cell types (for example, erythrocytes) increase their intracellular

NADH/NAD^+ ratio or the NADH level, in order to resist possible oxidative damage (Liang *et al.*, 2007; Ying, 2007). However, the change in nucleotide (NAD(H)) levels has also been linked to several diseases, such as sickle cell disease (Zerez *et al.,* 1990), neoplasia and ischaemia (Lohmann *et al.,* 1989), several age-associated diseases such as diabetes, cancers and neurodegenerative diseases; Parkinson's disease (Soriano *et al.,* 2001; Greenamyre *et al.,* 2001; Zhang *et al.,* 2002; Lin and Guarente 2003). Notably, several studies suggest that the change in NAD levels might modulate protein activities, and have an effect on cell functions (Ying, 2006; 2008). For instance, an augmentation of intracellular NAD^+ levels following CD38 knock out leads to SIRT activation with positive consequences on cell physiology (Barbosa *et al.,* 2007). One possible explanation is that CD38, as a member of the cyclase family, appears to be a major NAD consuming enzyme in cells. Thus, CD38 limits the availability of NAD to all other consumers.

1.2 Members of the ADP-ribosyl cyclase family

As mentioned above, NAD^+ is a substrate in the production of a novel Ca^{2+} messenger, cyclic ADP-ribose (cADPR; Lee *et al.,* 1989). Generally, cADPR is produced from NAD^+ by ADP-ribosyl cyclase activity, and there are three main members of the ADP-ribosyl cyclase family. The first ADP-ribosyl cyclase was described in the ovotestis of a marine invertebrate, the sea slug (*Aplysia californa*). The ADP-ribosyl cyclase from *Aplysia* is a soluble protein with a molecular weight of ~30 kDa. It generates cADPR as the predominant product of its enzymatic activity (Clapper *et al.,* 1987; Lee *et al.,* 1989). The second member of the ADP-riboysl cyclase family is CD38, which is the mammalian homologue of the *Aplysia* cyclase, with a single chain of 45 kDa (Mehta *et al.,* 1996; Ortolan *et al.,* 2002). CD38 was discovered by Reinherz *et al.*

(1980), while working on T lymphocytes by using the monoclonal antibody OKT10, and it was known then as a surface antigen (T10; Katz *et al.*, 1983). Several years later, T10 came to be known as 'cluster of differentiation 38' (CD38; Pallesen and Plesner, 1987). The third member of the cyclase family is CD157, a mammalian homologue of CD38, with a crystal structure that shows a high degree of structural homology with CD38 and the *Aplysia* cyclase as well (Yamamoto-Katayama *et al.*, 2002). CD157 is a 42-45 kDa surface molecule, identified as a bone marrow stromal cell antigen-1 (BST-1), also known as Mo-5 (Kaisho *et al.*, 1994). Each of the CD38 and CD157 glycoproteins has a polypeptide core of 280-300 amino acids (Liu *et al.*, 2005).

In addition to the well-known members of the ADP-ribosyl cyclase family, recent reports indicate the presence of CD38- and CD157-independent ADP-ribosyl cyclases. The next addition to the ADP-ribosyl cyclase family is an NAD(P)-catabolising enzyme from *Schistosoma mansoni* (*Sm*NACE; Kuhn *et al*., 2006).

1.3 Distribution of CD38

CD38 is distributed in a number of human and non-human tissues. It has been detected on the sarcolemma in skeletal and heart muscle, in addition to CD38 localization in the human brain (Mizuguchi *et al*., 1995; Fernandez *et al*., 1998). The CD38 molecule has been also found at various locations, including the normal prostatic epithelial cells (Kramer *et al*., 1995); pancreatic islet cells (Koguma *et al*., 1994; Mallone *et al*., 2002); cornea (Sizzano *et al*., 2007); the kidney; and intra-parenchymatous fibrous septa in the thyroid (Fernandez *et al*., 1998). Moreover, CD38's presence has been also documented in the inner nuclear envelope, for instance, in the rat hepatocytes, in addition to its localization in the plasma membrane (Khoo and Chang, 2000).

CD38 as a cell surface receptor is expressed in cells of hematopoietic origin (Terhorst *et al*., 1981). However, its expression has been most appropriately termed 'discontinuous' (Jackson and Bell, 1990) since CD38 expression is repeatedly changeable as bone marrow precursors develop into mature elements of the various lineages. For instance, in B cells, CD38 expression is tightly regulated during B cell ontogenesis and is highly present in bone marrow (BM) precursors. However, it is down-regulated in resting normal B cells and then is expressed in terminally differentiated plasma cells (Malavasi *et al*., 1994). CD38 expression is also changeable in T cells (Deaglio *et al*., 2001). Furthermore, studies suggest that CD38 is down-modulated during differentiation into immature human monocyte-derived dendritic cells and expressed again upon maturation induced by Lipopolysaccharide (LPS; Fedele *et al*., 2004). CD38 is also expressed by cells of the innate immune system, including circulating and residential natural killer (NK) cells (Mallone *et al*., 2001). Collectively, in the immune system, CD38 is expressed by immature hematopoietic cells, down-regulated by mature cells and re-expressed at high levels by activated lymphocytes; T cells, B cells, dendritic cells and NK cells (Funaro *et al*. 1990). CD38 is also expressed in the BM (Byk *et al*., 2005), granulocytes (Fujita *et al*., 2005), circulating monocytes (Zilber *et al*., 2000), on the surface membrane of erythrocytes and platelets (Zocchi *et al*., 1993; Ramaschi *et al*., 1996) and circulating osteoclast precursors (Shalhoub *et al*., 2000). CD38 has been also detected in lamina propria cells in the gut (Fernandez *et al*., 1998). Finally, it is worth mentioning that CD157 expression is also involved in most tissues, including the hematopoietic system, like CD38 expression, but the tissue distribution of CD157 is limited compared to CD38 (Ortolan *et al*., 2002).

1.4 CD38 (the type-II & -III glycoprotein) and cyclase crystal structures

The cyclase crystal structure reveals a homo-dimer; the enzyme is a bean-shaped molecule with most of the β sheets in the carboxyl domain, while the helixes are in the amino domain (Fig. 1.3 A; Prasad *et al*., 1996). The two domains are separated by a central cleft, with the active site located in a pocket near the cleft, as shown by crystallography and site-directed mutagenesis (Munshi *et al*., 1999), with a catalytic residue identified as Glu179. It is interesting to note that for the ADP-ribosyl cyclase, 86 of its 256 amino acid are identical to those in CD38, and an additional 110 amino acids are conservative substitutions (States *et al*., 1992). However, the structure of human CD38 is more complicated than the cyclase structure (Jackson and Bell, 1990). The structure of CD38 consists of an amino tail of 21 residues, a transmembrane segment of 23 residues and a large carboxyl domain of 256 residues that contains four glycosylation sites (Fig. 1.3 B; Jackson and Bell, 1990). The equivalent residue of Glu179 in CD38 is Glu226, which represents the catalytic residue of CD38 (Munshi *et al*., 2000).

The crystal structure of CD38 has revealed a molecule with a high degree of structural conservation with the cyclase. Thus, it was suggested that the overall homology between the two proteins is 69% (States *et al.,* 1992). However, Liu and others (2005) reported that these proteins have about 34% protein sequence identity. CD38 has a single binding pocket for multiple enzymatic activities, and it was observed that CD38's critical residues are localized in the carboxyl terminal and spread out in the last 100 amino acid residues of the protein (Munshi *et al.,* 2000). Other studies have shown that the CD38 active site is constructed by helices α5 and α6 from the N-terminal domain and helix α7 and strand β5 from the C-terminal domain (Fig. 1.3

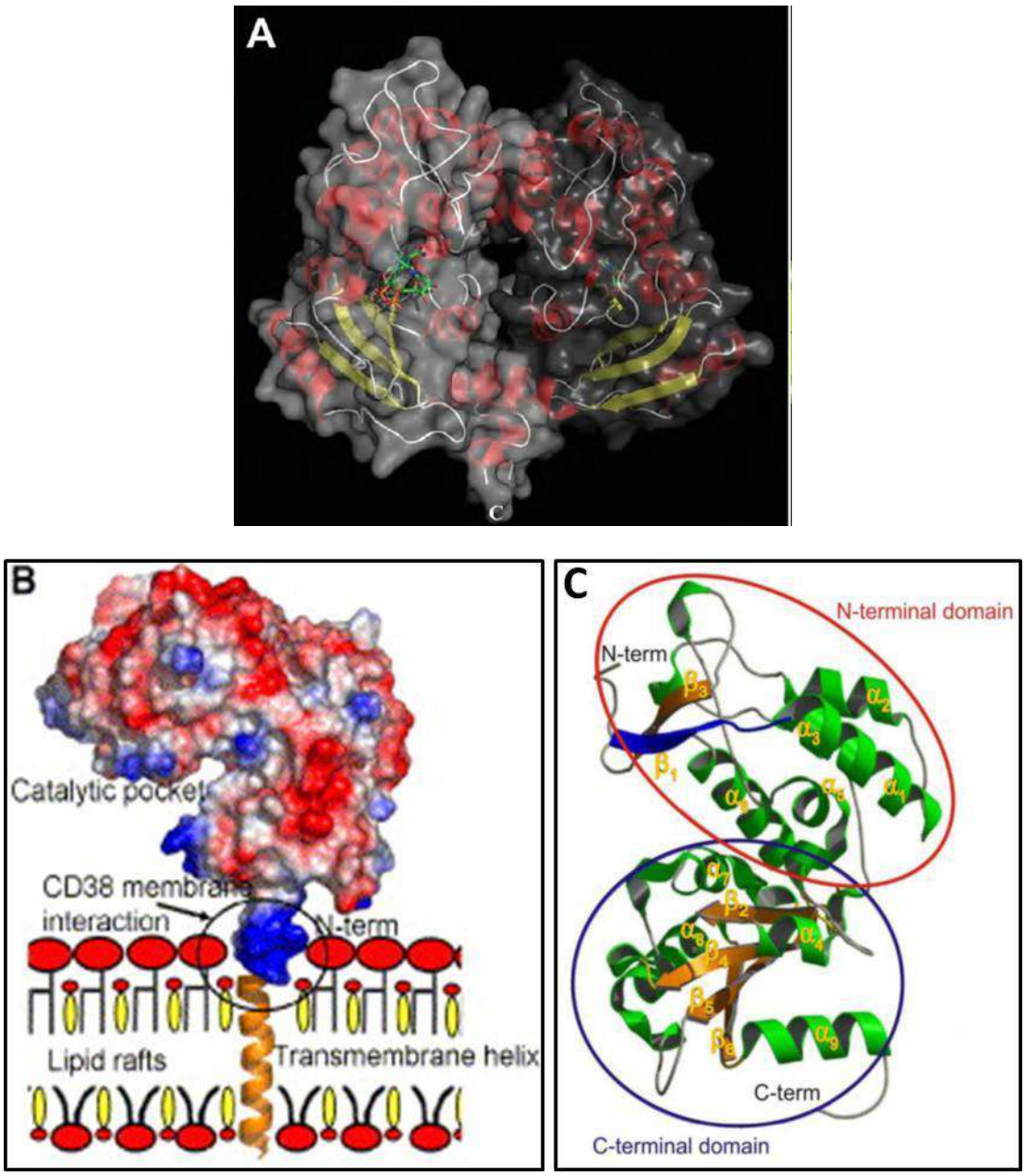

Figure 1.3 Structures of ADP-ribosyl cyclase and CD38. (A) The Aplysia ADP-ribosyl cyclase is a homo-dimer and the surfaces of the two monomers are coloured differently. Transparent grey revealing the secondary structures underneath. The colour code is: helix-red, β-sheet-yellow, coil-grey. The NAD molecules bound at the active sites are rendered using sticks. Colour code is: nitrogen-blue, oxygen-red, phosphorus-yellow, carbon-green. The letter C indicates the carboxyl end (adapted from Lee, 2012). (B) CD38 structure shows its membrane interaction. (C) The overall structure of human CD38. The N-terminal structures (in the red circle) and the C-terminal structure circled in blue (adapted from Liu *et al.*, 2005).

B). These two distinct domains are connected by a hinge region composed of three peptide chains including: residues 118-119, 143-144, and 200-201 (Liu *et al*., 2005).

It is important to note that there are many types of membrane proteins with different arrangements, as shown in Fig. 1.4, and CD38 is one of these proteins that spans from the internal to the external surface of the biological membrane (integral protein). Moreover, CD38 was initially classified as a type II transmembrane glycoprotein (Fig. 1.4b), with an extracellular carboxyl active domain (Jackson and Bell, 1990), expressed both the cADPR synthesizing and hydrolyzing activities. However, a recent thorough study by Zhao *et al.* (2012) showed that CD38 has the characteristics of a type III integral membrane protein, in which the C-terminus would be in opposite orientation to that in a type II membrane protein, so that the active site of CD38 would face the cytoplasm, with an extracellular N-terminal tail (Fig. 1.4a). Furthermore, some considerable studies have reported that the full-length CD38 can form dimers on the cell surface (Moreno-Garcia *et al.*, 2004) or even oligomers (Ferrero and Malavasi, 1999; Fig. 1.5).

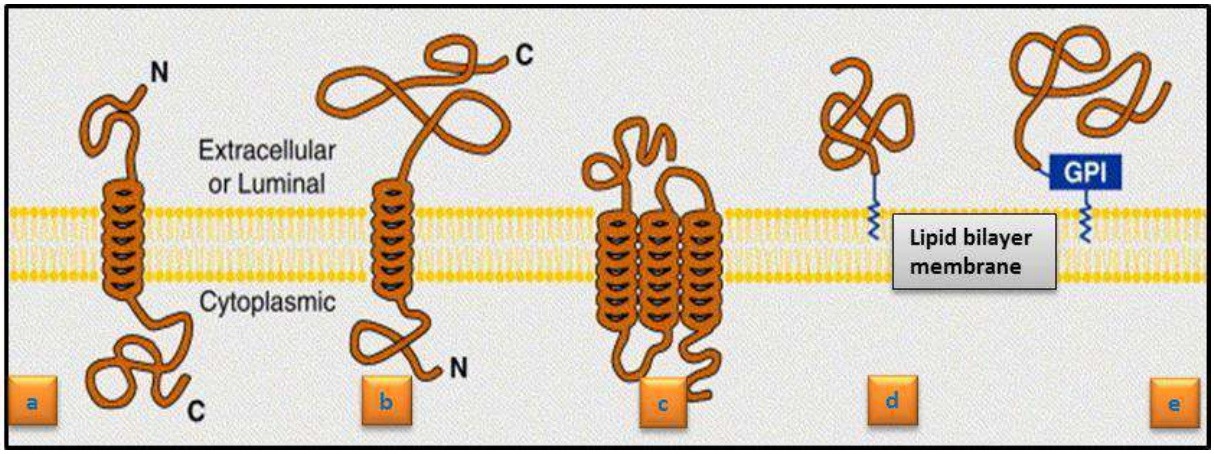

Figure 1.4 Schematic representation of different types of integral membrane proteins as follows (a) type-1 transmembrane, (b) type-2 transmembrane, (c) multipass transmembrane, (d) lipid-chain anchored membrane, and (e) GPI-anchored membrane (modified from Cai and Chou, 2006).

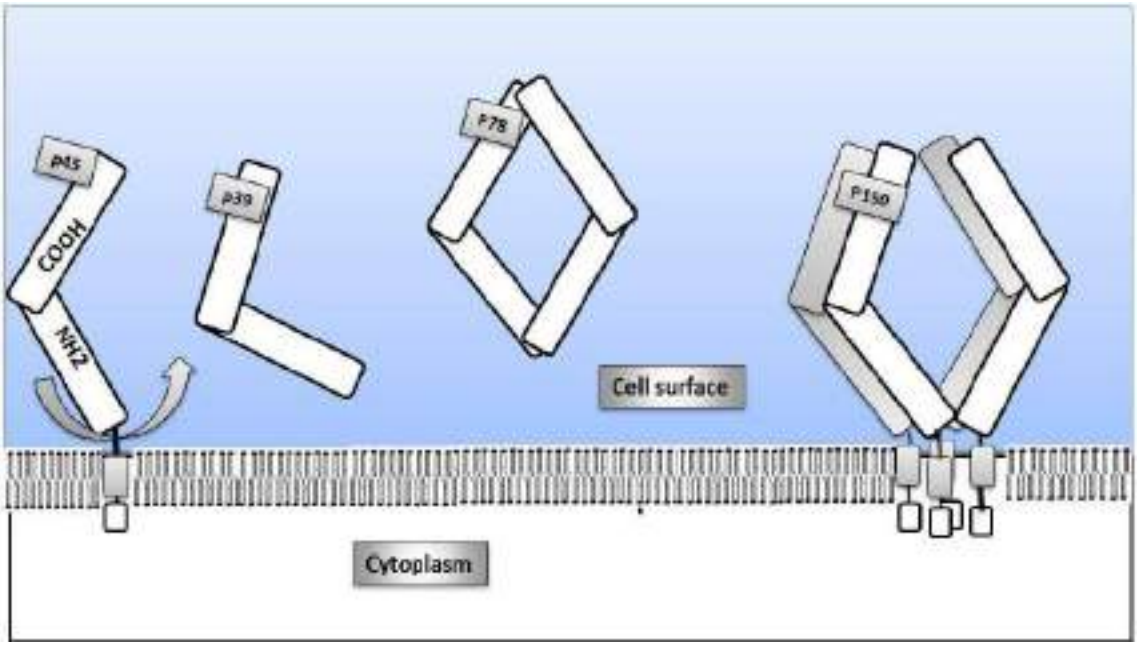

Figure 1.5 Simplified diagram representing monomeric, dimeric and oligomeric forms of CD38. Cleavage of the surface membrane form gives rise to p39 (soluble), its dimeric form is p78 and p190 represents a tetramer of the membrane form (modified from Ferrero and Malavasi, 1999).

The similar glycoprotein to CD38, CD157, also exhibits both monomeric and dimeric forms (Malavasi *et al.*, 2008). The C-terminal end of CD157 is anchored to the plasma membrane, by a glycophosphatidylinositol (GPI) molecule, while the N-terminal region, which includes the catalytic domain, is out of the membrane (Funaro *et al.*, 2009). Therefore, and on the cell surface membrane, the two molecules (CD38, CD157) are oppositely oriented with respect to one another (Ferrero and Malavasi, 1999).

1.5 CD38 as a cell surface receptor

CD38 has multiple functions through its roles as an enzyme and a receptor (Deaglio *et al*., 1996). As a receptor, CD38 is expressed in various cell lineages, where it mediates cell-cell interactions and delivers transmembrane signals. The role of CD38 as a receptor was first identified by means of agonistic monoclonal antibodies (mAbs), which suggested the existence of a non-substrate surface ligand, namely CD31/platelet endothelial cell adhesion molecule-1; PECAM-1 (Deaglio *et al.,* 1998). CD38 receptor functions are regulated through interactions with its non-substrate ligand, CD31, which is expressed in a variety of cells including endothelial cells, platelets and nurse-like cells (for example, macrophages and epithelial cells; Deaglio *et al.,* 2000; 2005). CD38/CD31 crosstalk has been extensively analyzed in a number of different environments, ranging from T lymphocytes to B, NK, and myeloid cells, from normal to pathological situations (reviewed in Deaglio *et al.,* 2000). For instance, CD31 interaction with CD38 induces activation, proliferation, cell adhesion and cytokine release in lymphocyte subsets (Deaglio *et al.,* 1998). CD38/CD31interactions also lead to increased B-cell proliferation and survival, through direct cooperation with CD100, a cell surface receptor member of the semaphorin family known as sema 4D (Kikutani and Kumanogoh, 2003). Other proposed ligands for CD38 include hyaluronate in humans (Nishina *et al.,* 1994), and an unidentified 130-kDa glycoprotein in mice (Wykes *et al*., 2004).

Several lines of evidence indicate that the receptor functions mediated by CD38 are regulated at multiple levels (Malavasi *et al.,* 1984). The first level involves the dynamic structure of CD38, which allows a monomer to dimer transition, which modulates the functions of the molecule (enzyme and receptor functions). Additional control is provided by the dynamic localization of

CD38 in lipid microdomains of the plasma membrane (Pavon *et al.*, 2006). A significant fraction of the membrane CD38 pool is localized in cholesterol-rich regions, while the remaining fraction of CD38 is localized in the raft pool (Deaglio *et al.*, 2007a). That localization makes it possible for CD38 to expand its interaction horizontally and frontally with molecules other than its substrate (NAD), forming large supramolecular complexes; thus it attracts transducers in spite of its short tail (Rah *et al.*, 2007).

Extensive observations that were made on CD38 receptor functions suggest that CD38 controls specific signalling pathways in B cells, T cells, NK cells, and monocytes. However, CD38 associations with surface molecules are lineage-dependent, and they also vary according to the maturation steps within each lineage (Deaglio *et al.*, 2001). For instance, CD38 signalling in B cells and in human or murine systems (Funaro *et al.*, 1993; Lund *et al.*, 1996) depends on the presence of a functional B-cell–receptor (BCR) complex. CD38-associated molecules in human B cells include the CD19/CD81 complex, the chemokine receptor CXCR4, and adhesion molecules, such as CD49d (Deaglio *et al.*, 2007a; 2010). The ability of CD38 to deliver its signals in B cells appears completely linked to the stage of maturation. Thereby, the presence of blocking mAbs in cultures of $CD19^{+}$ B-cell precursors suppresses B-cell proliferation and induces apoptosis (Kumagai *et al.*, 1995). However, in mature circulating B lymphocytes, CD38 ligation is followed by activation, apoptosis inhibition, proliferation and cytokine secretion (Zupo *et al.*, 1994; Funaro *et al.*, 1997).

Furthermore, in T cells, the CD38 molecule is also associated with the T-cell receptor (TCR)/CD3 complex (Zubiaur *et al.*, 1999), and it has been shown that CD38 initiated functional signals in a subset of membrane rafts containing CD3 (Zubiaur *et al.*, 2002; Munoz *et al.*, 2003).

The observation in immature T cells indicated that CD38 enhances apoptosis when it is cross-linked with a goat anti-mouse antiserum or interacts with CD31 (Tenca *et al.,* 2003). However, it has been shown that following T-cell activation, the final outcome includes cytokine secretion and cell proliferation (Malavasi *et al.,* 2008).

In monocytes, CD38 signalling has been shown to be associated with HLA class II and CD9 molecules. The CD38/HLA class II/CD9 complex shares a common pathway of tyrosine kinase activation, and cytokine secretion in human monocytes (Zilber *et al.,* 2005). CD38 expression in human monocytes was found also to be regulated in response to proinflammatory cytokines (Musso *et al.,* 2001). CD38 expression is also known as a marker of the transition of monocytes to dendritic cells (DC) induced by inflammatory processes (Fedele *et al.,* 2004). Furthermore, CD38 mediates important signalling that is involved in dendritic cell migration; the CD38/cADPR signalling pathway is required for the migration of immature dendritic cells to CXC ligand 12 (CXCL12) and of mature dendritic cells to CC ligand 19 (CCL19) and CCL21 (Partida-Sanchez *et al.,* 2004a; 2004b).

CD38 is also expressed by resting and activated natural killer (NK) cells; it forms part of a supramolecular complex that includes CD16. Indeed, CD38-CD16 association controls an activation pathway that includes Ca^{2+} fluxes, increased expression of HLA class II and CD25, tyrosine phosphorylation of cytoplasmic substrates (such as ZAP-70 and ERK), release of cytokines and cytotoxic responses (Mallone *et al.,* 2001). Collectively, the general events that take place after CD38 activation in several cell lineages include calcium (Ca^{2+}) mobilization from cytosolic stores, as well as the triggering of the phosphorylation of a cascade of intracellular substrates, including phosphatidylinositol 3-kinase, leading to the activation of

nuclear factors (such as the nuclear factor-κB complex), and the secretion of cytokines (Kitanaka *et al.,* 1997; Deaglio *et al.,* 2000).

Additionally, in neutrophils, CD38 signalling plays an important role in the regulation of cell trafficking; it has been shown that trafficking of neutrophils to sites of infection and inflammation is dependent on CD38 expression (Partida-Sanchez *et al.,* 2001; 2003). This process is controlled through cADPR production, which is triggering by the release of intracellular Ca^{2+} (Partida-Sanchez *et al.,* 2004b). Finally, as with CD38 receptor functions, CD157 also transduces activation signals, but no non-substrate ligand equivalent to CD31 has been described for CD157 (Malavasi *et al.,* 2006).

1.6 CD38 as active enzyme

CD38 is pleiotropic in function (Malavasi *et al.,* 1994); it is considered as the major NAD-consuming enzyme in humans (Malavasi *et al.,* 2008). CD38 is capable of catalyzing four major enzymatic reactions: NAD glycohydrolase (NADase), cyclic adenosine diphosphate ribose (cADPR) hydrolase, base-exchange reactions and ADP-ribosyl cyclase activity (Fig. 1.6 A, B). The ADP-ribosyl cyclase activity generates cADPR, and the NADase activity generates adenosine diphosphate ribose (ADPR) directly from NAD (Lee, 2006), while the cADPR hydrolase activity generates ADPR from cADPR (Howard *et al.,* 1993). However, it has been observed that the majority of the NAD (~95%) is converted to ADPR, and only a minor fraction of the total product appears to be cADPR (Howard *et al.,* 1993). Finally, CD38 can also use $NADP^+$ as a substrate and, in the presence of nicotinic acid (NA), to catalyze the exchange of the nicotinamide (Nam) group of $NADP^+$ with nicotinic acid, producing NAADP and nicotinamide (Lee, 2006). This reaction predominates in acidic conditions, while at neutral and alkaline pH the

enzyme mainly catalyzes cyclization of NAD^+ (Aarhus *et al.*, 1995). Furthermore, Graeff *et al.* (2006) documented that CD38 may also catalyse the hydrolysis of NAADP to ADP-ribose 2'-phosphate (ADPRP) at acidic pH. CD38 is also known to metabolize analogs of NAD, such as nicotinamide guanine dinucleotide (NGD) and nicotinamide hypoxanthine dinucleotide (NHD), releasing cyclic compounds (Cyclic guanosine diphosphate ribose (cGDPR) and cyclic inosine diphosphate ribose (IDPR), respectively) with fluorescent properties, but without calcium-releasing activity (Graeff *et al.*, 1994a). cGDPR, unlike cADPR, is a poor substrate for the hydrolase activity of CD38, and thus its measurement provides the basis of a continuous assay of cyclization for distinguishing CD38-like enzymes (with cyclase activity) from classical NADases (Graeff *et al.*, 1994a).

It is noteworthy that there are a number of critical residues that are highly conserved across the ADP-ribosyl cyclase family, and that have an essential role in the major enzymatic activities. For example, there are twelve conserved cysteine residues in the cyclase family, with only four of them (Cys119, Cys160, Cys173 and Cys201) having an essential role in the cADPR synthetic and hydrolytic activities of CD38 (Tohgo *et al.*, 1994). Moreover, the carboxylic domain of CD38 contains Cys275, which contributes to the NAD glycohydrolytic activity of CD38 (Hoshino *et al.*, 1997). Disulfide bonds between cysteine residues are important for the catalytic activity of CD38, as it has been shown that CD38 enzymatic activity can be inhibited by reducing agents such as dithiothreitol, 2-mercaptoethanol or reduced glutathione (Tohgo *et al.*, 1994; Zocchi *et al.*, 1995). Furthermore, three of the critical residues, Trp125, Trp189 and Glu226, are also highly conserved across the ADP-ribosyl cyclase family, with two of them (Trp125 and Trp189) essential for positioning NAD in the CD38 binding pocket, via hydrophobic interactions (Munshi *et al.*, 2000). However, a unique critical residue to CD38 is

Lys129; it is known to form a hydrogen bond with cADPR (Tohgo *et al.*, 1997). Additionally, there are two critical acidic residues in the catalytic domain of CD38 that are necessary for the pH-dependent base-exchange reaction: Glu146 and Asp155 (Graeff *et al.*, 2006).

It has been reported that CD157 shares a similar enzymatic function with CD38 (Malavasi *et al.*, 2006), except that CD157 does not produce NAADP. Surprisingly, CD38 knockout mice studies suggest that CD157 might undergo modification to enhance its cyclase activity to produce cADPR in some cells and tissues (Partida-Sanchez *et al.*, 2001; Lee, 2012). However, CD157 catalytic activity is one hundred-fold lower than that of CD38 (Hussain *et al.*, 1998).

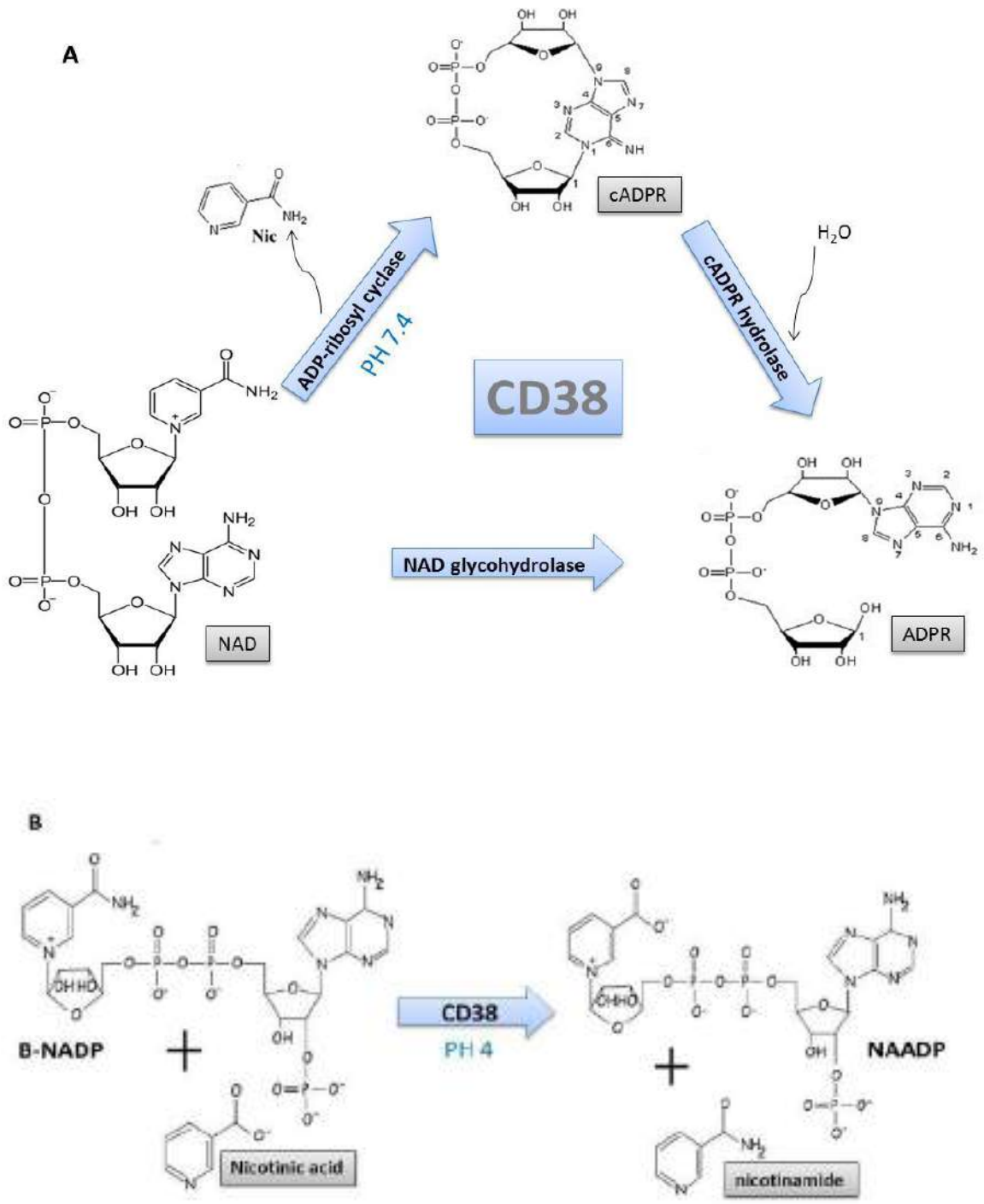

Figure 1.6 Schematic representation of CD38 (A) cyclase and hydrolase reactions by using β-NAD as substrate (Modified from Zhang *et al*., 2011). (B) Base exchange reaction in the presence of β-NAD with the pH optimum of 4 (modified from Yamasaki *et al.,* 2005).

1.7 The interdependence between CD38 enzymatic and receptor functions

CD38 as a cell surface receptor and a multifunctional enzyme has drawn the attention of several studies, focusing on how it is that the single molecule (CD38) has a multifunctional role (receptor and enzymatic functions), and what the role of the enzymatic activity of CD38 is in the initiation of the signalling cascade. Indeed the answer to these questions is still not completely known, because the possibility of finding CD38 inhibitors is still limited, in addition to the complexity of CD38 being a multifunction enzyme with a variety of enzymatic products. However, the initial hypothesis is that they are completely unrelated, as enzymatic mutants and enzyme inhibition of CD38 have no effect on its receptor functions in human B, T, and myeloid cells (Lund, 2006; Congleton *et al.*, 2011).

The alternative hypothesis by Malavasi *et al.*, (2011) and Vaisitti *et al.*, (2011), is that CD38 enzymatic functions are regulated through interactions taking place between CD38 and different proteins or molecules that are critical for cell homeostasis. This suggests that the human CD38 enzymatic activity is not only limited in function by the availability of the substrate (NAD), but also by the opening or closing of the enzymatic site that is further controlled by the interactions with other non-substrate ligands (Malavasi *et al.*, 2011; Vaisitti *et al.*, 2011). Indirect evidence in support of this hypothesis comes from the crystal structure of CD38, which has shown CD38 as a dimer coupled to different ligands (Zhang *et al.*, 2011). In addition, the study by Liu *et al.*, (2005) suggested that CD31 binding regulates the access of NAD to its enzymatic site. A possible explanation is that CD31 acts as modulator of CD38's three-dimensional structure and thus alters its propensity to bind the substrates or to initiate signalling (Liu *et al.*, 2005).

The membrane localization of CD38 in close association with signalling receptors is suggested to initiate enzymatic and receptorial coupling machinery important for signal transduction (Munoz *et al.*, 2008). Moreover, the products of the enzymatic activities of CD38 might be necessary for the receptor functions. For instance, it is believed that a direct contribution of cADPR to the signalling process is induced after CD38 binds with agonistic mAbs in humans (Hoshino *et al.*, 1997; Munshi *et al.*, 2000). Thus, CD38 provides a connection between Ca^{2+}-modulation via cADPR and the classical signalling cascades that are responsible for the activation of Ca^{2+}-dependent kinases and initiating antigen receptor signalling (Deaglio and Malavasi, 2006). Collectively, the functions attributed to CD38 are linked either to enzymatic or receptor functions. However, the final outcome is dependent on the interactions with other ectoenzymes and/or signalling molecules, which vary according to tissue and sub-cellular localization (Deaglio *et al.*, 2008).

1.8 Visualization of the cyclization reaction (enzyme-NAD interaction)

Until recently, it was not possible to visualize the wild type cyclase complexes with its substrate NAD, or to visualize cADPR formation, without modification. The excellent study by Kotaka *et al.* (2012) solved the previous difficulties of visualizing CD38 with its substrate, without limitations, by crystallography. The previous restriction was that CD38 converted NAD to its products during crystallization, and hence the only option was to use an inactive mutant of CD38, e.g. E226Q or E179G, or even to use substrate analogs that are resistant to enzymatic conversion. However, even with the limitations in the previous results, they were still consistent with the results recently obtained by Kotaka *et al.* (2012). Generally, the cyclization can proceed with either NAD, to produce cADPR, or with its analog, ara-2'FNAD, which, like NAD, is a

substrate for the *Aplysia* cyclase and CD38, except with the substitution of a fluorine atom at the 2'-position of the adenylyl ribose (Liu *et al*., 2008; Zhang *et al.,* 2011; Kotaka *et al*., 2012). It has been found that ara-2'F-NAD, or NAD enters the active site pocket with its nicotinamide-end first, which interacts with the catalytic residue Glu226 in CD38 and Glu179 in the cyclase. The interaction is not via the anomeric carbon (C1) of the terminal ribose, the cyclization site, but through the two -OH groups of the ribose, forming hydrogen bonding with the carboxyl group of the catalytic residue (Liu *et al.,* 2006; Kotaka *et al*., 2012). This leads to straining of the ribose ring and a cleavage of the glycosidic bond to release the nicotinamide group.

Moreover, Lee (2012), using cyclase crystallographic information, identified 22 folding conformations (folding states) during the interaction of NAD with the enzyme to produce a cyclic compound, of which only 3 are shown in Figure 1.7. The conformations started from an extended (initial) state (coloured yellow) in which the adenine ring stacks parallel and interacts hydrophobically with Tyr81. During the intermediate state (transparent) the N1 of the adenine brings closure to the anomeric carbon C1 of the terminal ribose. In the fully folded state (coloured cyan) the adenine interacts with Trp140 and the N1 of the adenine is only 5.2 Å from C1 in order to form the cyclization linkage (Lee, 2012). The same crystallography technique has also been applied to CD38 to visualize the folding process (Zhang *et al.,* 2011).

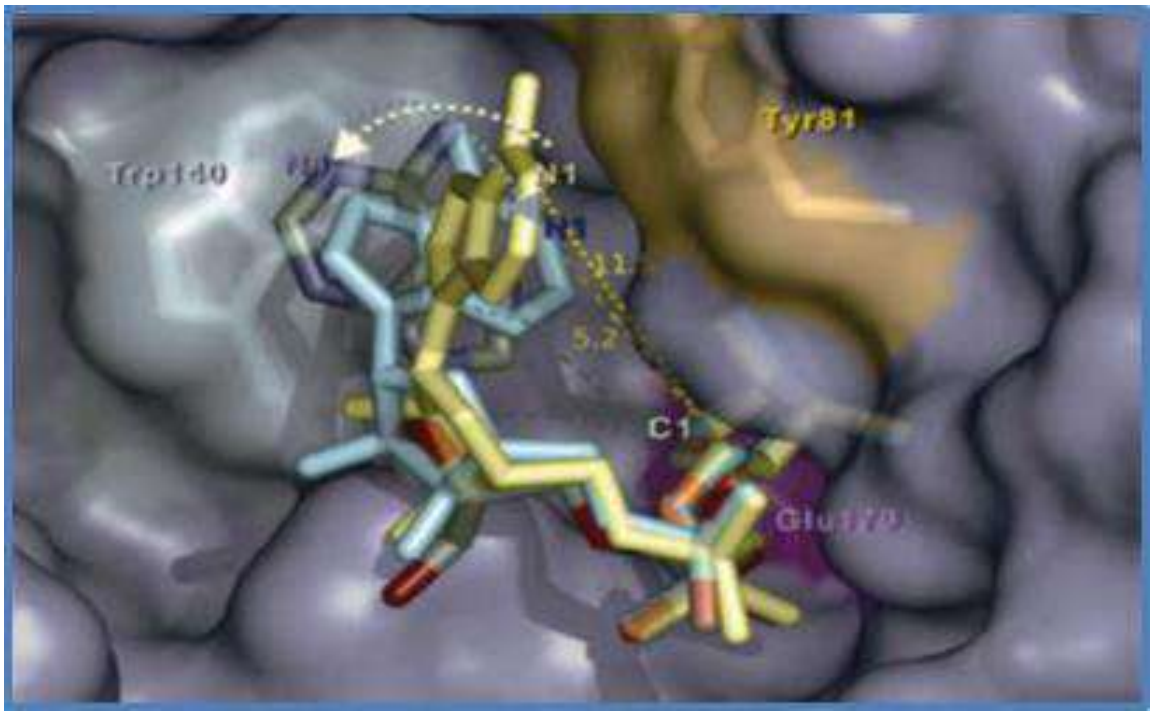

Figure 1.7 Visualization of the ara-2'FNAD cyclization reaction catalyzed by the cyclase. Adapted from Lee (2012).

1.9 The Second Messengers (cADPR and NAADP)

There are several known calcium mobilizers. First, inositol trisphosphate (IP_3), a second messenger that facilitates Ca^{2+} mobilization from its endoplasmic reticulum (ER) stores, was first shown in pancreatic acinar cells after activation by carbachol (Streb *et al.,* 1983, Churchil *et al.,* 2002). Several years later, a second active calcium inducer (cADPR) was purified by Lee *et al.* (1989). cADPR as a second messenger was found to induce calcium release from sea urchin egg homogenates through a variety of mammalian cells, including human cells (Dargie *et al.,* 1990; Lee, 2002). Evidence suggests that cADPR is an endogenous modulator of the Ca^{2+}-induced Ca^{2+} release (CICR) mechanism in cells, which is known to be mediated via the ryanodine receptor,

RyR (cADPR main target) in the endoplasmic reticulum (Lee *et al.*, 1995a). The activation of RyR by cADPR requires the presence of accessory proteins, such as calmodulin (Thomas *et al.*, 2002) and FK506-binding protein; FKBP (Zhang *et al.*, 2009b).

The third and the fourth calcium mobilizers are NAADP (Lee and Aarhus, 1995) and ADPR, which also play important roles in Ca^{2+} signalling (Lee, 2006). While ADPR acts on plasma membrane transient receptor potential cation channel member 2 (TRPM2), the NAADP channels have been identified as the two-pore channels (TPCs) in lysosomes, and the main role of NAADP in Ca^{2+} releasing correlates positively with the expression of TPC proteins (Perraud *et al.*, 2001; Brailoiu *et al.*, 2009; Calcraft *et al.*, 2009).

Indeed, CD38 activity to produce either NAADP or cADPR is dependent on its environment and is regulated by pH (Lee, 2006). For example, at physiological pH, CD38 cyclises NAD to produce cADPR, and also breaks it down to ADP-ribose, inactivating its signalling function. However, that it is able to synthesise and hydrolysise NAADP only at acidic pH, confirms that CD38 could be located in two separate environments in cells and perform different Ca^{2+} signalling functions. Therefore, CD38 is known as a unique Ca^{2+}-signalling enzyme that is responsible for cADPR and NAADP production in various cells (Lee, 2012). The first demonstration was in sea urchin spermatozoa, which contain micromolar concentrations of NAADP (Billington *et al.*, 2002). It has been shown that the synthesis of NAADP can be stimulated by several stimuli, including those that elevated cADPR synthesis (extensively reviewed by Lee, 2012). Furthermore, it was proposed that NAADP may serve as an initial Ca^{2+} inducer, whose signal may be amplified by cADPR- and IP_3-dependent Ca^{2+} release (Guse and Lee, 2008).

Interestingly, studies revealed that these two novel Ca^{2+} messengers (NAADP and cADPR) can act either individually or in coordination, depending on stimulus type, suggesting a crosstalk between the two calcium-mobilizing pathways (Park *et al.,* 2011; Kang *et al.,* 2012; Lee, 2012). Also, it is worth mentioning that the entry of cADPR into cells is either mediated via CD38, or by members of the equilibrative (ENT2) and the concentrative nucleoside transporters; CNT2 and CNT3 (De Flora *et al.,* 2004) as suggested mechanisms to resolve the CD38 'topological paradox'. However, the NAADP transporter has not been identified, although it has been suggested that the proteins involved in NAADP transport are different from those characterized for cADPR transport (Billington *et al.,* 2006). In conclusion, these messengers bind via different receptors and channels involved in the regulation of Ca^{2+}, and activate important signalling pathways, for instance, muscle contraction (uterus and bronchi) and gland secretion (pancreas). These functions were initially identified in CD38 knockout mice studies or mice modified to over-express CD38 (Jin *et al.,* 2007). They have also been confirmed in human disease models (Munesue *et al.,* 2010).

1.10 Role of CD38/second messengers in pathophysiological conditions

1.10.1 CD38 and obesity

Obesity is a major disease, defined as an increase in the body's storage of fat, causing health problems leading to increased mortality (Sorensen *et al.,* 2010). It increases the risk of a number of health conditions, including hypertension, adverse lipid concentrations, and type 2 diabetes (National Institutes of Health, 1998). However, the biochemical explanation for this disease is still unclear. Recently, Barbosa *et al.* (2007) described a novel and unique role for the enzyme CD38 as a necessary molecule in the biochemical pathway that leads to the development of

obesity, as confirmed by CD38 knockout mice studies. CD38 has been implicated in the regulation of a wide variety of signalling pathways in numerous cell types (Galione and Churchill, 2000). For instance, CD38 hydrolase activity (NADase) has a key role in the regulation of intracellular NAD levels and subsequently regulates NAD-dependent deacetylases such as sirtuins; also known as SIRT enzymes (Aksoy *et al.,* 2006). Importantly, SIRT enzymes have been implicated as regulators of energy metabolism, cell life span (longevity) and activation of peroxisome proliferator-activated receptor γ co-activator-1α (PGC-1α; Rodgers *et al*., 2005). The latter is known as a co-activator with pleiotropic function (Knutti and Kralli, 2001). It plays a significant role in energy metabolism and reduces the problems of obesity (Baur *et al*., 2006), by controlling the function and biogenesis of the mitochondria (Lin *et al.,* 2005). Recent studies have shown that activation of SIRT (by resveratrol) can protect laboratory animals from a high fat diet-induced obesity and its deleterious effects, by increasing levels of PGC1-1α, cellular mitochondrial numbers, and energy expenditure (Lagouge *et al*., 2006).

However, in the case of CD38-deficient mice, one of the possible mechanisms for mice's resistance to diet-induced obesity is mediated via activation of the NAD-dependent deacetylase (SIRT)/PGC1α pathway (Baur *et al*., 2006). It has been proposed that increasing intracellular levels of NAD following CD38 deficiency will promote activation of the SIRT enzymes. SIRT activation leads to the activation of PGC1α (Fig.1.8), which is involved in protection from obesity (Barbosa *et al*., 2007).

Furthermore, several reports have highlighted a crucial role of CD38 as a novel pharmacological target to treat metabolic diseases via NAD^+-dependent pathways. Thus, the manipulation of NAD^+ metabolism has emerged as a reasonable strategy to improve metabolic syndromes, such

as protecting against obesity. More recently, a study by Escande *et al*. (2013), reported that *in vitro* and *in vivo* inhibition of CD38 activity (via quercetin and apigenin) results in elevated cellular NAD levels, decreased overall protein acetylation and improved lipid homeostasis.

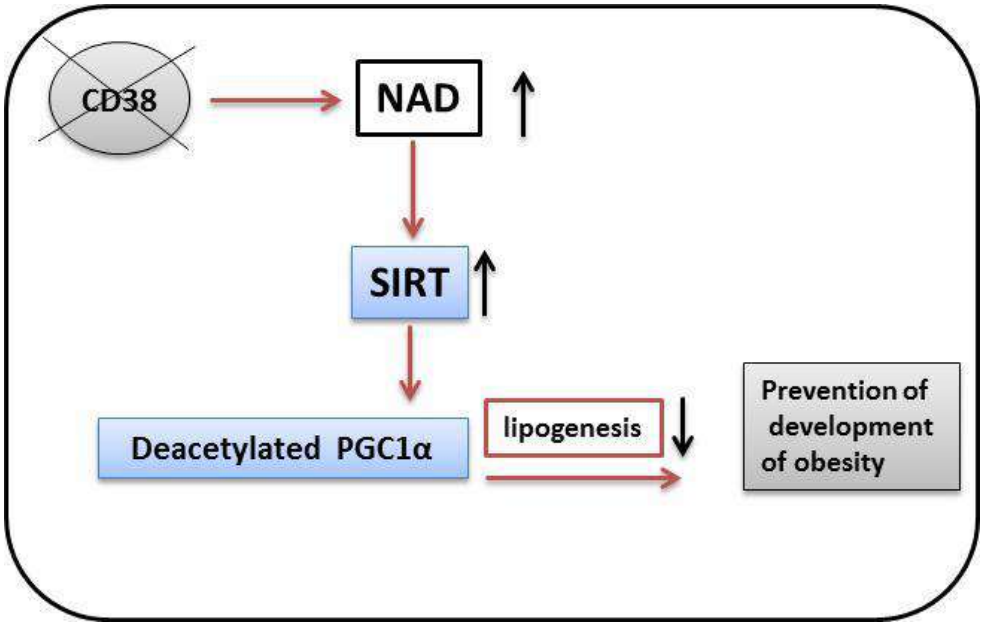

Figure 1.8 The crucial role of CD38 deficiency in preventing the development of obesity through activation of SIRT/PGC1α following NAD elevation.

In summary, in addition to the knockout of CD38, the inhibition of CD38 activity, and elevation of sirtuin activity were successful mechanisms for preventing the development of obesity, which is part of the NAD manipulation strategy. Another suggested mechanism that might have a beneficial effect is through the activation of one of the NAD biosynthesis pathways to increase NAD levels, which again could activate the SIRT enzymes, consequently leading to an increase in PGG1α activity and reduce the problems of obesity. Successful completion of these proposed

studies will lead to a better understanding of obesity and may lead to new therapeutic approaches for this condition.

1.10.2 CD38 and diabetes

Diabetes is a metabolic disorder characterised by chronic hyperglycaemia with disturbances of carbohydrate, fat and protein metabolisms, resulting from the destruction of insulin production by beta cells in the islets of Langerhans (type 1 diabetes), or from an impairment in insulin secretion; type 2 diabetes (Harris, 1989; Atkinson and Maclaren, 1994). The role of CD38 products in insulin signalling has been demonstrated in diabetes patients by several studies. The first pathway proposed for insulin secretion by glucose is mediated by the CD38-cADPR system in pancreatic β-cells (Okamoto *et al*., 1997). It is suggested that in the process of glucose metabolism, the generation of ATP induces cADPR accumulation by inhibiting the cADPR hydrolase activity of CD38, since the ATP produced competes with cADPR for the binding residue, Lys129, of CD38 (Kato *et al*., 1995). cADPR then stimulates insulin secretion by mobilizing intracellular Ca^{2+} from the endoplasmic reticulum (Noguchi *et al*., 1997). The CD38/cADPR system prevents β-cell apoptosis through activation of RyR2 in diabetes (Paraskevas *et al.,* 2001). The evidence shows that the Arg140Trp mutation on CD38 might be responsible for the development of type II diabetes mellitus, via the impairment of glucose-induced insulin secretion (Yagui *et al.,* 1998). Furthermore, CD38-deficient mice studies have shown an alteration in Ca^{2+} levels, in addition to a reduction in the responsiveness to insulin, which is regarded as a survival factor; consequently CD38 deficiency increased islet apoptosis (Paraskevas *et al*., 2001; Johnson *et al*., 2006). The apoptosis leads to decreased β-cell mass, and a disruption of islet architecture (Bonner-Weir, 2000). Another pathway involves the CD38/NAADP system, which mediates Ca^{2+} mobilization by insulin in human pancreatic β-

cells. It has been shown that NAADP-generating enzymes may be involved in insulin signalling. Thus, CD38 has important roles in controlling the anti-apoptotic signalling pathway in pancreatic β-cells (Johnson *et al*., 2006).

The causal relationship between CD38 and insulin release in humans has been further investigated, showing that auto-antibodies (a marker of autoimmunity in human diabetic patients) to CD38 might be playing a key role in impaired glucose-induced insulin secretion (Ikehata *et al.,* 1998). Auto-antibodies against CD38 have been found in sera from Caucasian type 1 (insulin-dependent, 13.1%) and type 2 (non-insulin dependent, 9.7%) diabetic subjects (Pupilli *et al.,* 1999). They have also been found in 13.8% of Japanese non-insulin dependent diabetes (NIDDM) patients along with abnormalities of both the CD38-cADPR signal system and effects on insulin secretion (Ikehata *et al.,* 1998; Mallone *et al*., 2001a). The different results of studies may result from the use of different types of islet samples.

Altogether, these studies might indicate that the auto-antibodies altered the *in vivo* ADP-ribosyl cyclase activity of islet CD38 and impaired glucose-induced insulin secretion. Further studies have confirmed that the absence of CD38 accelerates development of autoimmune diabetes in non-obese diabetic (NOD) mice (Chen *et al.,* 2006). In summary, CD38 has a regulatory role in insulin secretion by glucose in β-cells, via its metabolites, the calcium mobilizers (NAADP, cADPR), and that CD38 deficiency may contribute to the pathogenesis of diabetes (Fig. 1.9).

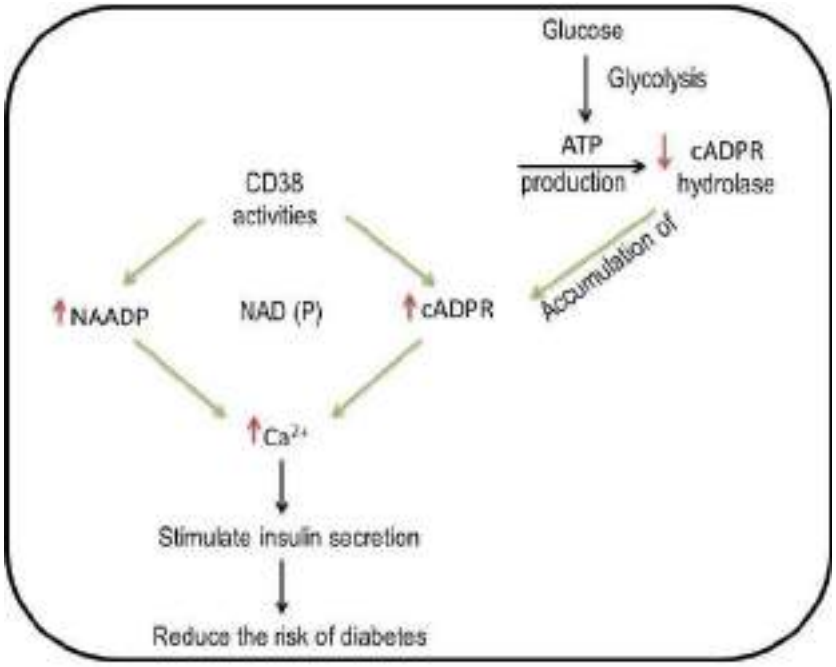

Figure 1.9 Simple diagram showing the role of CD38 activities and its products in protection against diabetes.

1.10.3 CD38 and Chronic Lymphocyte Leukaemia (CLL)

Chronic lymphocyte leukaemia (CLL), a B-cell malignancy, is the most frequent leukaemia in the western world, and is characterised by increased lymphocytosis (an increase in the number of lymphocytes) that results from the accumulation of a population of $CD5^+/CD19^+/CD23^+$ mature B lymphocytes in the peripheral blood, bone marrow (BM) and lymphoid nodes; LN (Rozman and Montserrat, 1995; Van Bockstaele *et al.*, 2009). It is also defined as a disease characterized by a dynamic balance between cells circulating in the blood and cells located in permissive niches in lymphoid organs (Zenz *et al.*, 2010).

There are two subgroups of CLL patients, according to CD38 expression, which correlates with different clinical outcomes (Damle *et al.,* 1999). CLL patients show either an indolent or a progressive course (Caligaris-Cappio and Hamblin, 1999). The two patient subgroups, with $CD38^+$ or $CD38^-$ CLL, differ clinically in several ways, including overall survival (Ibrahim *et al.*, 2001), time to first treatment (Morabito *et al.,* 2002), bias toward male gender (Damle *et al.*, 1999), number of leukaemic cells with atypical morphology (Morabito *et al.,* 2002), extent and level of adenopathy, lactate dehydrogenase, β-microglobulin levels (Ibrahim *et al.,* 2001; Domingo-Domenech *et al.,* 2002) and absolute lymphocyte counts (Del Poeta *et al.,* 2001). Hence, $CD38^+$ CLL patients have an unfavourable clinical course with a more advanced stage of the disease, poor responsiveness to chemotherapy, and a shorter survival state compared to $CD38^-$ CLL patients (Morabito *et al.,* 2002). Initial studies indicated that CD38 might be useful as a surrogate marker for the absence of mutations in immunoglobulin variable (IgV) genes in CLL patients (Damle *et al.,* 2007). Furthermore, the correlation between CD38 expression levels and cells' susceptibility to apoptosis makes this molecule a valuable prognostic marker and a disease modifier in leukaemia; CLL (Malavasi *et al*., 2008).

Researchers have confirmed that in combining CD38 with other negative prognostic markers, such as the cytoplasmic kinase zeta1-associated protein of 70 kDa (ZAP-70) and CD49d (Morabito *et al.,* 2009), cytogenetic abnormalities, CD23, b2m, p53 function and cell size (Shanafelt *et al.,* 2004), all together provide complementary prognostic information in CLL. It has been documented that CD38 ligation leads to phosphorylation of the activatory tyrosines within the proliferation marker ZAP-70 (Roos *et al*., 2008). It has been suggested that CD38 in association with ZAP-70 in CLL may contribute to the signals mediated by the B cell receptor complex (BCR; Chen *et al.,* 2002). This relation may explain why the simultaneous expression

of the two molecules is considered an efficient identifier of the high-risk patient subset (Schroers *et al.,* 2005). Therefore, patients with $CD38^+$ $ZAP\text{-}70^+$ clones are more responsive to activation of intracellular proteins than $CD38^+$ $ZAP\text{-}70^-$ patients (Deaglio *et al.,* 2007a). Moreover, $CD38^+$ CLL clones express specific activation markers in addition to $ZAP\text{-}70^+$, that are not found in $CD38^-$ CLL clones (Damle *et al.,* 2002), such as expressing high levels of CD69 and human leukocyte antigen (HLA)-DR (Damle *et al.,* 2007). Another characteristic of the $CD38^+$ and $CD38^-$ CLL subgroups is variable telomerase levels (Damle *et al.,* 2004). Lastly, they differ in high-risk genomic abnormalities (Krober *et al.,* 2002) in the development of new DNA mutations (Ottaggio *et al.,* 2003).

The earliest investigations of the role of CD38 in CLL pathogenesis and progression, was *in vitro* activation of CD38, elicited by agonistic mAbs that induced a portion of the CLL clone (10%-30%) to proliferate (Deaglio *et al.,* 2003). The following studies substituted the mAb with the CD31 ligand, which proved the same proliferation effect (Deaglio *et al.,* 2005). Noticeably, there are many indications of the significant association between CD38 expression and chemotaxis in CLL (Deaglio *et al.,* 2007a; Vaisitti *et al.,* 2010). The first indication came from a functional cooperation between CD38 and CXC receptor 4 (CXCR4), using a CD38 agonistic mAb which was able to enhance the chemotaxis of CLL cells in response to CXCL12 chemokine. However, this effect was inhibited by blocking mAbs. This functional cooperation was partial, owing to the co-localization of CD38 and CXCR4 in the same membrane region (Vaisitti *et al.,* 2010). Furthermore, a recent study has confirmed that co-expression of CXCR4 and CD5 creates a percentage of newly born cells that is proximally 10 times higher in $CD38^+$ than in $CD38^-$ clones (Calissano *et al.,* 2009).

A strong relationship between CD38 expression, CLL cell migration to solid tissues and clinical outcome exists, and that CD38 expression might reflect *in vivo* CLL cell activation (Fig. 1.10). Interestingly, the variable activation status may decline over time, leading to the conversion of $CD38^{+}$ cells to $CD38^{-}$ cells, but is reactivated again when the cells are recruited into lymphoid tissues (Calissano *et al.,* 2009).

The most favourable conditions for expansion of CLL clones exist in two separate proliferation centre (PCs) sites; in lymphoid nodes (LN) and BM (Jaksic *et al.,* 2004), where a favourable microenvironment which provides growth and survival signals mediated by CD38 is available (Deaglio *et al.,* 2005). In the proliferation centres, Leukaemic cells come into contact with accessory cells, such as T lymphocytes (Patten *et al.,* 2008), follicular dendritic (FDC), stromal, endothelial, and mesenchymal cells (Malavasi *et al.,* 2011) and some cytokines and chemokines, as shown in Figure 1.10.

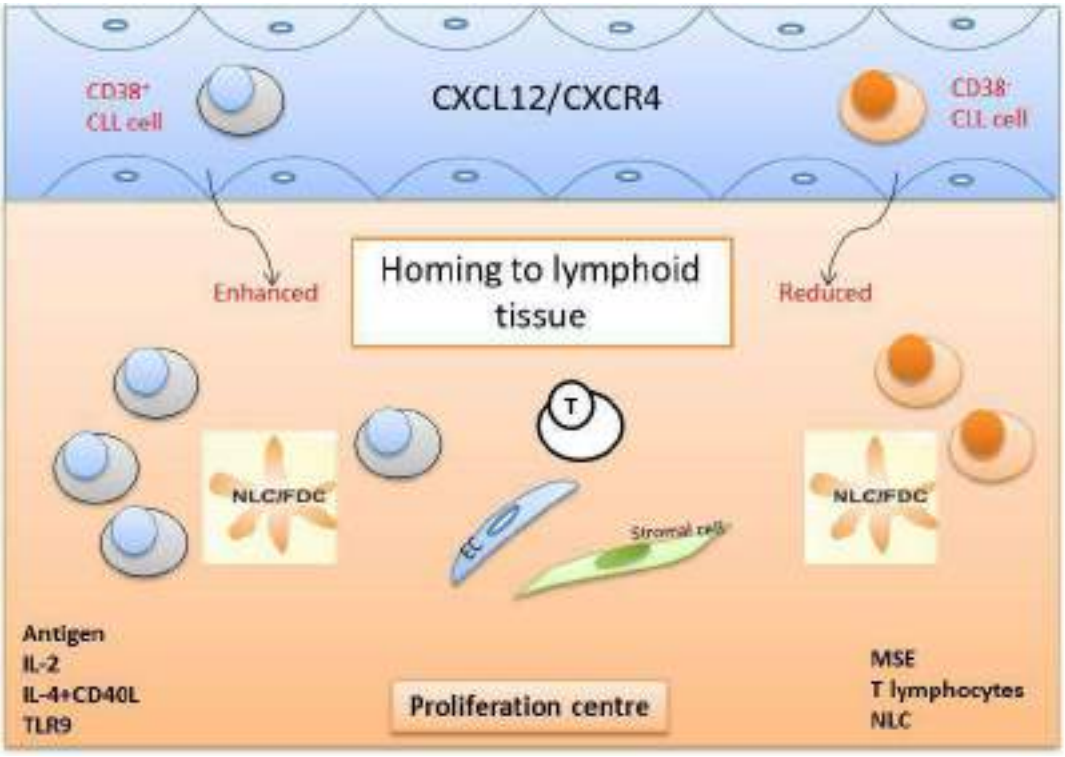

Figure 1.10 Hypothetical model of the interactions between CLL cells and distinct environments, suggesting a role for CD38 in the pathogenesis of CLL. $CD38^+$ CLL cells (grey) are more sensitive to CXCL12 signals, with a higher propensity to home to lymphoid tissues than the $CD38^-$ (orange). CLL lymphocytes in LN (PCs) come into contact with nurse-like (NLC) cells, follicular dendritic (FDC) cells, stromal cells, endothelial cells (EC), mesenchymal, and T cells. The presence of these environments, in addition to the cytokines and toll-like receptors (TLR) lead to CLL cell proliferation and disease progression; these events are more apparent in the $CD38^+$ subsets (adapted from Malavasi *et al.*, 2011).

The initiating event for this activation is still unclear, though a study by Chiorazzi and Ferrarini (2011) which has suggested BCR signalling as a factor promoting cellular stimulation, as $CD38^+$ CLL cells are generally more responsive to BCR signalling *in vitro*, which is not always the case in $CD38^-$ clones (Morabito *et al.*, 2010). However, evidence for involvement of CD38 in the BCR signalling pathway is indirect and linked to lateral associations with CD19 and CD81 and to the co-localization in the same lipid rafts as the BCR (Deaglio *et al.*, 2007b). Hence, besides BCR signalling, $CD38^+$ cells also respond to signals coming through chemokine and other receptors (Lopez-Giral *et al.*, 2004). For instance, nurse-like cells (NLC) that are present in solid

lymphoid tissues *in vivo* express CD38 ligand (CD31), and the interaction between CD38 and CD31 in this system promotes proliferation and survival (Deaglio *et al.,* 2005; Burger *et al*., 2009). Several reports have shown that CD31/CD38 signals that regulate the adhesion and chemotactic response of CLL cells are part of a molecular circuit involving the CCL3 and CCL4 chemokines, and the integrin CD49d (a4), the latter being a negative prognostic marker in CLL (Zucchetto *et al.,* 2009). Collectively, trafficking of a CLL cell to the proliferation centre might affect the cell's capacity to express more activation markers such as ZAP-70 and CD49d. Moreover, the percentage of $CD38^{+}$ CLL cells might also be extended, favouring survival/proliferation of CLL cells over apoptosis (Malvasia *et al.,* 2011). Additionally, the ability of leukaemic cells to recirculate from blood to lymphoid organs (the homing process) is also regulated by specific subsets of adhesion (integrin) molecules and by matrix metalloproteinases (MMPs). The latter play a significant role in mediating cell proliferation and prevention of apoptosis in association with chemokine receptors (Vaisitti *et al.,* 2011) by degrading the extracellular matrix to facilitate cell migration. One example of MMPs in CLL is MMP-9 (Kamiguti *et al.,* 2004), which is found to be involved in CLL cell migration and survival (Vaisitti *et al.,* 2011). However, targeting the CLL MMPs is suggested, to block cell trafficking to LN and BM (Deaglio *et al.,* 2010).

Recently, studies have indicated that nicotinamide phosphoribosyl transferase (NAMPT), the rate-limiting enzyme in the salvage NAD biosynthesis pathway in leukocytes, also exerts pro-survival activity in CLL, as recently confirmed from *in vitro* and *vivo* studies, suggesting the existence of a CD38/extracellular NAMPT (eNAMPT) loop in CLL cells, where CD38 consumes NAD and generates nicotinamide, triggering eNAMPT expression and activation to

resynthesize extracellular NAD levels. Finally, by this pathway pro-survival and activation signals will be generated in CLL (Audrito *et al.,* 2012).

In summary, the coexistence of a large supra-molecular complex, derived from the formation of extracellular and intracellular molecules in B-CLL cells, where CD38 looks to be a bridging element cooperating with all these molecules, might be one of the reasons for the higher migratory potential of $CD38^+$ CLL (Willimott *et al.,* 2007). This might provide an initial explanation for the clinical observation that patients with $CD38^+$ CLL clones have more aggressive disease with poor patient outcome. However, whether CD38 expression can affect the CLL homing process, through modulation of extracellular NAD^+ levels, or the generation of Ca^{2+} active compounds, or through structural re-organization of the membrane, still needs to be completely investigated (Vaisitti *et al.,* 2011).

Altogether, CD38 has been implicated in multiple pathological conditions. Therefore, to further assess CD38's physiological functions and to investigate the role of its products in other pathophysiological environments, several CD38 ablation and knockdown studies have been established. For instance, CD38-knockout mice studies have shown a highly depleted level of endogenous cADPR (Partida-Sanchez *et al.,* 2001). The consequence of cADPR depletion and the impairment of its metabolism caused multiple abnormalities and defects (reviewed in Lee, 2012), including in neutrophil chemotaxis and bacterial clearance (Partida-Sanchez *et al.,* 2001); bone resorption (Sun *et al.,* 2003); aortic muscle contraction (Mitsui-Saito *et al.,* 2003); regulation of airway tone in response to agonists (Deshpande *et al*., 2005); oxytocin secretion and social behaviour (Jin *et al.,* 2007); fibrosis after hepatic damage (Kim *et al.,* 2010); and inflammation after cerebral ischemia (Choe *et al.,* 2011). Recently, Xu *et al.* (2012) suggested a

beneficial role for the CD38/cADPR pathway in mouse coronary arterial myocytes (CAMs). In addition to the interesting role of cADPR, the functions regulated by NAADP/TPC are also significant (reviewed in Galione *et al.,* 2011). All these functions might also be disrupted in CD38 knockout mice, referring to the importance of the NAADP role in addition to cADPR as the main CD38 products. In conclusion, most previous and recent studies have supported the role of CD38/cADPR signalling cascade in various pathophysiological conditions in human and animal models.

1.10.3.1 CD38 as a possible therapeutic target in human leukaemia

The distinct differences in CD38 expression between normal cells and their leukaemic counterparts has made it attractive for the design of therapeutic protocols driven either by cells or by monoclonal antibodies (mAbs; Fig.1.11). These mAbs have a high ability to select $CD38^+$ tumour cell lineages, in addition to the stability of the complex (mAb-target) on the cell surface (Maloney *et al.,* 1999). However, in addition to the positive points, the limitation with *in vivo* use of anti-CD38 mAbs, is its widespread expression in multiple cell types and differentiation stages, in addition to a presence of CD38 expression in the brain, pancreas, and retina (reviewed in Malavasi *et al.,* 2008). These substantial limits, however, have not prevented the design of models for *in vivo* applications. One of these designs includes antibody-dependent cellular cytotoxicity against $CD38^+$ lymphoid cell lines (Stevenson *et al*., 1991).

Additional studies have developed anti-CD38 immunotoxins capable of killing human myeloma and lymphoma cells (Bofill *et al.,* 1994). Other models are based on either the use of antibodies alone (Tesar, 2007), or conjugated to toxins; mostly for purging applications (Bolognesi *et al.,* 2005), or conjugated to radiopharmaceuticals. In this design the mAbs are used as carriers of

radiopharmaceuticals delivering a lethal hit either by surface or cytoplasmic irradiation (Mehta *et al*., 2004). These models have been applied in myeloma and acute leukaemia cases (Stevenson, 2006). The mechanisms of action for using antibodies alone as a therapy include the inhibition of the migration function that is considered critical for CLL progression. This inhibition might be the result of the action of a mAb binding a specific domain of CD38 and disturbing ligation of a chemokine (CXCL12) to its receptor. Alternatively, a divalent anti-CD38-anti-CXCR4 therapeutic reagent might also provide simultaneous binding to CD38 and CXCR4, thereby increasing ligand specificity (Deaglio *et al.*, 2008).

CD38 can also be used as a target for gene therapy by using oncolytic viruses as anticancer drugs. These viruses propagate in tumour tissue and destroy it without causing excessive damage to normal or non-cancerous tissues, through selective targeting of CD38 (Nakamura *et al.*, 2005). The tumour cell is killed by the oncolytic virus as it takes over the cellular translational and transcriptional machinery, ultimately leading to an induction of cell necrosis or apoptosis (Parato *et al.*, 2005).

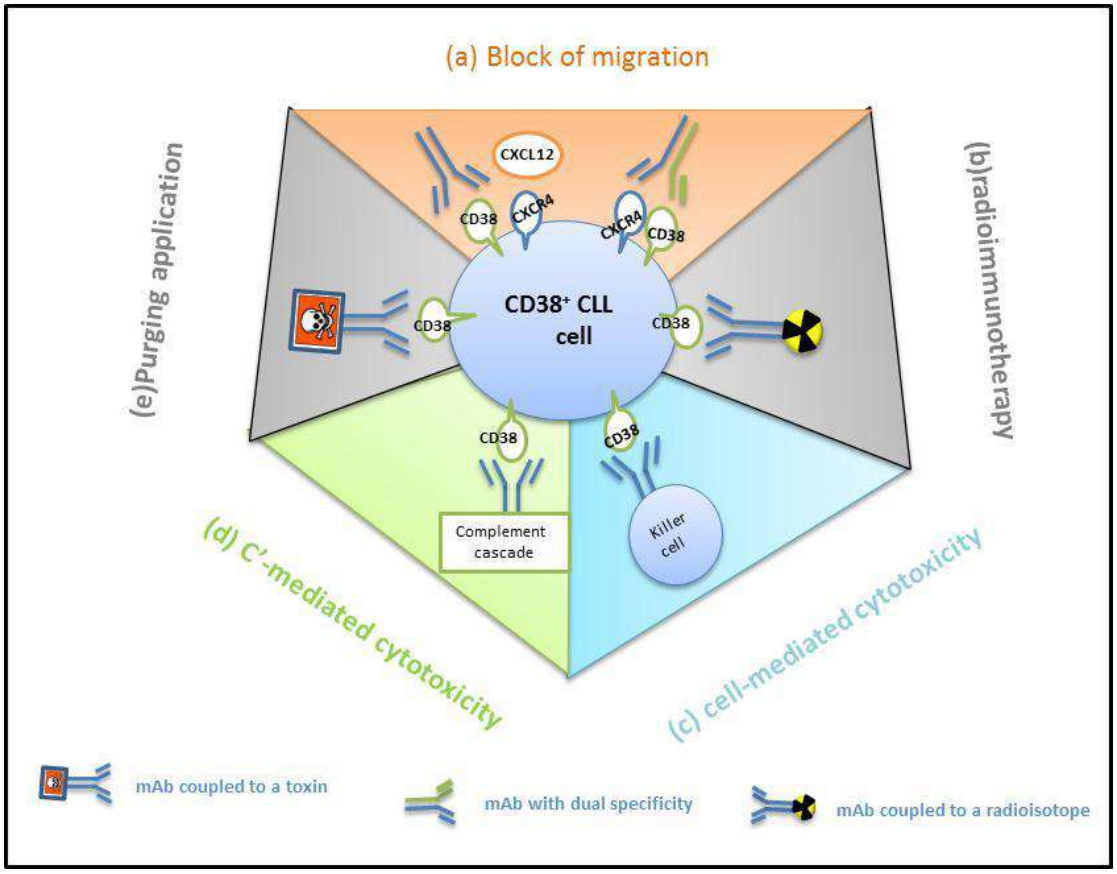

Figure 1.11 Potential applications of CD38 as a therapeutic target (adapted from Deaglio *et al.*, 2008).

Recently, two CD38 mAbs have been in clinical development: a humanized mAb; SAR650984 and a human mAb; daratumumab (de Weers *et al.*, 2011; van der Veer *et al.*, 2011). Alternatively, a useful and distinct approach could rely on the use of inhibitors of the enzymatic activities of CD38 instead of the mAbs strategy (Kellenberger *et al.*, 2011). This might be a useful strategy when CD38 inhibition is used as a therapeutic target in leukaemia and obesity patients. On the other hand, using activators of CD38 enzymatic activity might be important for other diseases, for instance diabetic patients.

In summary, several observations have suggested that CD38 is a potential therapeutic target for leukemia. Generally, targeting of CD38 may impair the proliferation of leukaemia cells, and might also render it more susceptible to conventional chemotherapy. However, more studies are still needed to investigate the role of CD38 as a therapeutic target in leukemia, and probably other diseases.

Finally, it is worth noting that CD38 regulation induced by all *trans* retinoic acid (ATRA) was interestingly involved in the induction of human leukaemia cells' (HL60) differentiation to neutrophil-like cells, as well as restricted cell proliferation. It has been documented that ATRA-induced CD38 expression is mediated by direct transcriptional regulation via activation of a retinoic acid receptor (RAR) and retinoid x receptor (RXR) (Kishimoto *et al.,* 1998). However, it has also been indicated that phosphoinositide 3-kinase (PI3-K) is involved in the modification of CD38 antigen expression in the ATRA-induced granulocytic differentiation of HL60 cells (Lewandowski *et al.*, 2002). Another study by Shen and Yen (2008) documented a causal role for Cbl-CD38 interaction in promoting ATRA-induced differentiation of HL60; this interaction enhances mitogen-activated protein kinase (MAPK) signalling, leading to myeloid differentiation.

1.11 The HL60 cell line and induction of differentiation

The HL60 cell model was derived from a patient with acute promyelocytic leukaemia (Collins *et al.,* 1977). These myeloid-restricted precursor cells are a well-characterized model for studying the terminal differentiation processes. HL60 cells exhibit the typical properties of leukaemia: unlimited proliferation capacity, inability to respond to normal differentiation stimuli, and increased obstruction of apoptosis (Palis *et al.,* 1988). However, many agents are known to induce differentiation in HL60 cells, with the hope of treating cancer cells by overcoming their blocked differentiation through several suggested mechanisms. These include: inhibiting histone deacetylase, inhibiting topoisomerase, interfering with DNA and RNA synthesis, and disturbing signal transduction (Tsiftsoglou *et al.,* 2003). For instance, induction of promyelocytic HL60 cells to mature into neutrophil-like cells has been shown after 5-7 days culture with DMSO (Collins *et al.,* 1978) or 5 days culture with ATRA (Breitman *et al.,* 1980). In contrast, exposure of HL60 cells to phorbol 12-myristate 13-acetate (PMA) or to sodium butyrate under a mild alkaline condition induces differentiation into monocyte- and eosinophil-like cells, respectively (Fischkoff, 1988; Ahmed *et al.,* 1991). Interestingly, the differentiated HL60 cells have many of the functional characteristics of normal peripheral blood granulocytes, including phagocytosis, complement receptors (such as CR1, the C3b receptor, and CR3), chemotaxis, and the ability to reduce nitroblue tetrazolium; NBT (Collins *et al.,* 1978; Newburger *et al.,* 1979).

One of the recognised myeloid differentiation agents is all-*trans* retinoic acid (ATRA), the acid form of vitamin A. ATRA treatment has been shown to modulate the secretion of certain cytokines as well as the expression of different adhesion molecules, for instance CD38 (Gao *et al.,* 2007). CD38 upregulation was observed in several types of myeloid cells, for instance

human myeloid leukaemic cell lines HL60 and KG-1, as well as in freshly isolated cells from acute promyelocytic (APL) and myeloblastic (AML) leukaemia when exposed *in vitro* to ATRA and *in vivo* during oral treatment with ATRA (Breitman *et al.*, 1981; Drach *et al*, 1993, 1994). It has been observed that this effect is mediated by the activation of nuclear receptors, RAR and RXR, which act as ligand-inducible transcription factors. It has been suggested that ATRA-induced CD38 expression is mediated via a RAR-RXR heterodimer, rather than an RXR-RXR homodimer (Mehta *et al.,* 1997). Indeed, the nuclear receptors, RAR and RXR are encoded by distinct genes and bind to specific ligands and response elements. Each RAR and RXR family of receptors consists of three subtypes, each subtype being encoded by a distinct gene (Pfahl *et al.,* 1994; Sporn *et al.,* 1994). RAR subtypes can bind both ATRA and its isomer, 9-*cis* retinoic acid (9-*cis* RA), whereas RXR subtypes bind only 9-*cis* RA (Heyman *et al.,* 1992). Thus, each may specifically regulate the expression of subsets of retinoid target genes, such as CD38, during ATRA-induced granulocytic differentiation of HL60 cells (Drach *et al.,* 1994). These observations were confirmed by a study by Kishimoto *et al.* (1998) in which the presence of a retinoic acid-response element (RARE), known as a DR5 repeat, was described, in intron 1 of the CD38 gene.

ATRA has been used in clinical therapy for promyelocytic leukaemia (PML) patients with satisfactory results (Warrell *et al.,* 1991). ATRA was either used alone in APL therapy or in a combination regimen of ATRA with cytotoxic chemotherapy (Tallman *et al.,* 2002). Another example includes ATRA/ATO (arsenic trioxide) and anthracycline-based chemotherapy (Sanz *et al.,* 2009). However, the differentiation of APL cells by ATRA shows a side effect known as retinoic acid syndrome (RAS), the most dangerous side-effect of ATRA treatment (Mehta, 2000). RAS is marked by acute respiratory distress and pulmonary oedema (Gruson *et al,* 1998).

Interestingly, an interaction between CD38 and CD31 might be involved in the pathophysiology of this syndrome (Lewandowski *et al.,* 2002). The differentiation of APL cells by ATO has also shown a side effect similar to that found with ATRA (Sanz *et al.,* 2009).

1.12 CD38 and HL60 differentiation

Studies on CD38 expression during ATRA-induced HL60 differentiation are quite varied, as some of them suggest that for ATRA-induced CD38 expression during myeloid leukaemia cells differentiation, this effect is independent of differentiation and is mediated by RAR activation in HL60 cells (Drach *et al.,* 1994). Meanwhile, a further study has demonstrated that the degree of the cellular response to retinoic acid (cell differentiation or loss of viability) depends on the CD38 expression level (Lamkin *et al.,* 2006). Recently, Congleton *et al.* (2011) have confirmed that induction of CD38 expression promotes myeloid maturation, whereas knocking it down has an inhibitory effect on ATRA-induced differentiation, and that effect is mediated through CD38 receptor functions rather than its enzymatic functions. Hence, CD38 either enhanced or blocked cellular differentiation.

It has been shown that granulocyte differentiation inducers in HL60, including dimethylsulfoxide (DMSO), failed to induce CD38 expression, unlike the case with ATRA (Guida *et al.,* 2004). However, not only is CD38 expressed in ATRA-induced HL60 differentiation, but the differentiation of HL60 is also accompanied with expression of CD11b, CD45RO, CD11c, CD54 and CD36, and suppression of CD117 and CD44, as investigated in immunophenotyped studies using a CD antibody microarray (Barber *et al.,* 2008). Finally, in most previous studies on the link between CD38 expression and the differentiation process, one theme remains clear: CD38 expression affects the differentiation status and might cause this abnormal differentiation.

Therefore, by studying this process, an understanding of extracellular/intracellular CD38 levels is gained, and even how its role in regulating other intracellular factors might affect the differentiation process against a proliferation.

1.13 The strengths of the HL60 model

The HL60 cell line is a well-characterized model that is possible to differentiate into cells morphologically similar to normal neutrophils, monocytes, macrophages, and eosinophils (Breitman *et al.*, 1980; Fischkoff *et al.*, 1984). However, the promyelocytes would normally differentiate terminally into only granulocytes. Importantly, the HL60 cell line provides a continuous source of human cells expressing CD38 (neutrophil-like cells), after being stimulated with ATRA. These cells are grown in culture, and therefore a large number of cells are available for experimentation. This would be of high importance for assays that require large numbers of cells.

Additionally, it is well known that peripheral blood neutrophils are short-lived cells and once removed from the blood their viability is limited to several hours (Mauer *et al.*, 1960). Therefore, a long-lived cell line such as HL60 cells has been found to overcome such a shortcoming. These cells are stimulated to neutrophil-like cells in a manner similar to blood neutrophils, and stay alive for several days, which is especially important for researchers who are only interested in neutrophil studies. Finally, the HL60 cell line is a model of acute myelocytic leukaemia (APL), so use of these cells to study terminal differentiation allows one to discover new factors that might affect this maturation. Additionally, they might be used as a potential therapy for differentiation diseases like APL.

1.14 Objectives of the study

As a receptor and a multifunction enzyme, CD38 plays important roles in the pathophysiology of several human diseases. Several human studies suggest a potential key role for CD38 receptor functions in the development of leukemia (for instance CLL). However, the effect of the enzymatic function of CD38 on leukemia development needs to be established to find a relevant therapy for $CD38^+$ leukemia patients. In the current study it was hypothesized that inducing CD38 expression or its enzymatic activity might significantly degrade intracellular NAD levels and hence have effects on several NAD dependent processes in cells. To test this hypothesis, HL60 cells were used as a model for human leukaemia that is able to express CD38 when treated with ATRA. The hypothesis that CD38 might control NAD levels and its related metabolic reactions might be one of a number of possible mechanisms that are responsible for poor prognosis and other consequences in $CD38^+$ leukemia patients. The specific objectives were:

a) to develop methods for determination of NAD levels and CD38 activity;
b) to determine whether CD38 levels are differentially elevated, both intracellularly and extracellularly, during the time course of HL60 differentiation induced by ATRA, by measuring cyclase activity of CD38 (cyclase assay), CD38 protein expression by flowcytometry and Western blotting, in addition to measuring CD38 gene expression by qPCR;
c) to determine the intracellular NAD(H) levels during a time course of HL60 differentiation, using a cycling assay;
d) to develop a novel inhibitor of CD38 activity, in order to test our hypothesis;

e) to determine the physiological consequences of the effect of low NAD levels in the cells by measuring the NAD/NADH ratio, lactate levels, total glutathione, the lipid peroxidation state, DNA damage and cell apoptosis.; and

f) to investigate the possibility of regulating CD38 gene expression under multiple conditions, such as using a CD38 inhibitor (kuromanin), NAD biosynthesis inhibitor (FK866), increasing NAD levels, and using several hypoxia conditions.

CHAPTER 2

GENERAL MATERIALS & METHODS

2. Materials and Methods

2.1 Materials

The HL60 cell line was a kind gift from Anwar Al-mzaiel (University of Plymouth, UK), and the human B-lymphocyte-derived cell line (RAJI Cells) was obtained from ECCAC (European collection of cell culture). RPMI-1640, Fetal Calf Serum (FCS), L-glutamine, penicillin, streptomycin, and trypan blue were all from Lonza, Slough, UK. NGD; kuromanin and all-trans-retinoic acid (ATRA) were from Sigma-Aldrich Ltd. (Poole, UK); and PBS and NAD were from Melford Laboratories (Ipswich, UK). Antibodies for Western blotting, anti-human CD38 mouse monoclonal antibody was from BD Bioscience (Oxford, UK) and mouse monoclonal (10H) to PADPR was from Abcam (Cambridge, UK). M-MLV reverse transcriptase, dNTPs, random nonamers, SYBR Green, and other PCR reagents were purchased from Sigma-Aldrich Ltd. (Poole, UK).

2.2 Culture of HL60 and RAJI cells

The cells were maintained in suspension in Roswell Park Memorial Institute (RPMI-1640) medium supplemented with 10% heat-inactivated fetal calf serum, 100 U/ml penicillin and 100 µg/ml streptomycin, 2 mM L-glutamine, and kept at 37 °C in a 5% CO_2 humidified incubator. Cultures were passaged twice weekly by dilution in fresh medium to a density of 0.3×10^6 cells/ml in both 25 and 75 cm^2 flasks.

*2.3 HL60 and all-*trans *retinoic acid (cell differentiation)*

To induce HL60 differentiation with ATRA (Breitman *et al.*,1980), the cells (2.5×10^5 cells ml^{-1}) were incubated with 1 µM ATRA at 37 °C in a humidified atmosphere of 5% CO_2 for up to 5 days (Fig. 2.1). The cells were then washed twice in RPMI-1640, centrifuged at 200 × *g* for 5 min, and subsequently counted and assayed for further analysis. ATRA stock solution was dissolved in pure ethanol (99% v/v) at a concentration of 10 mM and diluted into the growth media to a final concentration of 1 µM ATRA; the final ethanol concentration in cultures was 0.01%. HL60 cells were also treated with ethanol (0.01%) as a control.

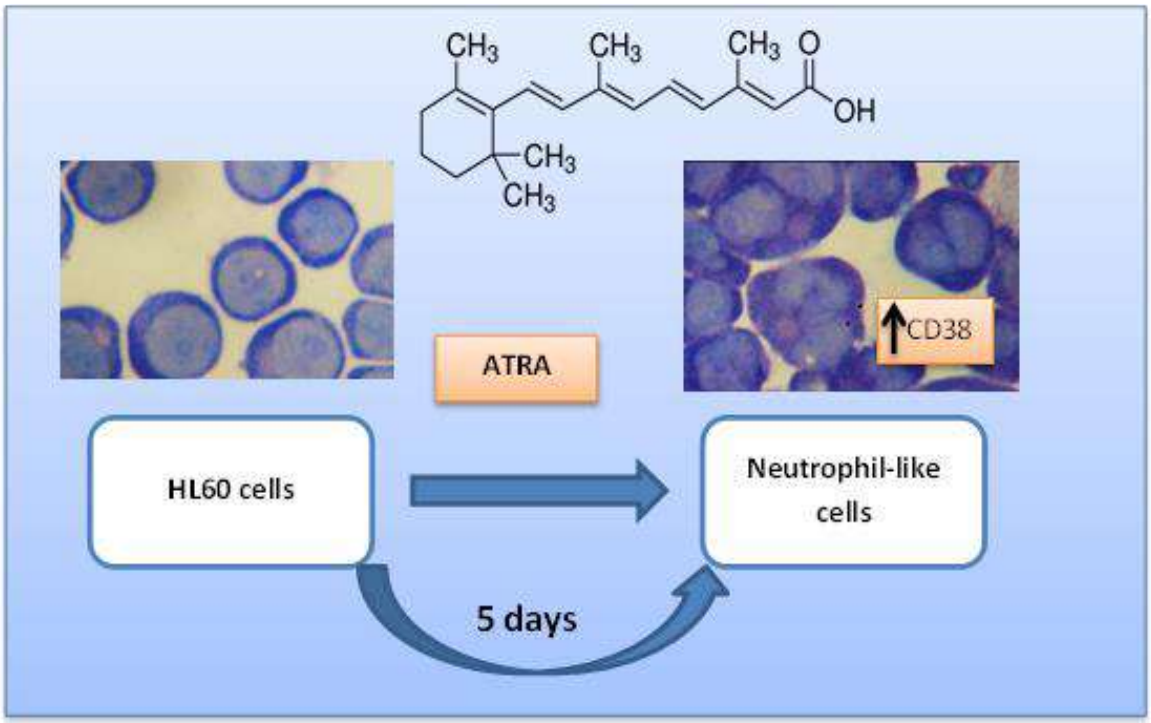

Figure 2.1 Diagram illustrating HL60 differentiation by ATRA over 5 days.

2.4 NBT differentiation assay

Differentiation of HL60 cells was assessed using the nitroblue tetrazolium (NBT) reduction test. Briefly, 100 µl of 1×10^6 cells ml^{-1} in RPMI media were incubated in 96 well plates with 100 µl of 2 mg/ml (0.2% w/v) NBT and 100 µl (200 ng/ml) of freshly prepared phorbol myristate acetate (PMA) in RPMI. After 30-60 min incubation at 37 °C in 5% CO_2 a humidified incubator, cells then were dissolved in 100 µl DMSO to solubilise the reduced NBT (formazan product). The absorbance of the solution was measured at 590 nm on a plate reader (VersaMax, Molecular Devices, Sunny Vale, CA).

2.5 Assessment of viability

A viability test was used to determine the number of viable cells present in cell suspensions; it was carried out on all cell samples before they were assayed in each experiment. This assay is based on the principle that live cells possess intact cell membranes that exclude the dye, trypan blue, whereas dead cells take up the dye.

In this test, cell suspension (10 µl) was mixed with 90 µl of 0.1% trypan blue, and then (after 5 min incubation) 10 µl from the mix (cells with trypan blue) were visually examined to determine whether cells had taken up or excluded the dye. In this assay, viable cells have clear cytoplasm whereas nonviable cells have a blue cytoplasm.

2.6 Cell proliferation assay (MTT)

To carry out the MTT assay, 10 µl of 5 mg ml^{-1} 3-(4,5-dimethylthiazole-2-yl)-2,5-diphenyl tetrazolium bromide (MTT) was added to 100 µl of cell suspension at a density of 1×10^6 cells

ml^{-1} in PBS (137 mM NaCl, 2.7 mM KCl and 10 mM phosphate, pH 7.4) in 96 well plates. The plate was incubated in a humidified incubator for 2-3 h at 37 °C to allow reduction of MTT. The reduced MTT was solubilized by the addition of 100 µl DMSO to each well and each sample was pipetted several times to aid dissolution. Plates were read in a plate reader (VersaMax, Molecular Devices, Sunny Vale, CA) set to 540 nm.

2.7 mRNA isolation and Quantitative Real-Time PCR

Levels of mRNA for CD38, GAPDH, CD157, IDO, NMNAT and NAMPT were determined in ATRA-treated and untreated HL60 cells during the time course of differentiation using quantitative real-time PCR. After cell incubation, total RNA was isolated using a commercially available GenEluteTM mammalian total RNA miniprep kit (Sigma, Poole, UK), which utilizes a column based technique to isolate and purify RNA. An On-column DNase-I treatment step was used to remove genomic DNA. RNA quantity (A_{260}) and purity (A_{260}:A_{280}) was measured using a Nandrop spectrophotometer (ND-1000; Labtech, UK). RNA (1 µg) from control and ATRA-treated HL60 cells was reversed transcribed to cDNA using M-MLV reverse transcriptase in thin-walled PCR tubes (Sigma, Poole, UK) using a GeneAmp PCR System 9700 instrument. RNA was denatured at 70 °C for 10 min in the presence of dNTPs (dATP, dCTP, dGTP, TTP; 0.5 mM) and random nonamers (1 µM); following the Sigma reverse transcription protocol.

Reaction mixes were cooled on ice for 5 min and then 1 unit of MMLV-reverse transcriptase was added to each. Reaction mixes were then incubated at room temperature for 10 min, 37 °C for 50 min and 94 °C for 5 min. cDNA samples were stored at 4 °C until use. Primer sequences were designed using the NCBI website and according to the mRNA sequence of each gene published

in the same website using primer Blast software. Primers (Table 1) were purchased from Eurofins MWG Operon (Germany), and all primers produced 100-105 bp products.

Quantitative RT-PCR was performed using a 96 well plate using the StepOne plus sequence detection system (Applied Biosystems, UK) and using the DNA-binding dye SYBR green for detection of PCR products. GAPDH was used as a housekeeping gene to normalise mRNA levels. cDNA was amplified by adding 2 µl to a final reaction volume of 25 µl containing SYBR green, 0.05 U/µl Taq polymerase, 300 nM reference dye and 0.2 µM of the specific primers. Reactions were performed under the following conditions: 94 °C for 2 min followed by 40 cycles of 94 °C for 30 s, 60 °C for 30 s and 72 °C for 30 s. The fluorescence obtained in the reaction was normalized using the reference dye included in the master mix. Results of the levels of CD38, GAPDH, CD157, IDO, NMNAT and NAMPT expression were indicated by the number of cycles required to achieve the threshold level of amplification. The C_t (cycle at threshold) value from control HL60 was compared with that of ATRA-treated cells using the $\Delta\Delta C_t$ methodology to determine the relative target quantity in samples (Livak and Schmittgen, 2001).

Genes	Primers	Size	Product (bp)
GAPDH	For:CCCACTCCTCCACCTTTGAC	20	100
	Rev:CTGTTGCTGTAGCCAAATTCGT	22	
CD38	For: GCACCACCAAGCGCTTTC	18	100
	Rev:TCCCATACACTTTGGCAGTCTACA	24	
CD157	For: GGGAAGGCAGCATGAAAGTC	20	105
	Rev: GGTCCACGCACTGTAAGAGCTT	22	
IDO	For: GCCTGCGGGAAGCTTATG	18	100
	Rev: TGGCTTGCAGGAATCAGGAT	20	
NMNAT	For: TCATTCAATCCCATCACCAACA	22	105
	Rev: AGGAGAGATGATGCCTTTGACAA	23	
NAMPT	For: TCCGGCCCGAGATGAAT	17	105
	Rev: TGCTTGTGTTGGGTGGATATTG	22	

Table 2.1 Primers used for qPCR experiments, the size and product was shown for each primer.

2.8 Assessment of CD38 expression during HL60 differentiation by western blotting

2.8.1 Plasma membrane and whole cell lysate preparation

75-100 µl pre-cooled lysis buffer (consisting of; 1% Nonidet (NP-40), 150 mM sodium chloride and 50 mM Tris HCl (pH 8.0) with freshly added a protease inhibitor (AEBSF 104 mM, Aprotinin 80 µM, Bestatin 4 mM, E-64 1.4 mM, Leupeptin 2 mM, Pepstatin A 1.5 mM)), were added to the cell pellet (2.5×10^6 cells ml^{-1}) with constant agitation for 20 min at 4º C. Cell lysate was centrifuged for 30 min at 6000 × g, 4º C. The supernatant was harvested in a fresh tube and stored at -20º C for further assays, and the pellet was discarded.

2.8.2 Preparation of Nuclear Extract

Cells nuclear extracts were prepared as described by Whiteside *et al.,* (1992). Cells were harvested in ice-cold PBS by centrifugation (6000 × g for 30 s) and washed once with ice-cold PBS. Cell pellets were then lysed in 150 µl hypotonic lysis buffer (HLB; consists of 10 mM HEPES, 1.5 mM $MgCl_2$, 10 mM KCl, 0.125% NP-40 with freshly added protease inhibitor and 1 mM DTT, pH 7.9). After incubation on ice for 5 min, lysates were centrifuged at 6000 × *g* for 1 minute, 4 °C. Cleared lysates (supernatant) were then moved to fresh tubes, frozen and stored at -20 °C for further estimation of cytosolic protein concentration.

The nuclei pellets were washed in HLB to remove contaminating cytosolic proteins. After washing the pellets, they were resuspended in 100 µl of hypertonic extraction buffer (HEB; consisting of 5 mM HEPES, 1 mM $MgCl_2$, 0.5 M NaCl, 0.2 mM EDTA and 25% glycerol with freshly added protease inhibitor cocktail (100 µl per 1 ml of lysis buffer; P8340, Sigma, Poole, UK) and 1 mM DTT, pH 7.0) for 1 h at 4 °C under agitation. After centrifugation (6000 × *g* for

10 min at 4 °C), supernatants containing the nuclear protein were moved to fresh tubes and stored at -70 °C.

2.8.3 Determination of protein concentration

Protein concentrations were assessed according to a simple protocol described by Bradford (1976). In this assay, 200 µl Bradford reagent was added to 50 µl of each sample and standard solutions of bovine serum albumin in 96 well plates. After 5 min incubation the absorbance was read at 595 nm using a plate reader. As blank, water was mixed with the Bradford reagent

The reference standard for the protein under test was bovine serum albumin (BSA), and concentrations between 0-20 µg protein ml^{-1} were used to generate a standard curve for each run of the assay. The concentration of protein in each sample was then interpolated from the standard curve.

2.8.4 Western blot assessment of protein expression

Total protein samples (20 µl containing 50 µg or 100 µg) were mixed with 5 µl of 5× loading buffer (60 mM Tris-chloride, pH 6.8, containing 2% (v/v) SDS, 10% (v/v) glycerol and 0.1% (v/v) bromophenol blue), and subsequently denatured by incubation for 5 min at 100 °C under reducing conditions with freshly added 5% (v/v) mercaptoethanol.

Equal amounts of protein were electrophoresed on 12% sodium dodecyl sulphate-polyacrylamide gel electrophoresis (SDS-PAGE) gels using standard conditions. The gel was run in 1 × SDS running buffer (192 mM glycine, 25 mM Tris base and 0.1% w/v SDS, pH 8.3) for 45-50 min. The voltage was set to 200. After electrophoresis, the protein-containing gel was sandwiched

between buffer-soaked filter papers. Polyvinylidene fluoride (PVDF) membranes were used and were placed immediately next to the gel. The sandwich was placed in the blotting tank full of 1× pre-cooled blotting buffer (192 mM glycine, 25 mM Tris base and 20% methanol) with the gel towards the anode, and the blot was run at 100 V for 36 min. Two sets of molecular weight markers were used to calibrate the gels as well as to assess transfer efficiency; prestained markers (10 kDa to 190 kDa; from Bioline Reagents Ltd., London, UK) and biotinylated (unstained) protein ladder (9 kDa to 200 kDa; from New England Biolabs, Hitchin, UK).

When blotting was complete, the membrane was blocked at room temperature by shaking in Tris-buffered saline-0.05% Tween 20 (TBS-T) solution containing 5% skimmed milk (w/v) for 1 h. The proteins were then (after blocking) probed overnight at 4 °C with the primary antibody (CD38 or PAR antibody) at a dilution 1:500 in 2.5% blocking buffer. After the incubation with the primary antibody, the membranes were washed 3 times for 5 min in TBS-T before the 1 h incubation with the HRP-conjugated secondary antibody (goat polyclonal anti-mouse IgG; Abcam Cambridge, UK), which was used with dilution (1:1000) and prepared in 2.5% blocking buffer.

The same washing steps were performed with TTBS before the membrane was soaked briefly for 5 min in the detection reagents. Before images were captured (exposed for a maximum of 10 min) the excess detection reagent was drained off by holding the membrane with forceps and touching the edge against a tissue. The plot, protein side down, was placed onto a fresh piece of Saran Wrap, wrapped up and any air bubbles gently smoothed out with the protein side up. Bands were visualized by electro generated chemiluminescence staining (Amersham

Biosciences, UK). Digital imaging with a charge-coupled device (CCD) camera-based imagery system was used (UVP EC3 Imaging system, Cambridge, UK).

2.9 NAD^+ assays

Multiple enzymatic cycling assays have been used for the determination of NAD^+ levels as follows.

2.9.1 Glucose 6-phosphate dehydrogenase (G6PDH)/diaphorase cycling assay

This assay was used to determine NAD^+ levels fluorimetrically; it consists of two enzymatic reactions. In the first reaction, NAD^+ is reduced to NADH catalysed by glucose 6-phosphate dehydrogenase (G6PDH). This reaction was conducted in the presence of an excess of glucose 6-phosphate. In the second part of reaction NADH is reoxidized to NAD^+, catalyzed by diaphorase. Diaphorase catalyzes the conversion of resazurin into the highly fluorescent resorufin (indicator reaction). Fluorescence was measured with excitation wavelength 530 ± 25 nm and emission wavelength 590 ± 35 nm.

2.9.2 Alcohol dehydrogenase cycling assays

This cycling assay involves a single enzyme catalysed reaction (Fig. 2.2). This assay was previously described by Bernofsky and Swan (1973), Self (1988) and Leonardo *et al.* (1996). In this system NAD^+ is first reduced to NADH catalysed by yeast alcohol dehydrogenase utilizing ethanol as cosubstrate, after which NADH reduces phenazine ethosulfate (PES), regenerating NAD^+ for the next cycle. The PES is then oxidized by passing electrons to a tetrazolium dye ; MTT (Self, 1988). The signal from the NAD is then amplified using an enzyme-cycling system.

The product of the reaction, a formazan dye, is measured spectrophotometrically at 565 nm. However, the method used for NAD determination in this thesis was a slight modification of alcohol dehydrogenase cycling assay described by Leonardo *et al.* (1996).

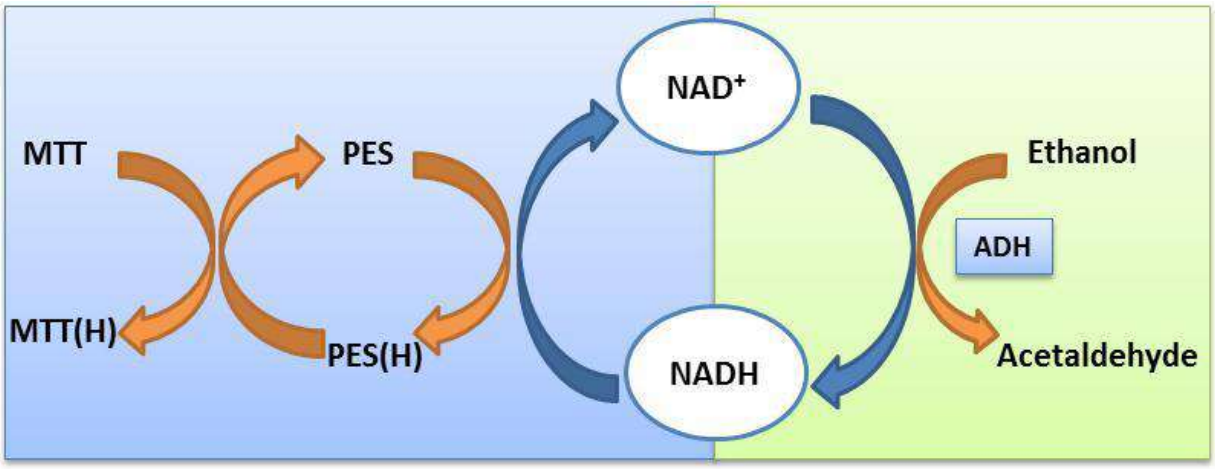

Figure 2.2 The principle of enzymatic cycling reaction for the colorimetric determination of NAD^+.

2.9.2.1 Modified NAD(H) cycling assay

NAD^+ and NADH were extracted (Fig. 2.3) by a modification of the protocol described by Leonardo *et al.* (1996). Cells with and without treatment were placed in microcentrifuge tubes and centrifuged at 7000 × *g* for 1 min. After removal of the supernatant, the pellets were immediately frozen in a dry ice-ethanol bath. For NAD^+ extraction, 250 µl of 0.2 M HCl were added to the frozen pellets or 250 µl of 0.2 M NaOH for NADH extraction. To extract NAD(H), samples were placed in a 100 °C water bath for 10 min and then centrifuged at 4000 × *g* for 5 min to remove cellular debris. NAD^+ or NADH-containing supernatants were transferred to fresh tubes and stored in -20 °C until needed. Extracted NAD^+ or NADH were assayed as described below.

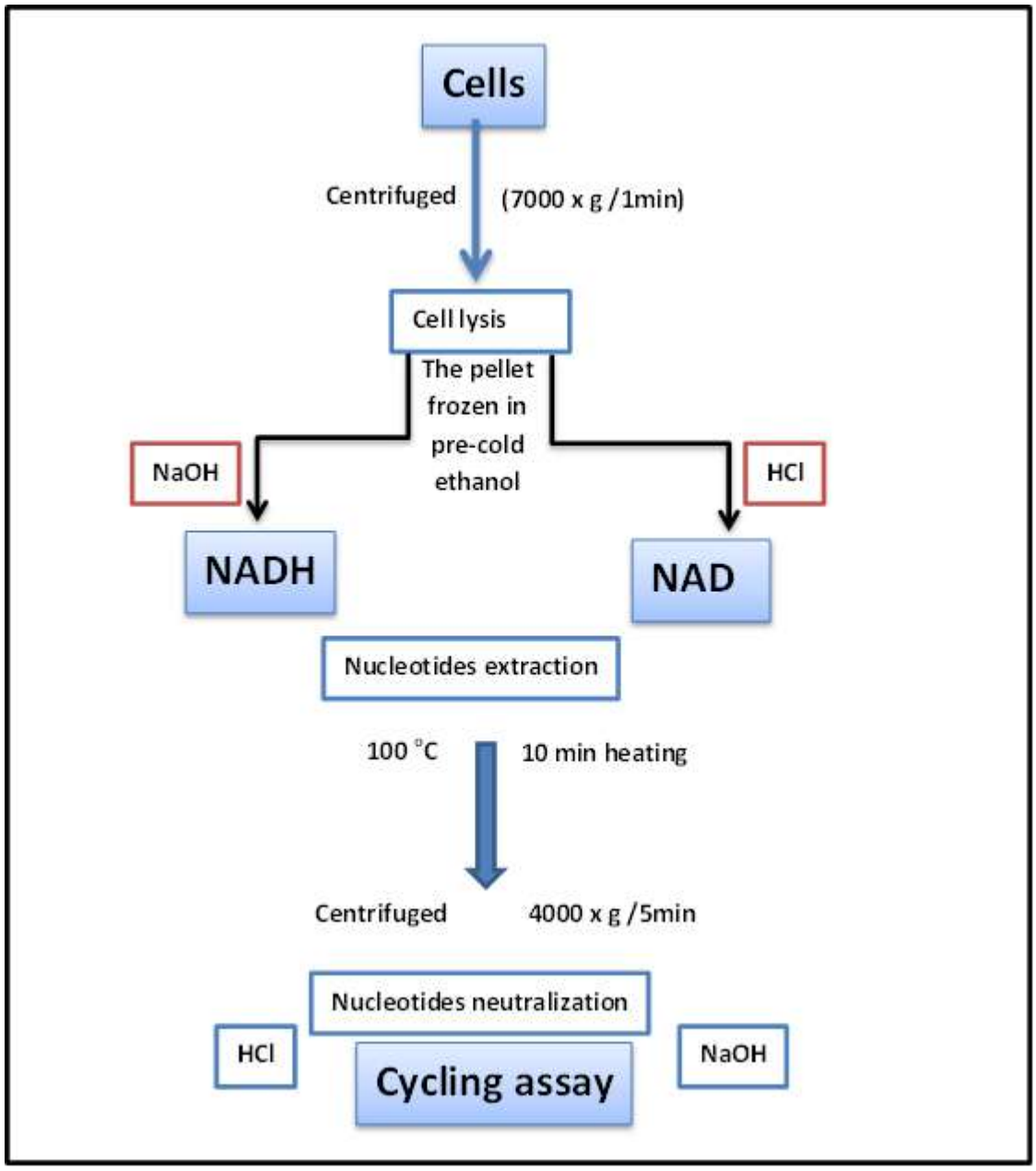

Figure 2.3 A simple diagram for nucleotides extraction and assay illustrating NAD^+ extraction by HCl and NADH extraction by NaOH.

For NAD(H) determination, the NAD^+, NADH recycling assays were performed in triplicate as follows: 49 µl of extracted NAD^+ (or NADH) was added to the following reaction mixture containing 151 µl of 98 mM of sodium bicine, pH 8.0, 24 mM of either NaOH (neutralizing base for NAD^+) or HCl (neutralizing acid for NADH), 1.63 mM of PES, 0.412 mM MTT, 19.6 µl of absolute ethanol, 3.92 mM of EDTA and 5 µl of yeast ADH (400 U/mg in 0.1 M bicine buffer, pH 8.0). The absorbance at 565 nm was recorded in a plate reader (VersaMax, Molecular Devices, Sunny Vale, CA), after 30 min incubation in the dark. NAD^+ and NADH standards from 5 to 60 µM were repeated with each separate experiment, to calibrate the assay (Fig. 2.4 A, B).

The reaction specifically detects NADH and NAD^+, but not NADPH nor $NADP^+$. The enzyme cycling reaction significantly increases the detection sensitivity and specificity. NAD^+ or NADH can be easily quantified by comparing with standards of NAD^+ and NADH. The NAD^+/NADH ratio was calculated by dividing intracellular NAD^+ levels by NADH levels in the same sample after they had been normalized to the cell number.

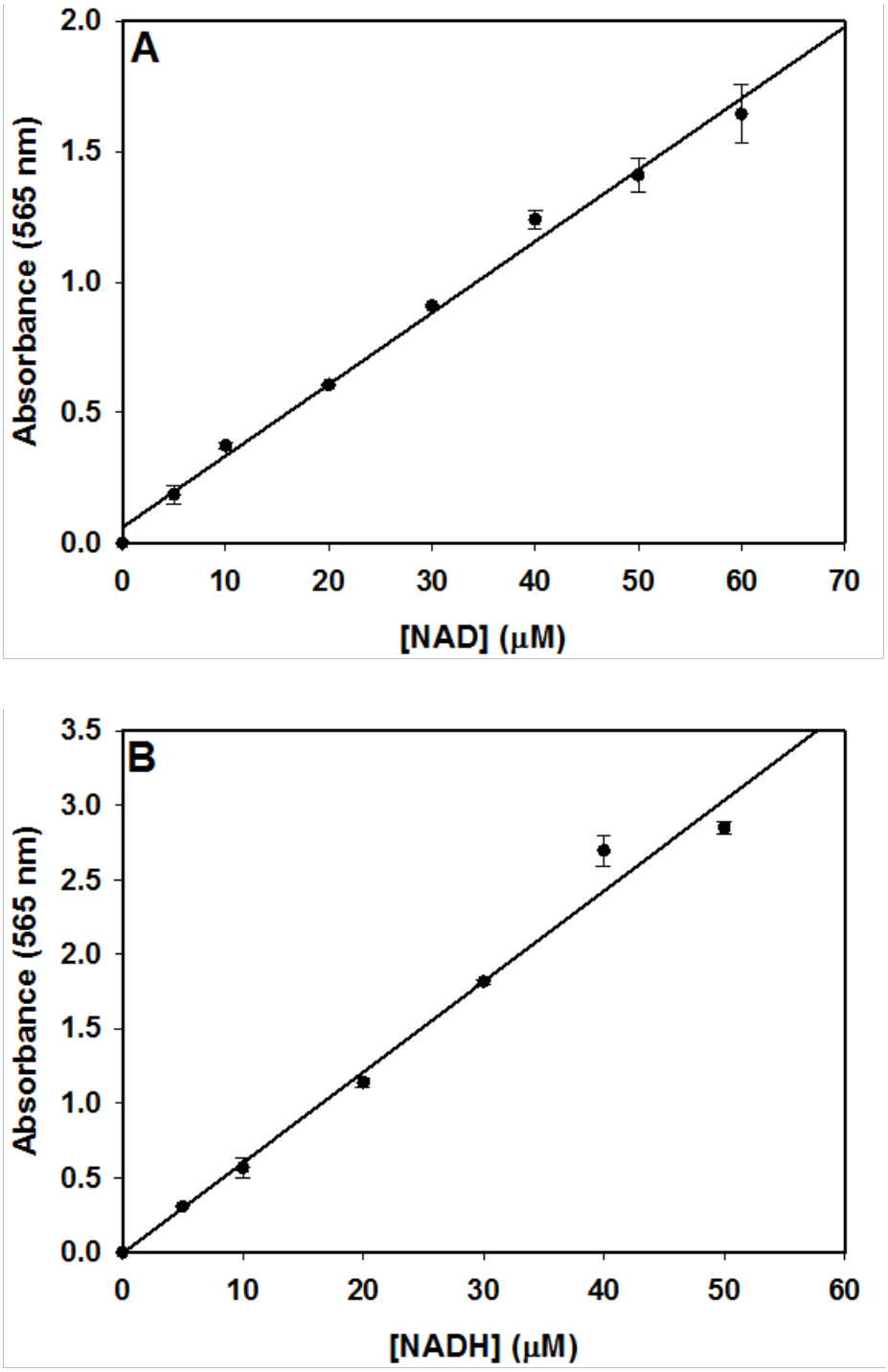

Figure 2. 4 (A) The NAD cycling assay. NAD (5-60 µM) extracted with HCl, the mixture was equilibrated in the dark at 25ºC for up to 30 min (r=0.99). (B) The NAD(H) cycling assay. NADH (5-30 µM) extracted with NaOH, the mixture was equilibrated in the dark at 25ºC for up to 30 min (r=0.99). Change in absorbance is recorded at 565 nm. Data are means ± SEM, n=3.

2.9.2.2 Effect of cell number on the sensitivity of the NAD assay

Intracellular NAD was determined in the HL60 cell line to examine the possibility of an effect of differences in cell number on NAD levels, which might potentially interfere with the results of treatment effects on NAD levels. Thus, different cell numbers were used to assess variations in NAD levels in HL60 cells. As shown in Figure 2.5, there were no apparent differences in NAD levels in HL60 cells observed using different cell numbers. Therefore, in subsequent studies, final cell numbers between 0.24×10^6 ml^{-1} and 0.98×10^6 ml^{-1} were routinely used in the experiments.

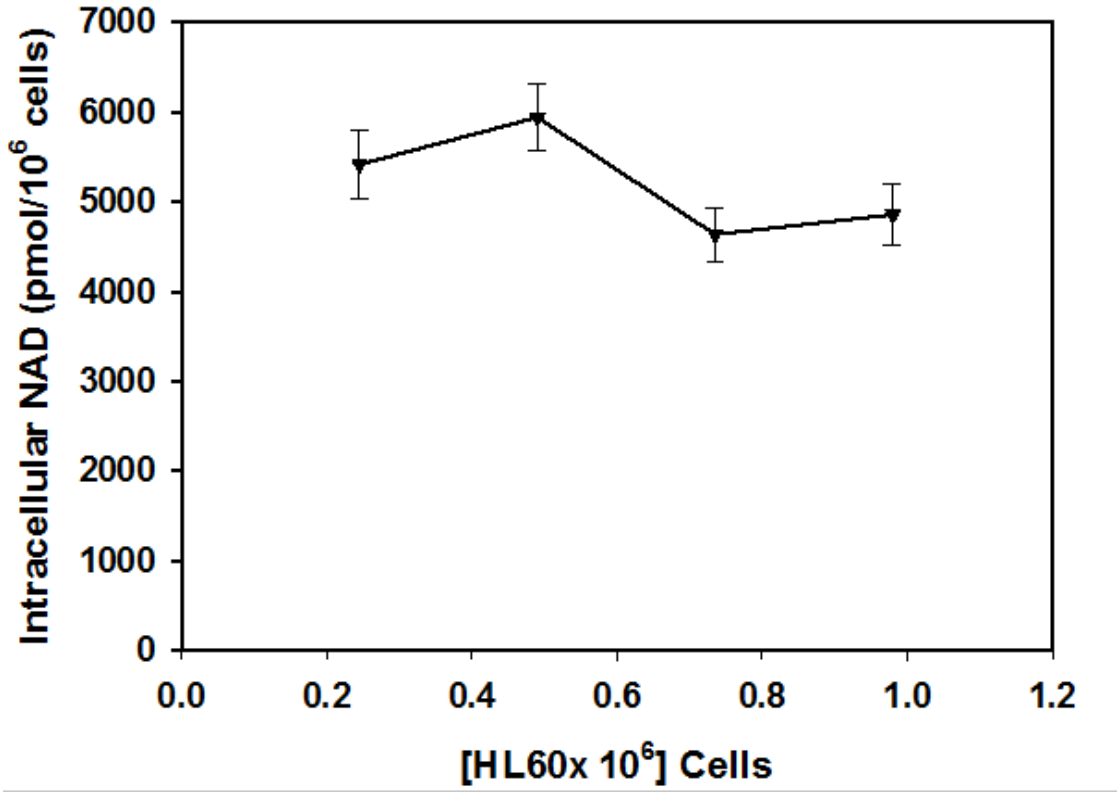

Figure 2. 5 Intracellular NAD levels determined in HL60 cells with cell density (0.24-0.98 × 10^6 cells ml^{-1}) and incubation time 30 min. Data are means ± SEM, n = 3 (7 measurements).

CHAPTER 3

THE EFFECT OF CD38 EXPRESSION ON NAD LEVELS IN HUMAN LEUKEMIA CELLS

3.1 Introduction

CD38 has a dual behaviour, with enzymatic and receptorial functions. As a receptor, CD38 controls signalling pathways involved in the activation, growth and survival of lymphoid and myeloid cells (Mallone *et al.*, 2001). The role of CD38 as a negative prognostic marker in CLL has also been widely confirmed (Matrai, 2005). The CLL published data, in which the levels of CD38 expression correlated inversely with patient outcome have generated much attention. In CLL, CD38 measurements have become more straightforward than those of IgVH mutation and other negative prognostic markers (Damle *et al.*, 1999). While much accumulated data has shown a distinct role of the CD38 receptor functions in the poor prognosis in CLL patients, to this author's knowledge nothing is known about the role of CD38 enzymatic functions in leukemia. To address this issue, HL60 cells, which express CD38 when treated with ATRA, were used as an available model for human leukaemia. Another leukemia cell line was also used in this study; RAJI cells (Burkitt lymphoma) also express the CD38 molecule (Trubiani *et al.*, 2008). Our hypothesis was based on the previous findings of Barbosa *et al.* (2007), who reported that in CD38 knockout (KO) mice, intracellular NAD levels are increased. Furthermore, another study in macrophages has shown that when CD38 is genetically deleted, an increase in intracellular NAD levels occurs (Iqbal and Zaidi, 2006). This might reflect the major role that CD38 has as an endogenous and extracellular regulator of NAD levels. Therefore, the hypothesis of this study was that NAD levels might be depleted in the case of CD38 upregulation. It was also expected that low levels of NAD, an important coenzyme for the network of enzymes involved in vital metabolic pathways in the cell, might have physiological consequences, such as in the case of leukemia patients where the $CD38^{+}$ subset of patients show poor prognosis and short survival.

It is worth mentioning that CD38 receptor functions in CLL have been well documented over many years by different groups (Deaglio *et al.,* 2008; Malavasi *et al.,* 2008). However, the purpose of the current study was to draw attention to the cellular enzymatic function of CD38 in the poor prognosis in leukemia. To do this, a number of approaches were used: HL60 cells were differentiated to neutrophil-like cells using ATRA, and CD38 protein levels, cyclase activity and CD38 mRNA levels were all investigated by different methods; the intracellular NAD levels were evaluated during the differentiation process by using a modified NAD cycling method; the levels of other enzymes that catalyse NAD-consuming reactions such as CD157, PARP, and sirtuins, in addition to the expression of NAD biosynthesis enzymes were all determined during the differentiation. The current study shows for the first time that when CD38 expression is induced by ATRA, intracellular NAD decreases significantly and that this high degree of NAD degradation correlates with CD38 expression.

3.2 Material and methods

3.2.1 Materials

RPMI-1640 medium, fetal calf serum (FCS), L-glutamine, penicillin, streptomycin, trypsin and trypan blue were all purchased from Lonza Ltd. (Slough, UK). NAD was from Melford (Ipswich, UK). NGD, kuromanin, ATRA, M-MLV reverse transcriptase, dNTPs, random nonamers, SYBR® Green and other PCR and western blotting reagents were all purchased from Sigma-Aldrich Ltd. (Poole, UK). FACS antibodies; phycoerythrin (PE)-conjugated anti-CD38 antibody and mouse IgG1 K isotype control (PE) were all from eBioscience Ltd. (Hatfield, UK). The MCF-7 cell line was a kind gift from Niketa Ferguson (University of Plymouth, UK).

3.2.2 Culture of the MCF-7 cell line

The adherent breast cancer cell line, MCF-7, was cultured in RPMI-1640 medium supplemented with 10% fetal bovine serum, 100 U/ml penicillin, 100 µg/ml streptomycin, and 2 mM L-glutamine. The confluent cells were passaged by treating them with 0.05% trypsin-EDTA (Life Technology, UK). The cells were maintained in culture at 37 °C and under a 5% CO_2 atmosphere with cell viability greater than 95% as assessed by trypan blue exclusion.

3.2.3 Measurement of the cyclase activity of CD38

CD38 cyclase activity was assayed by monitoring the conversion of nicotinamide guanine dinucleotide (NGD) to cyclic GDP-ribose (cGDPR), essentially as described previously (Graeff *et al.,* 1994; Genazzani *et al*., in: Putney, 2005). This method was applied to measure the cyclase activity for 1.3 - 2.0 × 10^6 cells ml^{-1} from both whole and lysed cells, and in nuclear extracts (see Sections 2.8.1and 2.8.2). The enzyme assay was started by adding 1.3 - 2.0 × 10^6 cells to a

reaction mixture containing 100 µM NGD and phosphate buffered saline (PBS), pH 7.4, to final volume of 0.75 ml in a UV-cuvette. The production of fluorescent cGDPR was monitored for 5-10 min fluorimetrically with an excitation wavelength of 300 nm and an emission wavelength of 410 nm, using an LS50B luminescence spectrophotometer (Perkin Elmer, UK). The initial rate was expressed as the change in fluorescence intensity per second (ΔF/s).

3.2.4 Detection of surface and intracellular CD38 during HL60 differentiation by fluorescence-activated cell sorter (FACS)

3.2.4.1 Flow cytometry for extracellular staining

Following treatment of HL60 cells (Section 2.3) with ATRA (1 µM), 1.5×10^6 cell ml^{-1} were washed twice with PBS. After this, pellets were resuspended in 100 µl of FACS staining buffer (PBS containing 1% w/v bovine serum albumin) and then incubated for 30 min at 4 °C followed by washing three times by centrifugation at 200 × g for 5 min. The pellets (1.5×10^6 cells) were resuspended in 100 µl FACS staining buffer, and 15 µl aliquots of cell suspension were incubated with either conjugated monoclonal anti-CD38 antibody (HIT2-PE, 0.25 µg/100 µl; 1:20 dilution), or isotype control-PE (0.25 µg/100 µl; 1:20) for 30 min at 4 °C in the dark. After incubation, cells were washed twice with 500 µl of FACS buffer and resuspended in 500 µl PBS. Samples were incubated on ice after mixing and kept in the dark to avoid photo bleaching until they were analysed. The samples were sorted on a BD FACSAria^{TM}II flow cytometer (Becton-Dickinson, USA), and data from 10,000 events were collected and analyzed by the BD FACSDiva version 6.1.3 software.

In each experiment, CD38 antibody conjugated to a fluorochrome (PE) was used to distinguish CD38 positive cells (cells that bind antibody) from CD38 negative cells (cells that did not bind

antibody) or from the isotype control (negative control). CD38 positive cells give much greater fluorescence intensity than CD38 negative or unstained and control cells.

Before analysis, cells were gated and the cell debris was discounted using the forward scatter (FSC) and side scatter (SSC) profiles (Fig. 3.1). Data were analyzed using WinMDI 2.8 software (Joe Trotter, Pharmingen, CA). Mean fluorescence index (mfi) was calculated as: mfi = fluorescence (test) – fluorescence (isotype control)/ fluorescence (isotype control).

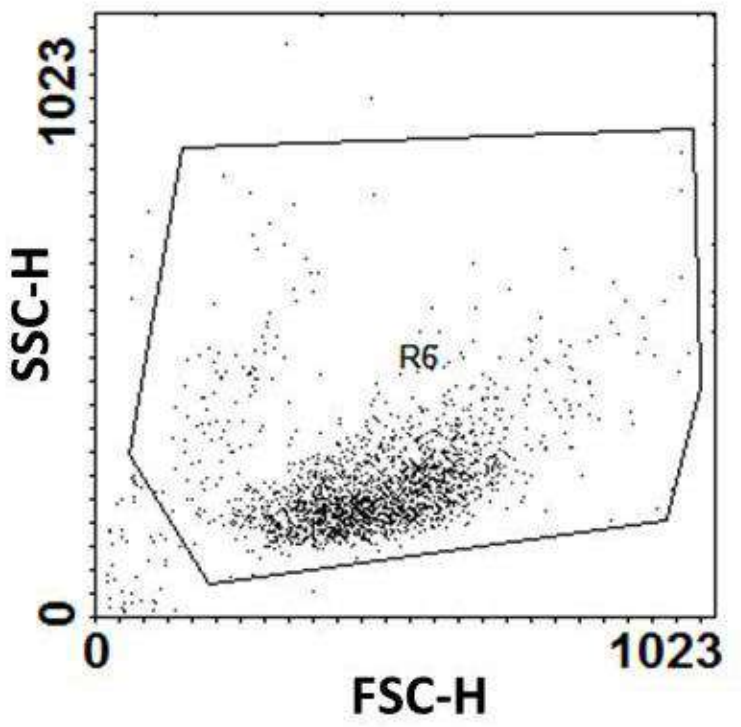

Figure 3.1 cells were gated and cell debris was gated out based on forward scatter (FSC) and side scatter (SSC) profiles as shown in the SSC-FSC dot plot, to analyse data by using WinMDI 2.8 software and to calculate mean fluorescence index.

3.2.4.2 Flow cytometry for intracellular staining

Intracellular staining was performed according to the protocol described by Jacob *et al.* (1991). Cells were harvested, washed twice with PBS at 200 × g for 5 min, and resuspended at approximately 1.5×10^6 cells ml^{-1} of PBS. Cell viability was assessed using trypan blue, and was not less than 99%. Cells were fixed with a 1× fixation buffer containing 4% paraformaldehyde (eBiosciences, UK) for 20 minutes on ice. For permeabilization, cells were washed twice with SAP buffer (PBS containing 2% v/v fetal calf serum and 0.3% w/v saponin). The cells were then stained for 30 min at 4 °C with the anti-human CD38 PE (0.25 µg/100 µl, clone-HIT2) in SAP buffer or with 0.5 µg/100 µl of mouse IgG1 K isotype control PE. After two washes in PBS containing 1% BSA and 0.1% saponin, cells were resuspended in 500 µl PBS and analyzed on a BD FACSAria^{TM}II flow cytormetry (Becton-Dickinson, USA). For each case studied, 10,000 events were processed, and data were analyzed using BD FACSDiva version 6.1.3 software. For negative controls, the primary antibody was omitted.

3.2.5 Co-culture of differentiating cells with MCF-7 cells and measurement of cell proliferation by MTT assay

The cell lines (HL60, RAJI, MCF-7 and differentiating cells) were maintained in culture at 37 °C under a 5% CO_2 atmosphere at cell viability greater than 95%. For the co-culture experiments, the adherent MCF-7 cells (2×10^5 cells/ well) were grown in six-well plates and incubated for 24 h. On the day of the experiment, 1 ml of 3×10^6 HL60 cells (3 days differentiated) were added to plates containing the adherent cells, and cultured for a further 24 h in the same medium and incubated at 37 °C. The supernatant containing the suspended, differentiated cells was collected

and washed with PBS. Cell proliferation was measured using the MTT cell proliferation assay as previously described (Section 2.6).

3.2.6 Determination of intracellular NAD levels in cells treated with CD38, PARP and Sirtuin inhibitors

HL60 cells (2.5×10^5 ml^{-1}) were seeded in a 25 cm^2 culture flasks and incubated with 1 µM ATRA for 3 days in the presence or absence of a PARP inhibitor (4-amino-1,8-naphthalimide, 1-30 µM) or a sirtuin inhibitor (sirtinol). The cells were then harvested and collected by centrifugation, washed and counted. The intracellular NAD was extracted and the level determined by the enzymatic cycling assay as previously described (Section 2.9.2.1).

The intracellular NAD levels was determined in HL60, RAJI or differentiating HL60 cells (2.5×10^5 cells ml^{-1}) treated with 1-30 µM kuromanin, an inhibitor of CD38 cyclase activity, at times up to 6 h. In addition to measuring NAD levels, both cell proliferation (MTT assay) and nitroblue tetrazolium reduction (NBT assay) were also determined in all cell lines after being treated with kuromanin at various concentrations and for different incubation times.

3.2.7 Statistical analysis

Statistical analysis of the data was assessed using Fisher's one way analysis of variance (Statview 5.0.1; Abacus concepts, USA) or Student's t-test as appropriate. Data are expressed as means ± SEM for three separate experiments in triplicate, unless otherwise stated. A difference of $P < 0.05$ was considered statistically significant.

3.3 Results

3.3.1 ATRA-induced HL60 mature granulocyte cell differentiation and inhibited cell proliferation

HL60 cells can terminally differentiate to granulocytic (neutrophil-like) cells after incubation with 1 μM ATRA for 5 days. To confirm this characteristic, the NBT assay was used to evaluate cell differentiation. NBT, a water-soluble dye, is widely used to detect the production of superoxide anions within phagocytic cells, and in the process it is reduced to an insoluble intracellular blue-black formazan. The measurement of superoxide anions is considered to be an accurate method for estimating the ability to generate a respiratory burst (Baehner *et al.*, 1976).

The results showed a significant increase (1-way ANOVA, $p < 0.01$) in the NBT reduction capacity (Fig. 3.2) in HL60 cells treated with ATRA for 5 days (0.51 ± 0.15), compared with treated cells at time zero (0.23 ± 0.068) and undifferentiated HL60 cells (0.14 ± 0.04), indicating mature granulocyte differentiation. These results are consistent with the previous reports that indicated that approximately 70-80% of HL60 cells matured towards granulocyte like cells after day 4 of differentiation (Imaizumi *et al.*, 1987).

Further evidence for cell differentiation induced by ATRA is provided by the morphological change of HL60 cell to neutrophil-like cells as determined by Wright-Giemsa-stained cytospin slide preparations. HL60 cells were successfully differentiated to neutrophil-like cells (Fig. 3.3). HL60 cells cultured without ATRA are predominantly promyelocytes with characteristic cytoplasmic granules, large nuclei. However, after 5 days of incubation with 1 μM ATRA, a high percentage of HL60 cells resembled mature granulocytes (mainly segmented neutrophils). Thus,

the results (Fig. 3.3) confirm that ATRA induces relatively extensive morphological differentiation of HL60 cells.

The proliferation capacity of HL60 cells after incubation with 1 μM ATRA was determined using the MTT assay. As illustrated in Figure 3.4, ATRA inhibited HL60 cell proliferation; reduction of cell vitality, compared with the untreated control (100 ± 0.2%), was evident after 24 h (87.8 ± 11.1%) and was significant on the 3^{rd} (75.2 ± 2.0%) and 5^{th} (74.9 ± 2.0%) days of differentiation. These results indicate that ATRA induces HL60 differentiation, but inhibits the proliferation process.

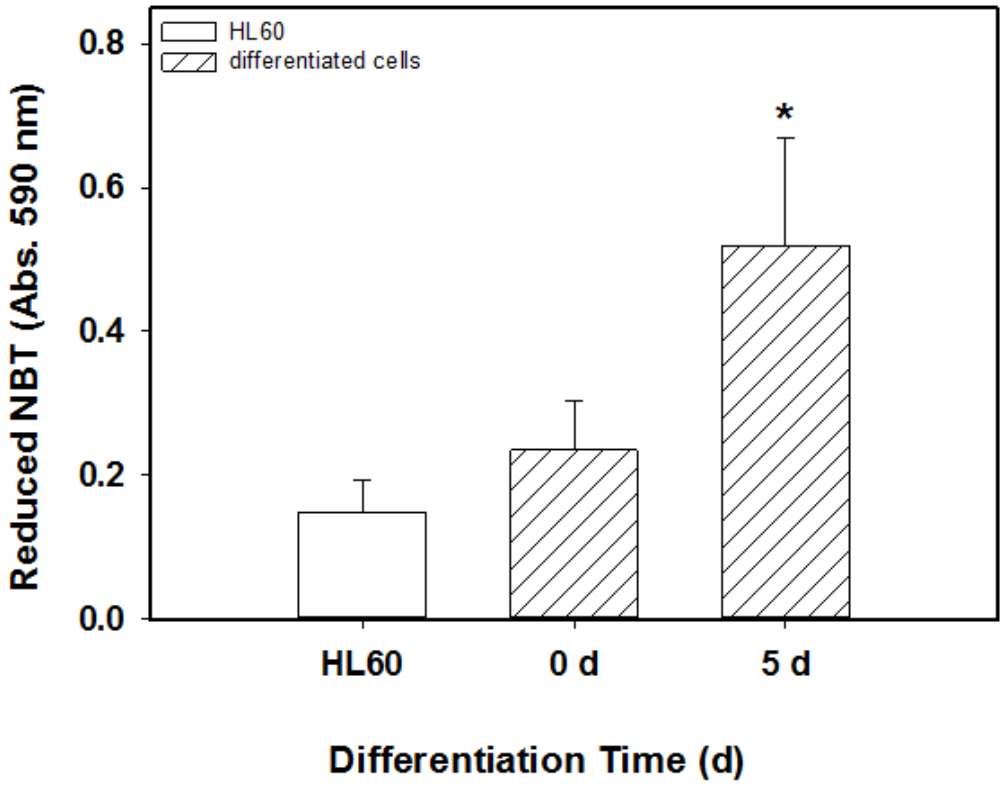

Figure 3.2 The NBT reduction ability of ATRA treated HL60 cells for 5 days comparing to untreated HL60 cells (as control). Data are means ± SEM, n = 3 (3-5 measurements per replicate). * denotes significant difference from the control, $P < 0.05$.

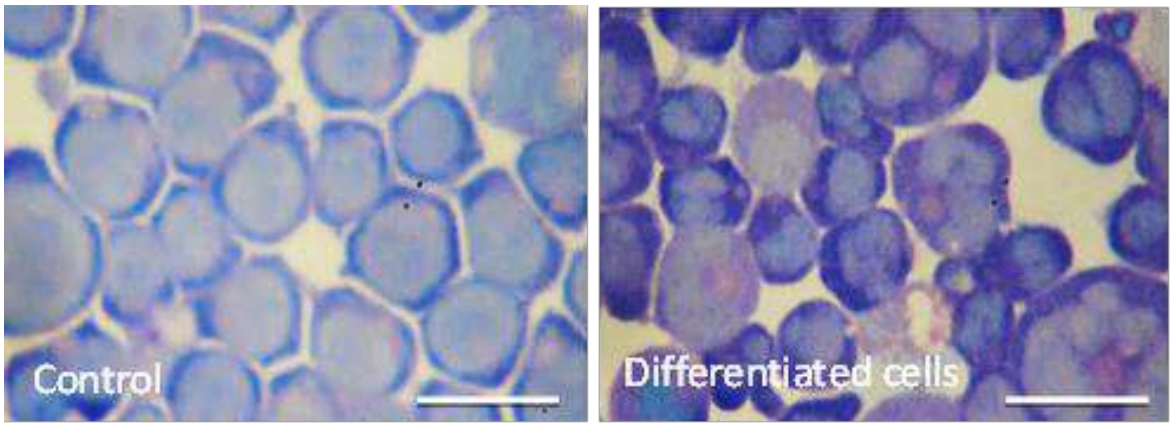

Figure 3.3 Morphology of undifferentiated (control) and differentiated HL60 cells. Differentiation was induced using ATRA for 5 days. Cytospin slide preparations of cell culture suspensions were stained with Wright-Giemsa stain and examined using light microscopy (×1000 magnification). Scale bar: 30 µm.

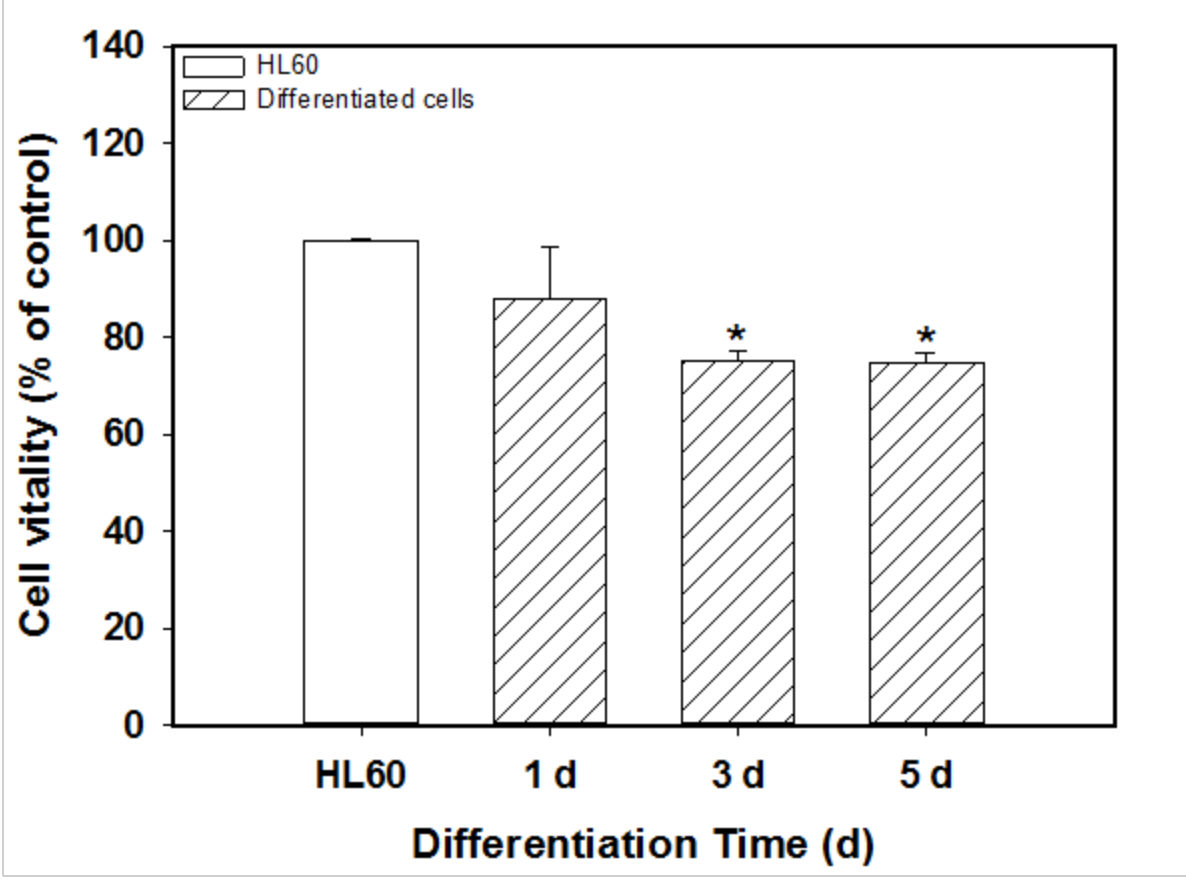

Figure 3.4 Effect of ATRA-induced HL60 differentiation over 5 days on cell vitality (MTT assay) as compared to the untreated control (HL60). Data are means ± SEM, n = 3 (3 measurements per replicate). * denotes significant difference from the control (HL60), $P < 0.05$.

3.3.2 ATRA-induced HL60 differentiation is accompanied by CD38 induction

Treatment of HL60 cells with ATRA was accompanied with upregulation of CD38 expression (Munshi *et al.,* 2002). However, the full mechanisms of CD38 regulation, and the initial induction time for its mRNA expression, cyclase activity and protein levels were not fully investigated during ATRA-induced HL60 differentiation. Therefore, in this Chapter, a time course of CD38 expression during HL60 differentiation was obtained. Also, a comparison of surface and intracellular CD38 protein levels and cyclase activity has been determined, which is first reported in this Chapter.

3.3.2.1 Measuement of CD38 mRNA expression by qPCR

The level of CD38 mRNA expression during cell differentiation was measured using real time PCR coupled with reverse transcription. qPCR analysis demonstrated that CD38 mRNA is expressed early, from 3 h of differentiation, and reached a maximum at 24 h in a time-dependent manner (Figure 3.5); thereafter it remained at a constant level. This finding suggests that ATRA induced transcriptional regulation of the CD38 mRNA, and also supports a previous finding of Uruno and colleagues (2011) that showed an early-phase increase of CD38 mRNA expression at 1.5-6 h after incubation of HL60 cells with ATRA. Furthermore, it was of particular interest to test whether the second member of the NADase/ADP–ribosyl cyclase gene family (Ferrero and Malavasi, 1997), CD157, would also show changes in gene expression during the differentiation. Therefore, CD157 mRNA expression in HL60 after treatment with ATRA was analyzed for up to 120 h. It was found that CD157 showed only a slight but significant increase after 3 and 5 days of differentiation (Fig. 3.5). Hence, CD157 does not appear to be upregulated during HL60

differentiation. These results suggest the possibility of CD38 being the major NAD-consuming enzyme that is expressed during HL60 differentiation, rather than its homologue, CD157.

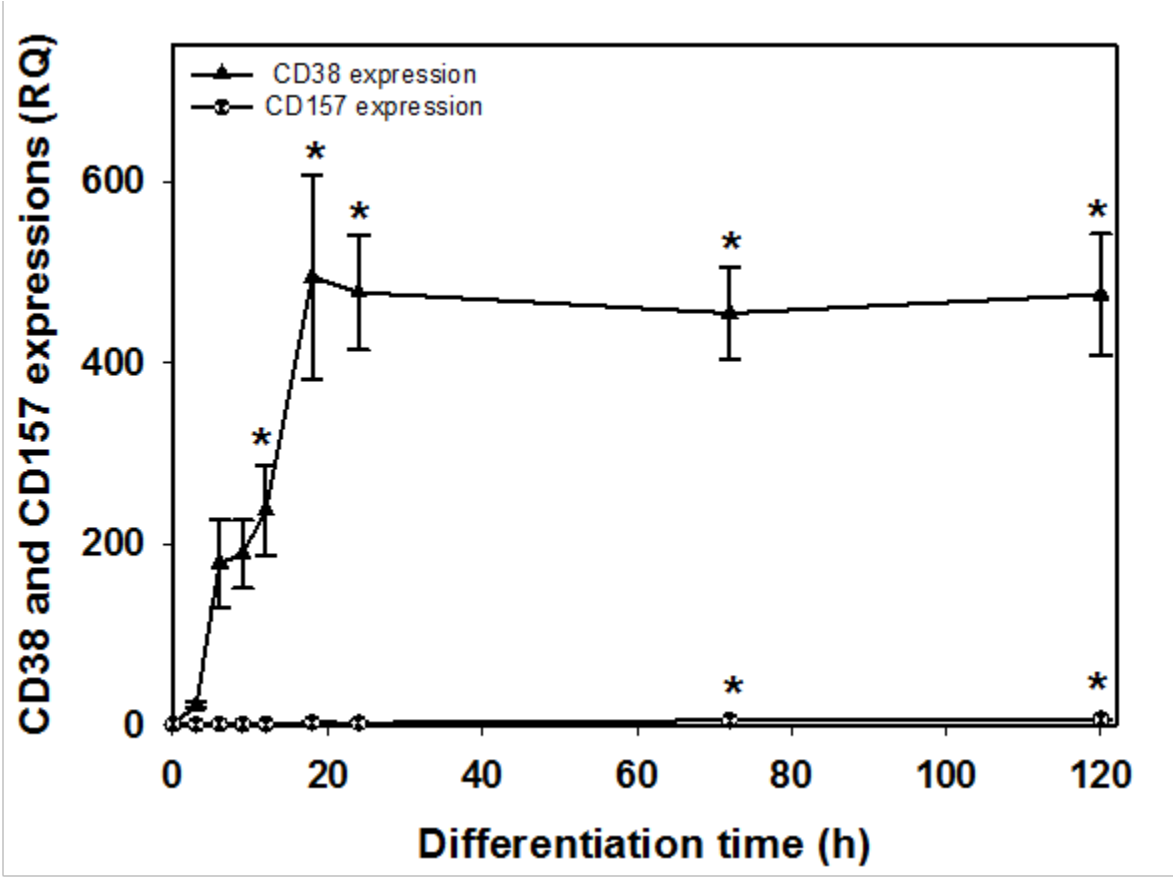

Figure 3.5 Time-course analysis of CD38 mRNA induction in HL60 cells treated with ATRA over 5 days differentiation showing the increase in CD38 expression, but not in CD157 expression comparing to untreated control (HL60). Data are means ± SEM, n = 3 (4-7 measurements per replicate). * denotes a significant difference from the control (HL60), $P < 0.05$.

3.3.2.2 Surface and whole cell lysate CD38 cyclase activity during HL60 differentiation

In light of previous evidence which showed that CD38 mRNA was upregulated during differentiation of HL60 cells, the relationship between gene expression and the active form of the protein was investigated. Therefore, in this study, the intracellular and extracellular cyclase activities of CD38 were explored. CD38 cyclase activity was measured for whole cell lysate (representing intracellular and extracellular cyclase activity), and viable differentiated cells (representing extracellular cyclase activity) as shown in Figure 3.6. There was a significant increase in the CD38 cyclase activity during the first 24 h of differentiation. CD38 activity reached its maximum level in both cases at 6 h during the differentiation, with lower activity seen at 8 - 12 h. However, at 24 h, a twofold increase activity was seen in both the cell lysate (200.0 ± 8.2%) and live cells (260.0 ± 29.7%) compared to the untreated control. It is noteworthy that CD38 cyclase activity in cell lysate was found to be (unexpectedly) lower than that of viable cells. One explanation is that using a lysis buffer might result in lowered enzymatic activity in comparison to that for viable cells. In addition, if it is possible that extracellular nucleotides (in this case NGD) are able to enter cells as previously reported by Billington *et al.* (2008a), then the NGD cyclization activity in viable cells might represent whole CD38 cyclase activity.

As confirmed above, CD38 is active during the early stages of differentiation. Therefore, the extracellular CD38 cyclase activity was further measured on the 1st, 3rd and 5th days both in HL60 cells and in differentiated HL60 cells. A significant increase in cyclase activity was shown (Fig. 3.7) on the third day of differentiation. Thereafter, the activity increased gradually up to day 5, as compared to the appropriate control. Altogether, the data presented in this section

confirm a continuing increase in CD38 activity during the *in vitro* differentiation process. This increase is initiated within 4 hours and progresses over the 5 days of differentiation.

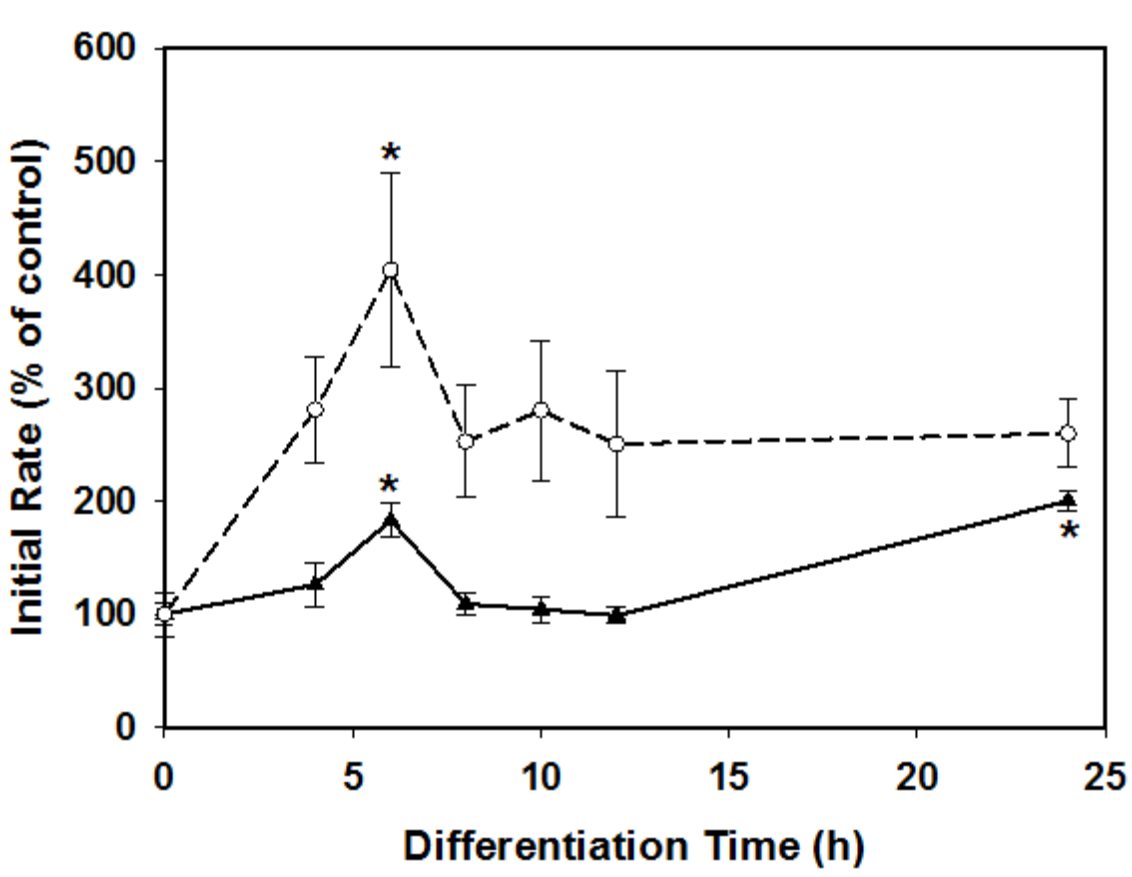

Figure 3.6 Time courses of measuring of CD38 cyclase activity in whole cell lysate (solid line) and in live cells (dashed line) in HL60 cells during differentiation using ATRA over 24 hours comparing to untreated control (100%). Data are means ± SEM, n = 3 (1 measurement per replicate). * denotes significant difference from the untreated control (HL60), $P < 0.05$.

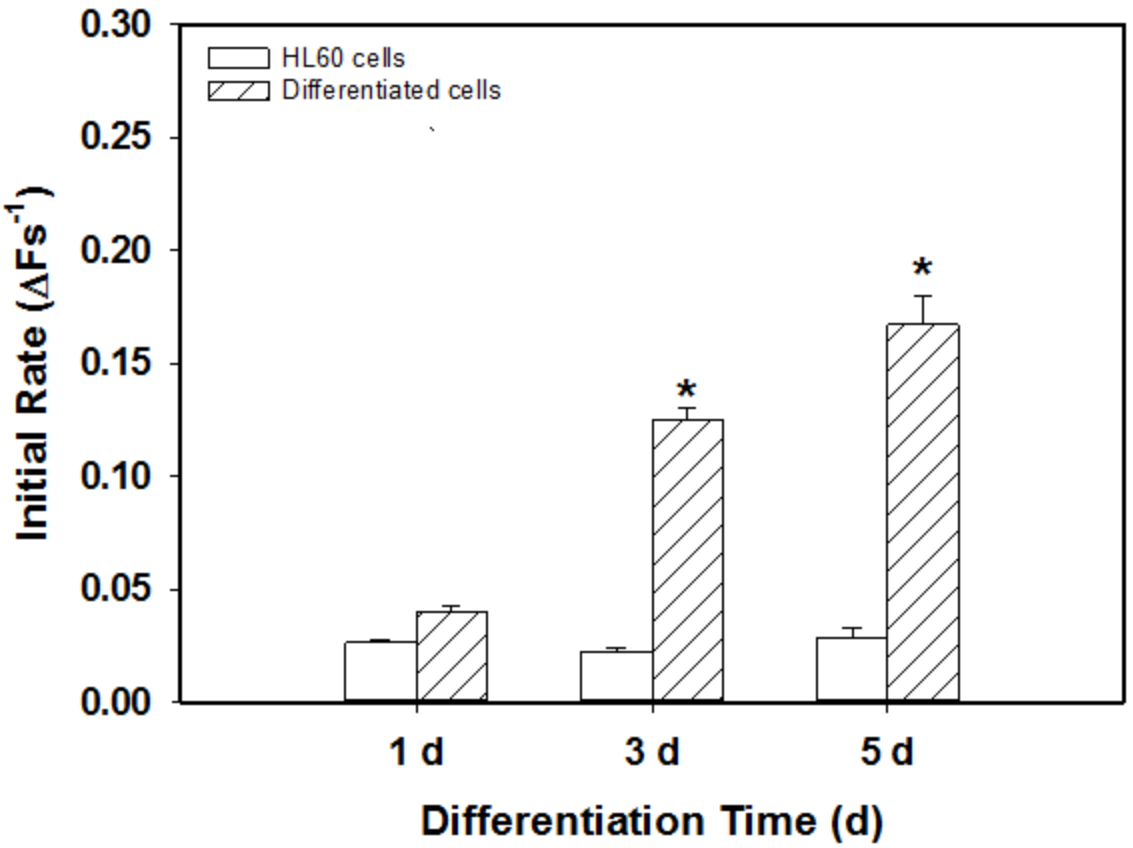

Figure 3.7 Time course of CD38 cyclase activity in HL60 cells treated with ATRA over 5 days comparing to each untreated control (HL60). Data are means ± SEM, n = 3 (3 measurements per replicate). * denotes significant difference from the appropriate control ($P < 0.05$).

3.3.2.3 Analysis of intracellular and extracellular CD38 by FACS

As stated above, a comparatively rapid increase in CD38 expression occurs in response to ATRA in HL60 cells. This can be conveniently measured by using flowcytometry, in addition to the previously measured ADP-ribosyl cyclase activity of CD38, using the NGD technique, or its mRNA expression using qPCR. Thus, CD38 expression was analyzed before and after permeabilization using saponin, to distinguish between surface and internal CD38 expression. Saponin is a detergent which complexes with membrane cholesterol and thereby disrupts the lipid structure (Schroeder *et al.,* 1998).

In the current work, extracellular staining with a CD38-antibody in HL60 cells was determined after treatment with 1 µM ATRA for 10 h, 18 h, 1 day, 3 days and 5 days as shown in Figure 3.8 A; 3.10 with significant differences in the CD38 positive cells being observed compared to the control. These results confirm that CD38 was significantly expressed at 10 h of differentiation, and up to 5 days. Parallel cultures of HL60 cells without the ATRA treatment and RAJI cells served as negative and positive controls, respectively (Figure 3.9).

Cell permeabilization with saponin, was also applied before staining with CD38 antibody in order to allow internal access which facilitates intracellular CD38 investigation in addition to measuring its surface localization. Unexpectedly, our findings (Fig. 3.8B) did not show an increase in the MFI from CD38 positive cells staining with a CD38-antibody compared to the extracellular staining. However, the results (Figure, 3.10) show more internal (total) CD38 expression at 10, 18, and 24 h differentiation compared to the undifferentiated HL60 cells.

The results suggest that, both in CD38 positive cells (RAJI) and during the differentiation, it seems likely that CD38 antibody was probably able to detect surface CD38 epitope better than the internal CD38 even under permeabilization circumstances. It might also suggest that CD38 is mostly expressed on the cell surface with less expressed intracellularly.

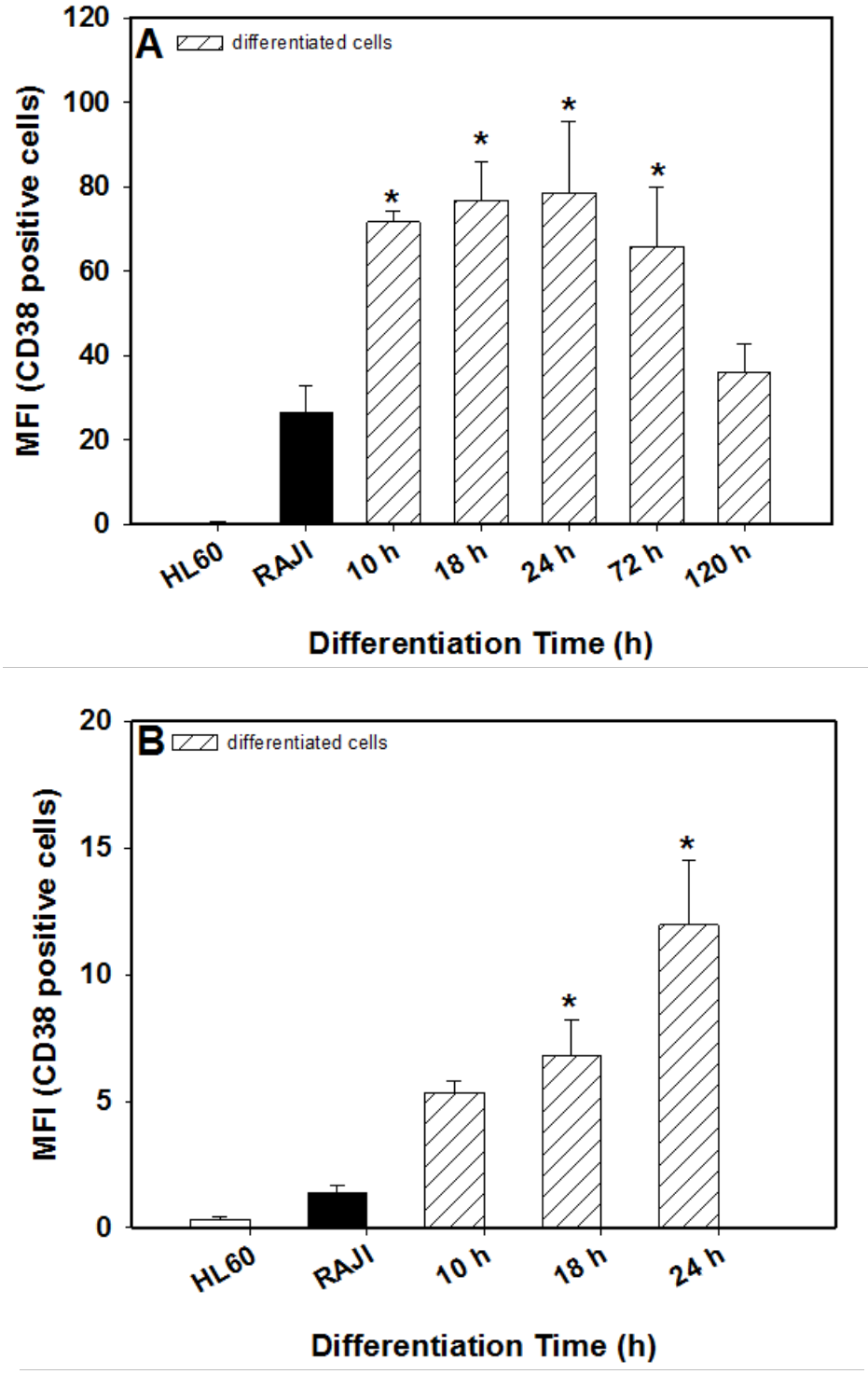

Figure 3.8 Expression of CD38 in HL60 cells treated with ATRA, analyzed by FACS after staining with CD38 antibody (HIT2-PE) and expressed as mean fluorescence index comparing to untreated HL60 cells (as control). (A) Extracellular CD38 expression from 10-120 hours of differentiation and (B) Total CD38 expression at 10, 18, and 24 h of differentiation. Data are means ± SEM, n = 3 (1 measurement per replicate). * denotes significant difference from the control ($P < 0.05$).

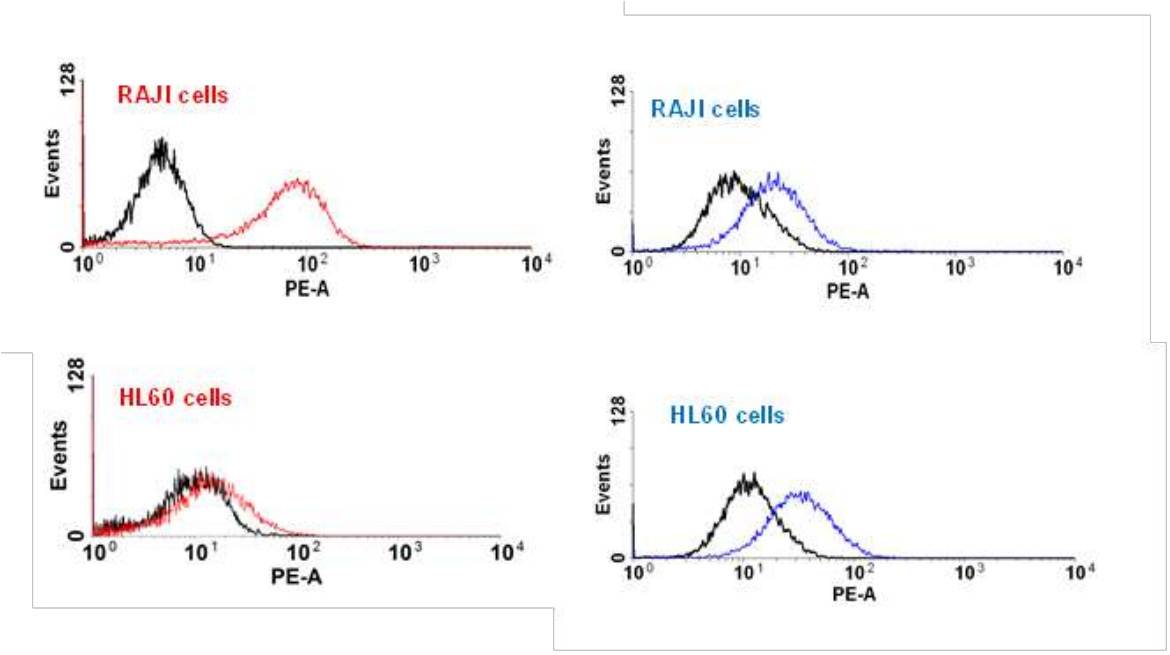

Figure 3.9 Expression of extracellular CD38 (red histograms) versus intracellular CD38 (blue histograms) in RAJI cells (positive control), and undifferentiated HL60 cells (negative control), in comparison with the Isotype control (IgG)-stained cells shown in the black histograms. Cells were stained with PE-labeled anti-CD38 mAb and analyzed by FACS. Data are representative of three independent experiments.

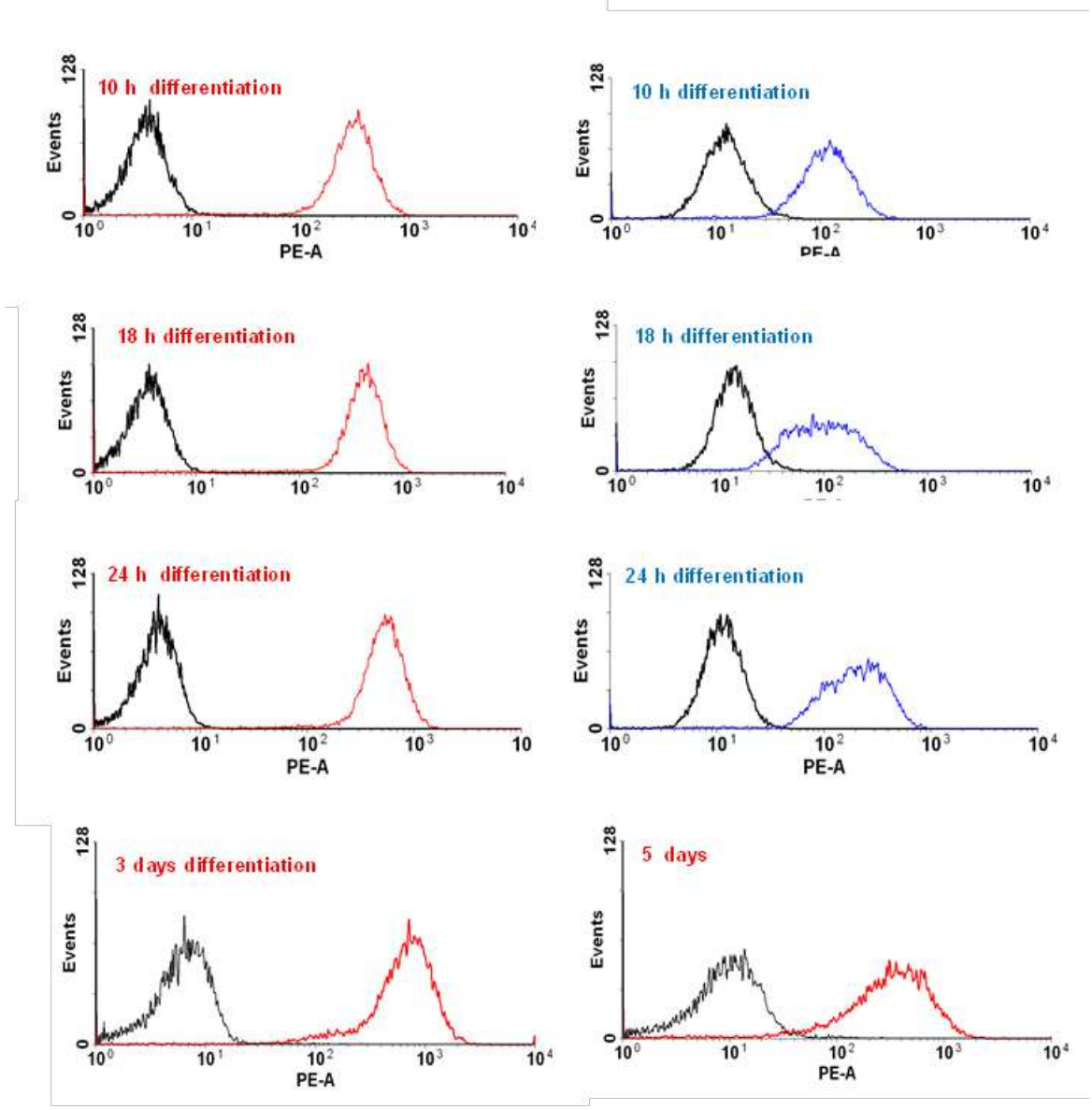

Figure 3.10 Expression of extracellular CD38 (red Histogram) versus intracellular CD38 (blue Histogram) in the time course of ATRA-induced HL60 differentiation, in comparison with the Isotype control (IgG) stained cells shown in the black histograms. Cells were stained with PE-labelled anti-CD38 mAb and analyzed by FACS. Data are representative of three independent experiments.

3.3.2.4 CD38 Western blots for whole cell lysate and nuclear extract

In this part of the work CD38 expression was investigated both in cell lysates from undifferentiated (control) and differentiating HL60 cells by Western blotting, in order to determine the time course of CD38 accumulation after ATRA treatment. An additional aim was to investigate the molecular forms of CD38 that are present in differentiating cells or the control on the plasma membrane and the subcellular location. Thus, Western blotting was used for all cell lysates under reducing and denaturing conditions by using a mouse monoclonal CD38 antibody. The results (Figure 3.11 A, B) showed that both HL60 cell lysate and differentiating HL60 cell lysate at 0-120 h (after ATRA treatment) possess a single 45 kDa monomer of CD38, but with different intensity. In all experiments, the positive control used, RAJI cell lysate always contained a single 45 kDa band form of CD38. A strong 45 kDa band corresponding to CD38 appeared after 10 h of incubation of HL60 cells with ATRA (Figure 3.11 A), with the maximum band intensity clearly shown on day 3 of differentiation. A weak 45 kDa band was observed in control cells as well as at 0, 3 and 6 h of differentiation. In addition, the results (Figure 3.11 A) confirmed that lysate from both differentiating and undifferentiated HL60 cells contain high molecular weight (HMW) forms of CD38 together with 60 kDa and 190 kDa molecular forms. A HMW form, 190 kDa has been observed clearly after 6 h of ATRA incubation with HL60 leukemic cells.

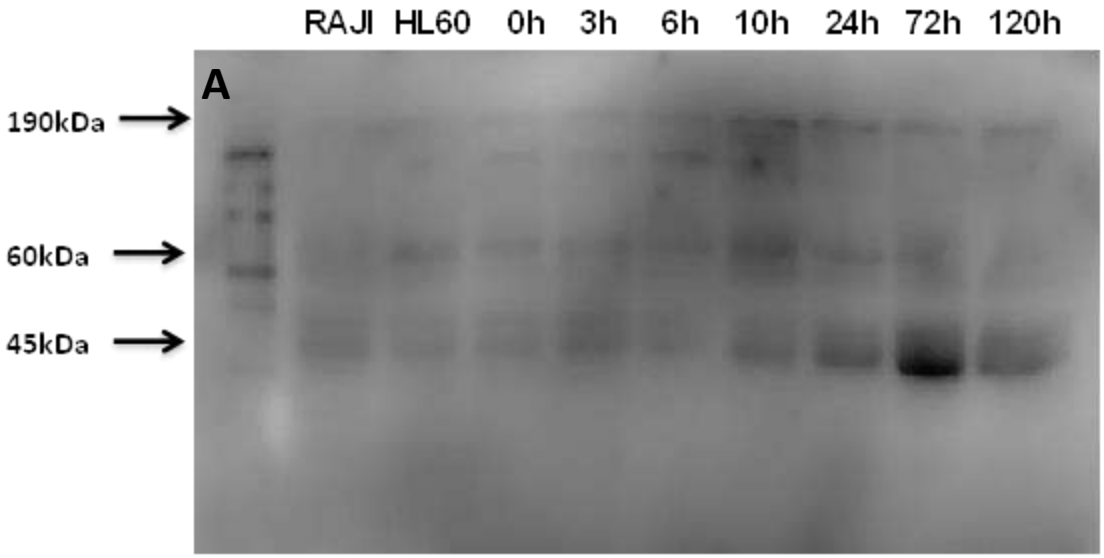

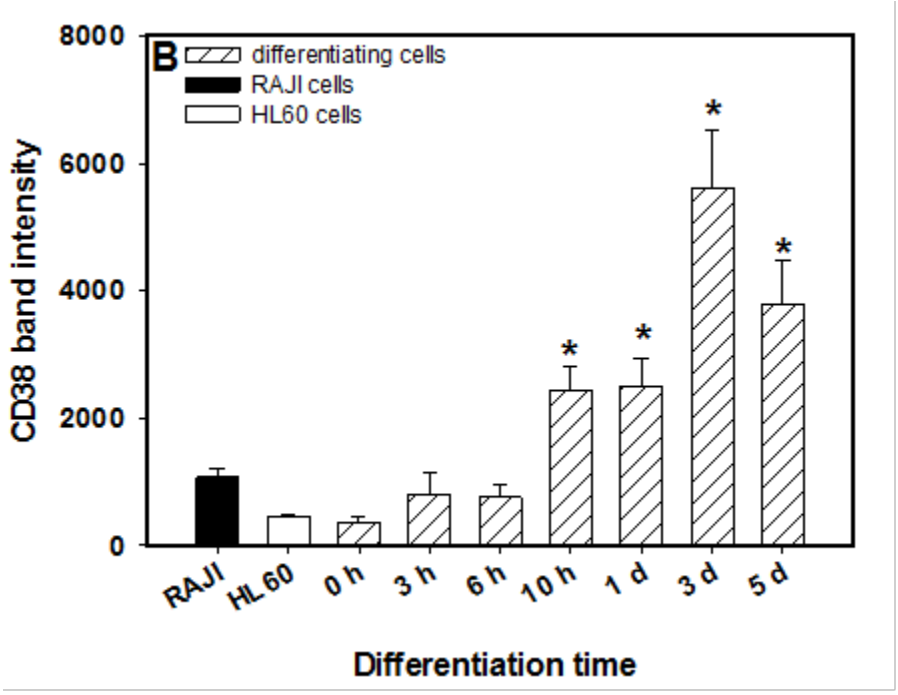

Figure 3.11 Time-course of ATRA treatment of HL60 cells over 5 days showing (A) Western blot of differentiating cells for CD38 showing the 45 kDa band corresponding to membrane CD38 under reducing, denaturing conditions and 12% SDS-PAGE. 100 µg of protein/ well were used each experiment with 1:500 primary antibody dilution (data represent 1 of the 3 separated experiments) (B) The luminescence intensity of CD38 single band 45 kDa. Data are means ± SEM, n = 3 (1 measurements per replicate). * denotes significant difference from the untreated control (HL60), $P < 0.05$.

In summary, the Western blotting results support FACS data, since the extracellular CD38 clearly appeared within 10 h of differentiation compared to undifferentiated HL60 cells. Therefore, as CD38 was expressed on the plasma membrane from early in the differentiation process, it seemed important to determine whether CD38 was also expressed intracellularly in the nuclei. Thus, to address this issue, the nuclei of ATRA-treated HL60 cells were extracted and the molecular forms of CD38 were investigated in both HL60 cells and HL60 cell lysate after 0, 10, 24 and 72 h of incubation with ATRA (Figure 3.12A). A weak 45 kDa band appeared at 24 h of differentiation and increased after 3 days of differentiation (Figure 3.12A). The same 45 kDa band, the monomeric form of CD38, was also seen in the RAJI cell nuclear fraction but was absent both in the undifferentiated HL60 cell lysate and in the cell lysate at 0 h and 10 h of differentiation. A high molecular weight (80 kDa) form of CD38 also appeared in nuclear fractions and was clearly visible in both RAJI cell lysate and after one day of HL60 differentiation.

It is important to mention that reducing conditions with mercaptoethanol were used in both the plasma membrane and nuclear fractions. Furthermore, ATRA-induced expression of CD38 on nuclei from HL60 cells was also investigated using the NGD assay (Figure 3.12B) at 10, 24 and 72 h after treatment with ATRA, and also using undifferentiated HL60 cells as a control. The results revealed NGD cyclization by CD38 activity which is clearly observed on the surface of nuclei after treatment with ATRA at 1 and 3 days. These and previous observations indicate that the majority of the CD38 cyclase activity occurred in the plasma membrane fraction and, to a lesser extent, in the nuclei, indicating that CD38 enzymatic activity might have an important role in the nucleus in addition to its extracellular activity.

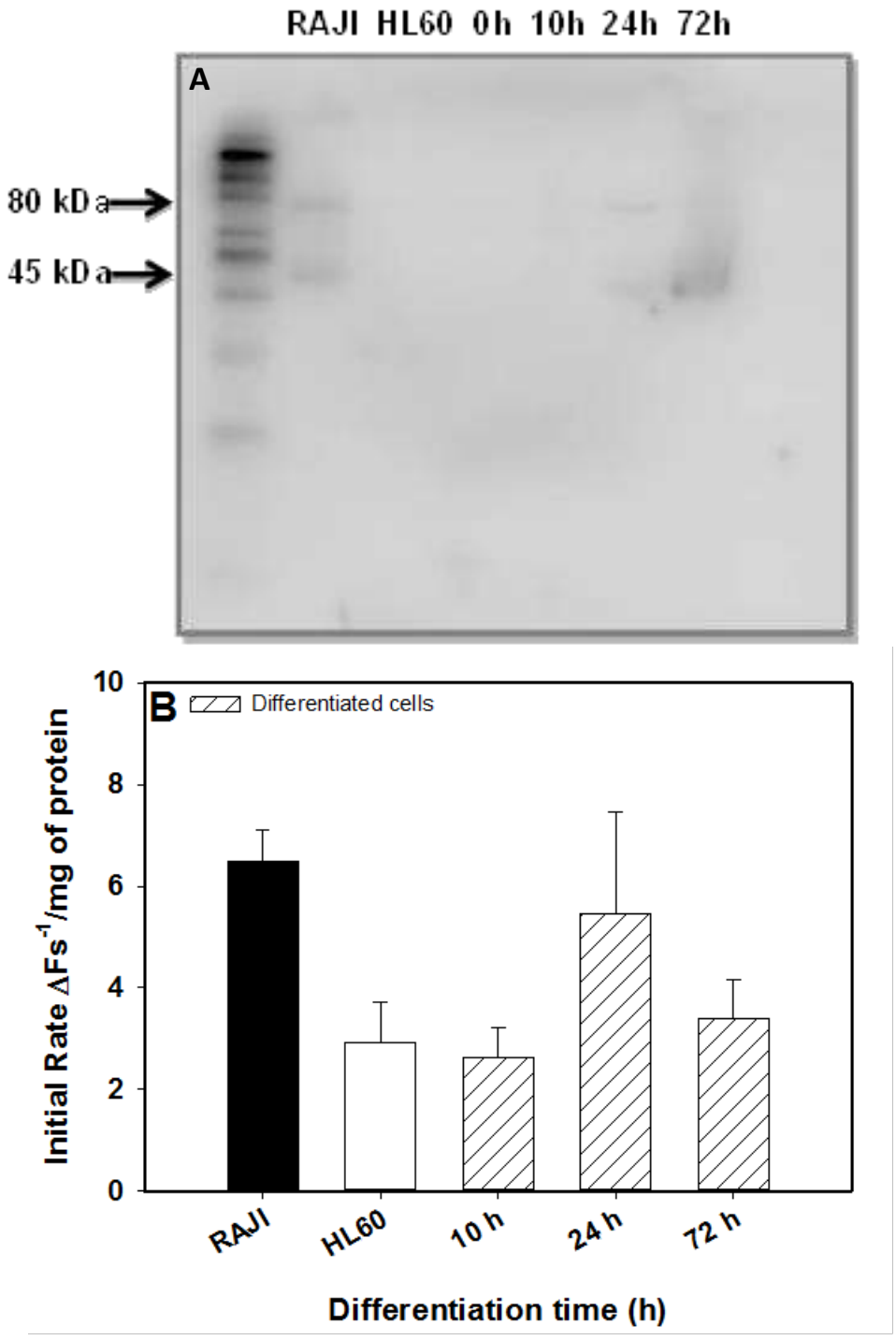

Figure 3.12 Time course of ATRA treatment of HL60 cells over 3 days showing (A) western blotting of nuclear CD38 under reducing and denaturing conditions. A 12% SDS-PAGE gel with 60 µg of protein/well was used in each experiment (gel shown representative of 3 experiments) (B) CD38 expression in the nuclear fraction was measured as the rate of cGDPR production from NGD. Data are means ± SEM, n = 3 (1 measurements per replicate). No significant differences in activity during differentiation and comparing to untreated control (HL60) were found ($P > 0.05$).

It is important to note that the nuclei used in this investigation were isolated by a conventional method (Whiteside *et al.,* 1992). The purity of a nuclear preparation can be characterized by either measuring the activity of an endoplasmic reticulum marker; glucose-6-phosphatase or a plasma membrane marker; 5-nucleotidase. (Colowick and Kaplan, in: Fleischer and Packer, 1974). However, this approach was not carried out because contamination of the nuclear extract could be excluded on the basis of the absence of CD38 protein in the extract; in HL60 cells, CD38 is localised in the plasma membrane and not in the nuclear membrane. Importantly, the respective findings of this investigation provide further evidence for ATRA-promoted nuclear and plasma membrane CD38 activation. CD38 was previously detected in nuclear membrane of differentiating cells (Yalcintepe *et al.,* 2005). Further reports have also revealed that CD38 enzymatic activity is present not only in the plasma membrane, but also in intracellular membranes of organelles such as mitochondria and nuclei (Yamada *et al.,* 1997; Liang *et al.,* 1999; Khoo *et al.*, 2000; Iqbal and Zaidi, 2006). Interestingly, in all of the work described in this Chapter, HL60 differentiation was accompanied by a large increase in CD38 expression and cyclase activity (both extracellular and intracellular) from early in the differentiation process. Thus, CD38 expression might not only serve as a marker of HL60 maturation to neutrophil-like cells, but the enzyme might also catalyse the degradation of NAD during ATRA-induced HL60 differentiation. This expression might have important consequences on cell metabolism.

3.3.3 Effect of CD38 expression on NAD levels during HL60 differentiation

High levels of CD38 expression and cyclase activity were observed during ATRA-induced HL60 differentiation. Therefore, it was of importance to investigate the effect of this increased expression on the levels of the substrate of CD38, NAD, during ATRA-induced HL60 differentiation. However, in order to evaluate NAD levels during differentiation, it was important to first examine the effect of ATRA on the NAD assay. Therefore, to address this issue, two concentrations of ATRA (10 nM and 1 µM) were analyzed along with a range of NAD concentrations (0.975 µM, 1.95 µM, 19.5 µM and 195 µM).

The results (Fig. 3.13) show that both 10 nM and 1 µM ATRA had no apparent effects on the NAD assay, even though 10 nM ATRA, at an NAD concentration of 19.5 µM, was the only concentration that exerted a significant effect on the NAD assay when compared to other NAD concentrations and the control (not treated with ATRA). Importantly, with 1 µM ATRA, the concentration which was used to induce HL60 differentiation, the results confirmed that there was no interference with the NAD assay.

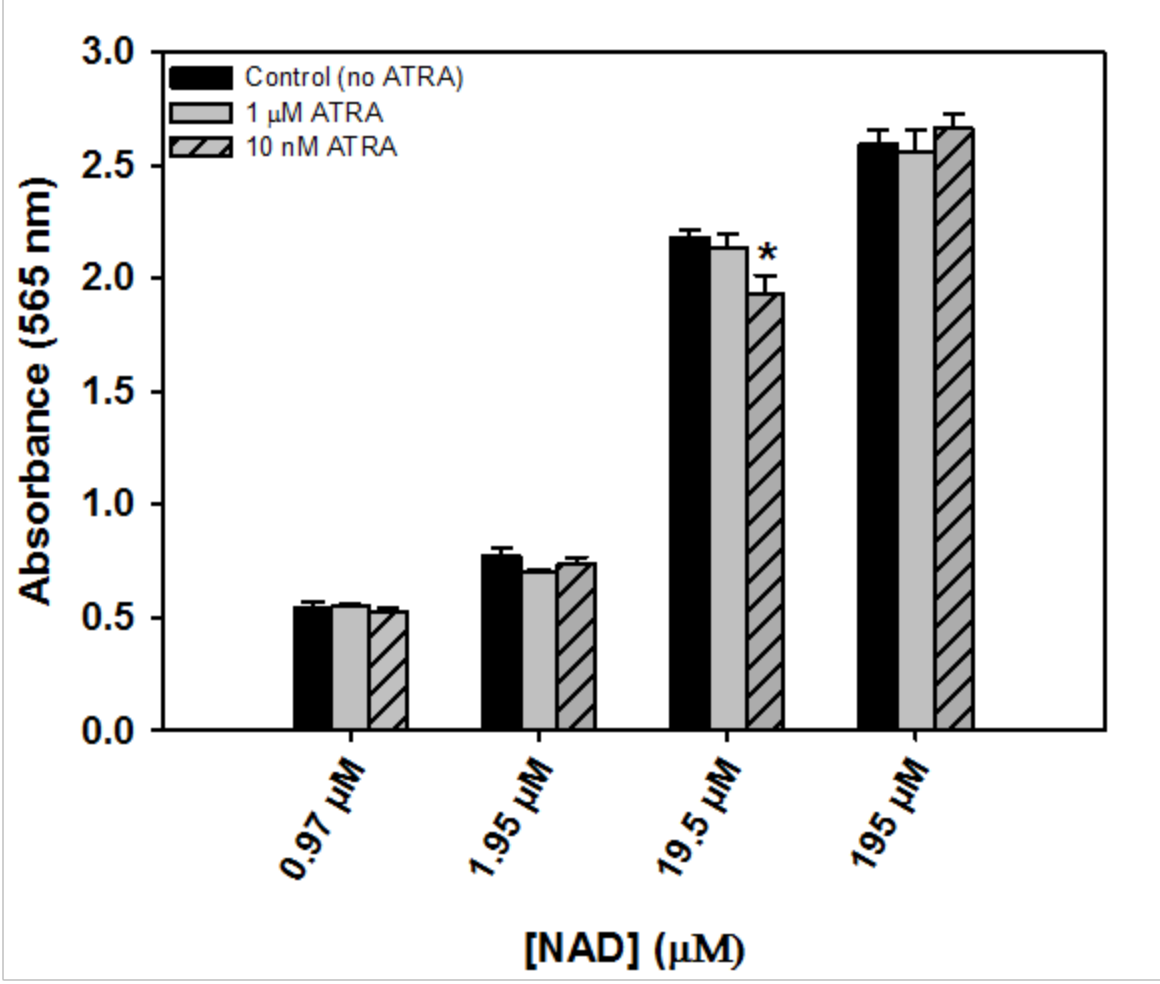

Figure 3.13 The effect of different ATRA concentrations (0, 10 nM and 1 µM) on the NAD assay, at a range of NAD concentrations (0.97, 1.95, 19.5 and 195 µM). Data are means ± SEM, n = 3 (3 measurements per replicate). * denotes significant difference from the appropriate untreated control ($P < 0.05$).

Thus, NAD levels were determined at 4 - 120 h of differentiation compared to the control (cells not treated with ATRA). Surprisingly, a substantial time-dependent decline in intracellular NAD levels was clearly detected in response to ATRA treatment in HL60 cells (Figure 3.14). There was a significant drop in NAD levels as differentiation occurred to 64.6 ± 8.9% on day 1, 47.3 ± 7.0% on day 3 and 40.5 ± 8.7% on day 5 compared to the control.

A significant decrease in the intracellular NAD levels was seen from early in the differentiation (4 h), and levels continued to drop up to 5 days. This rapid decline in NAD levels was concomitant with the rise of CD38 mRNA expression as seen in Figure 3.15. Interestingly, the latter was seen after 3 h, while NAD degradation started at 4 h differentiation time. These novel data might support a major role for CD38 as a regulator of intracellular NAD.

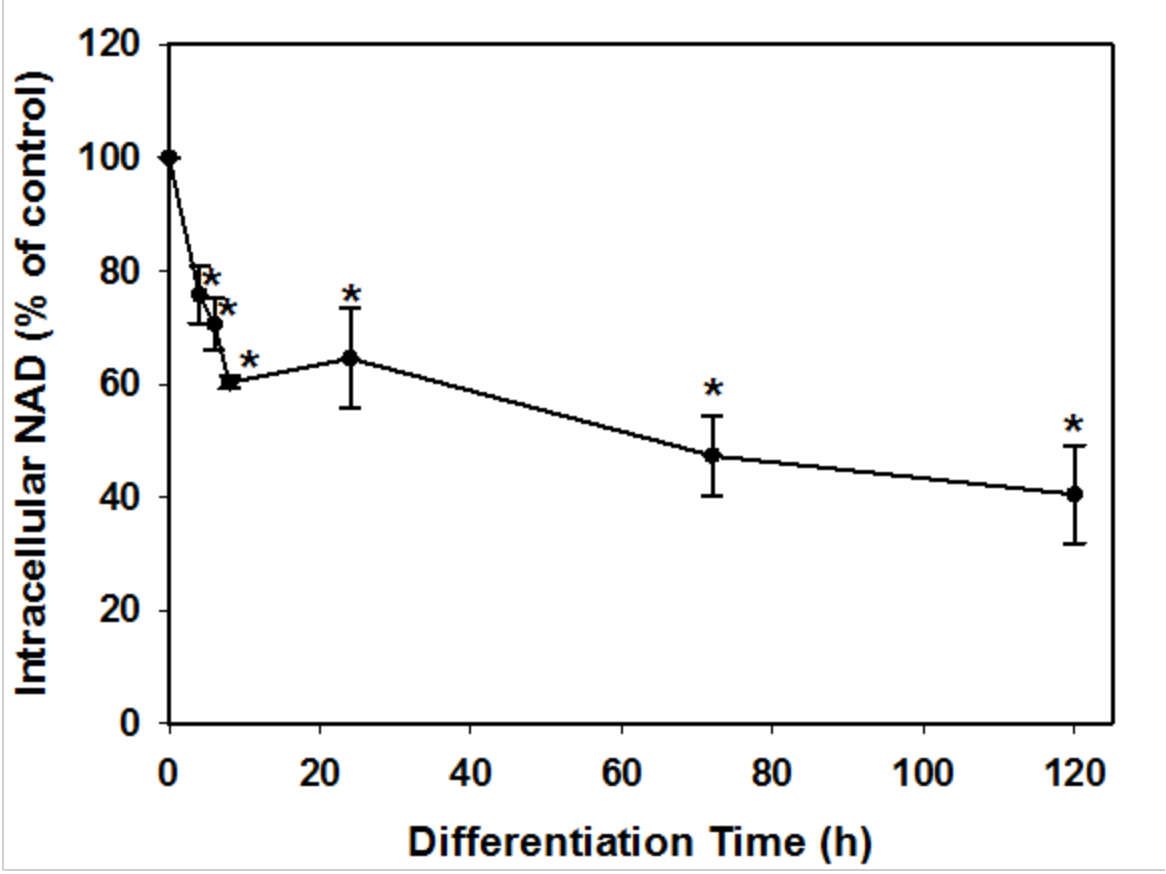

Figure 3.14 The decline in intracellular NAD levels during HL60 differentiation estimated over 5 days of differentiation and compared to untreated control (HL60). Data are means ± SEM, n = 3 (3 - 7 measurements per replicate). * denotes significant difference from the control (100% HL60), $P < 0.05$.

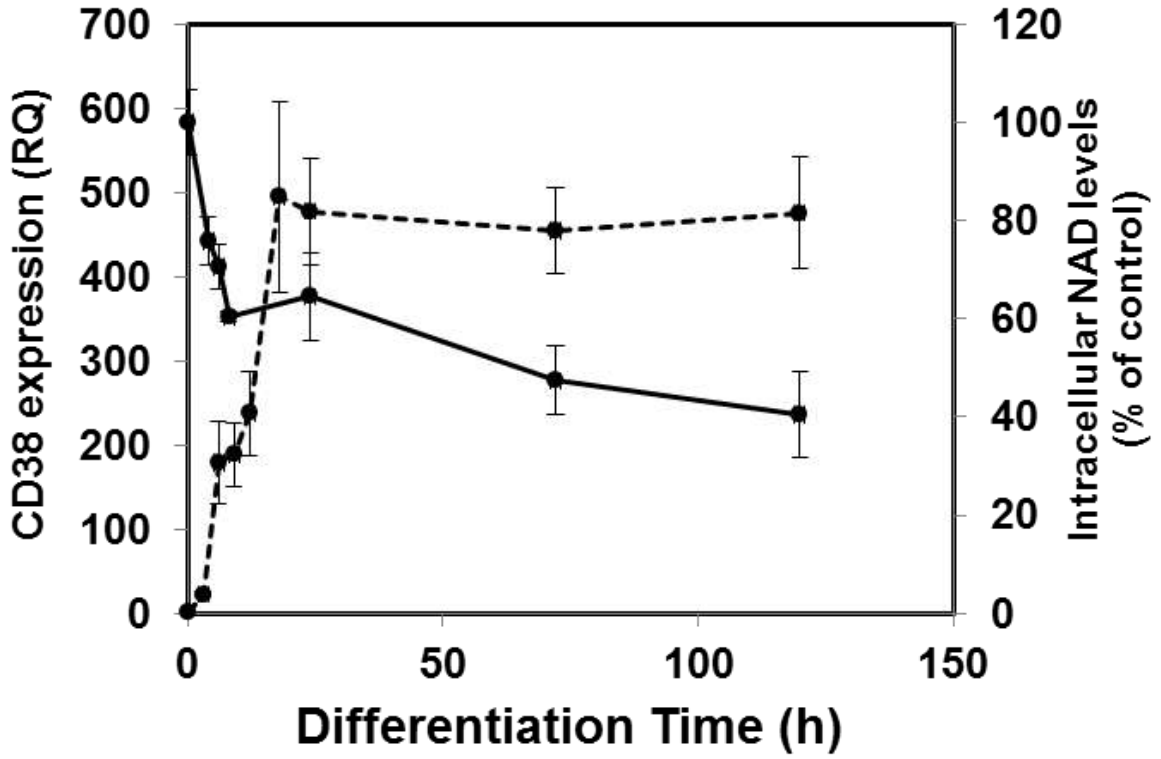

Figure 3.15 The decline in intracellular NAD levels (solid line), concomitant with CD38 mRNA induction (dashed line) during HL60 differentiation estimated over 5 days of differentiation and compared to untreated control (HL60). Data are means ± SEM, n = 3 (3 - 7 measurements per replicate).

3.3.4 Kuromanin inhibited NAD-cyclization activity of CD38 and elevated NAD levels, but PARP and sirtuin inhibitors had no effect on NAD levels during the differentiation

To establish whether the novel finding of low NAD levels during HL60 differentiation was due to upregulation of CD38 and its enzymatic activity as evaluated in the current study, it was hypothesized that inhibition of CD38 activity might lead to elevation of intracellular NAD. Therefore, a novel inhibitor of the NAD cyclization activity of CD38, kuromanin, was tested. It has recently reported that flavonoids such as kuromanin and luteolin act as inhibitors of human CD38 at low micromolar concentrations (Kellenberger *et al.*, 2011). Thus, the effect of the inhibition of the enzymatic activity of CD38 by kuromanin was investigated in both RAJI cells and the differentiating HL60 cells on intracellular NAD levels (Fig. 3.17). It is worth noting that RAJI cells show high CD38 activity compared to HL60 cells, but they have low intracellular NAD compared to HL60 cells (Fig. 3.16).

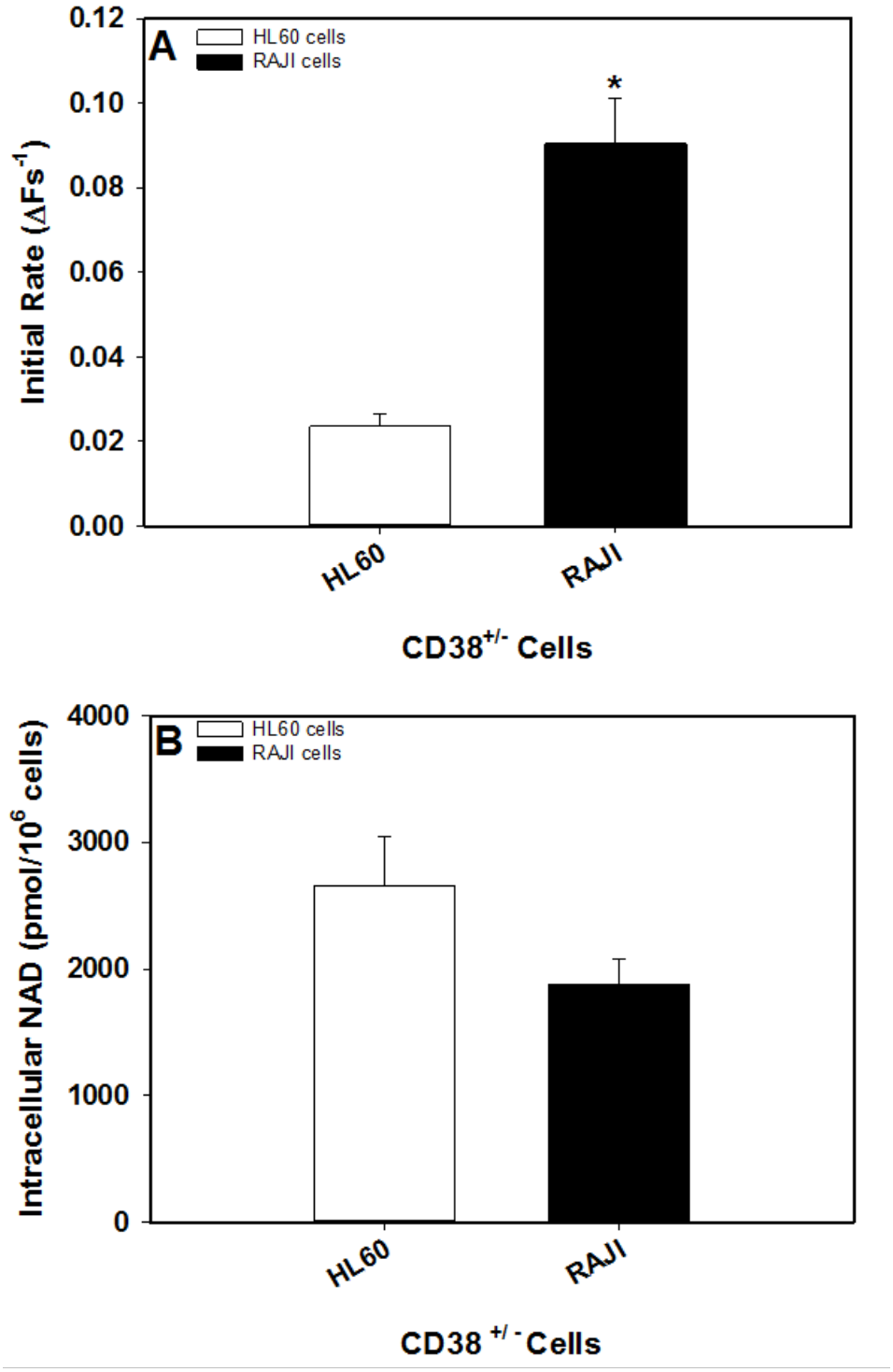

Figure 3.16 (A) CD38 cyclase activity in HL60 and RAJI cells as expressed as initial rate. (B) Intracellular NAD levels in HL60 and RAJI cells as expressed as pmol/10^6 cells. Data are means ± SEM, n = 2-3 (3-5 measurements per replicate). * denotes significant difference between group (Student's t test, $P < 0.05$).

In the current study, the effect of inhibition using 8 µM kuromanin on NAD levels was first investigated in RAJI and HL60 cells up to 2 h of incubation. The results (Fig. 3.17) show that RAJI cells have lower NAD levels than HL60 before kuromanin treatment, but they have higher NAD levels after kuromanin treatment, which might suggest that CD38 activity was inhibited by kuromanin.

Interestingly, Figure 3.18 A shows that inhibition of CD38 cyclase activity in RAJI cells with up to 30 µM kuromanin resulted in significantly elevated intracellular NAD levels after 6 h of treatment. As kuromanin leads to elevated intracellular NAD levels, the MTT assay was used to monitor cell vitality during kuromanin treatment. Cell vitality was not changed after 6 h incubation with kuromanin (Fig. 3.18 B), which might suggest that kuromanin has no effect on growth of RAJI cells after 6 h incubation, but nevertheless it significantly affects cell proliferation after 48 h incubation (Fig. 3.18 B).

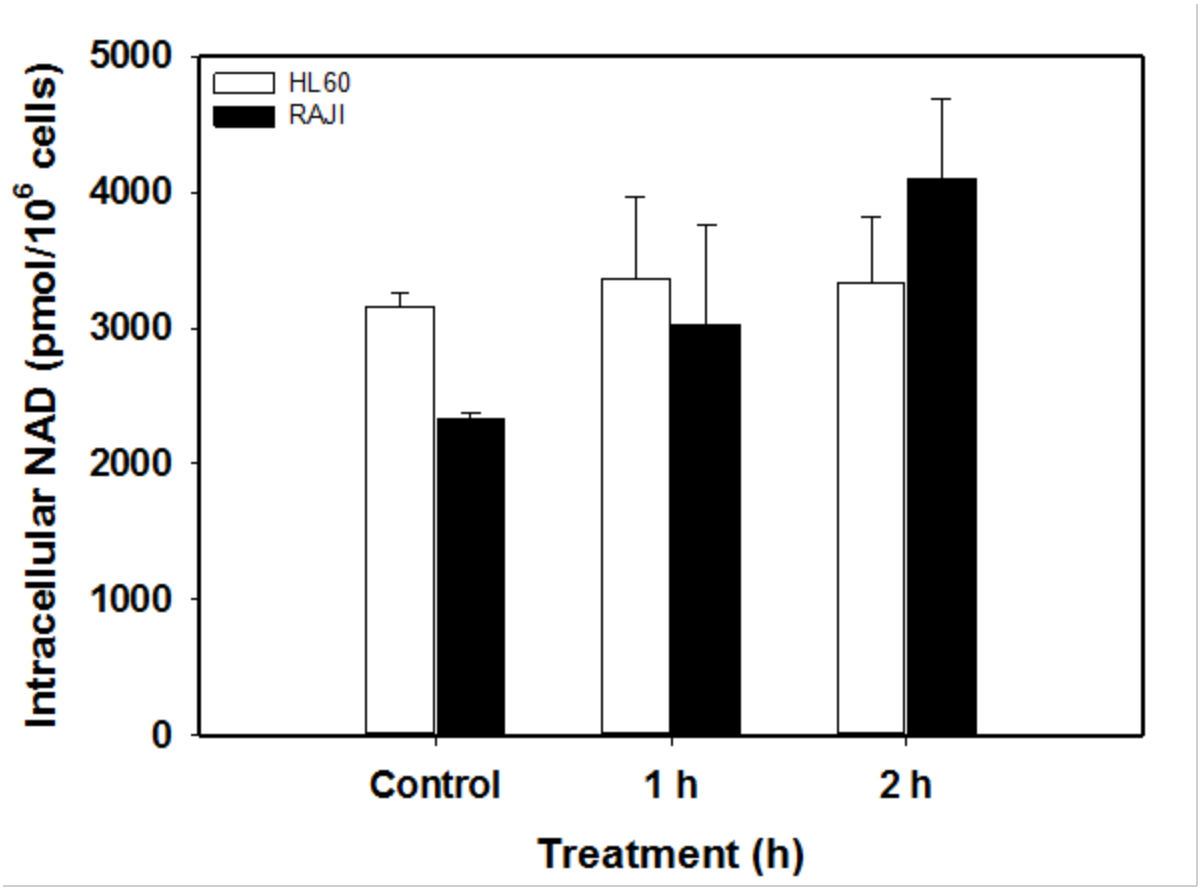

Figure 3.17 Intracellular NAD levels in RAJI and HL60 cells treated with kuromanin (8 µM) for up to 2 h comparing to appropriate untreated control (RAJI or HL60 cells). Data are means ± SEM, n = 3 (4-5 measurements per replicate), $P > 0.05$.

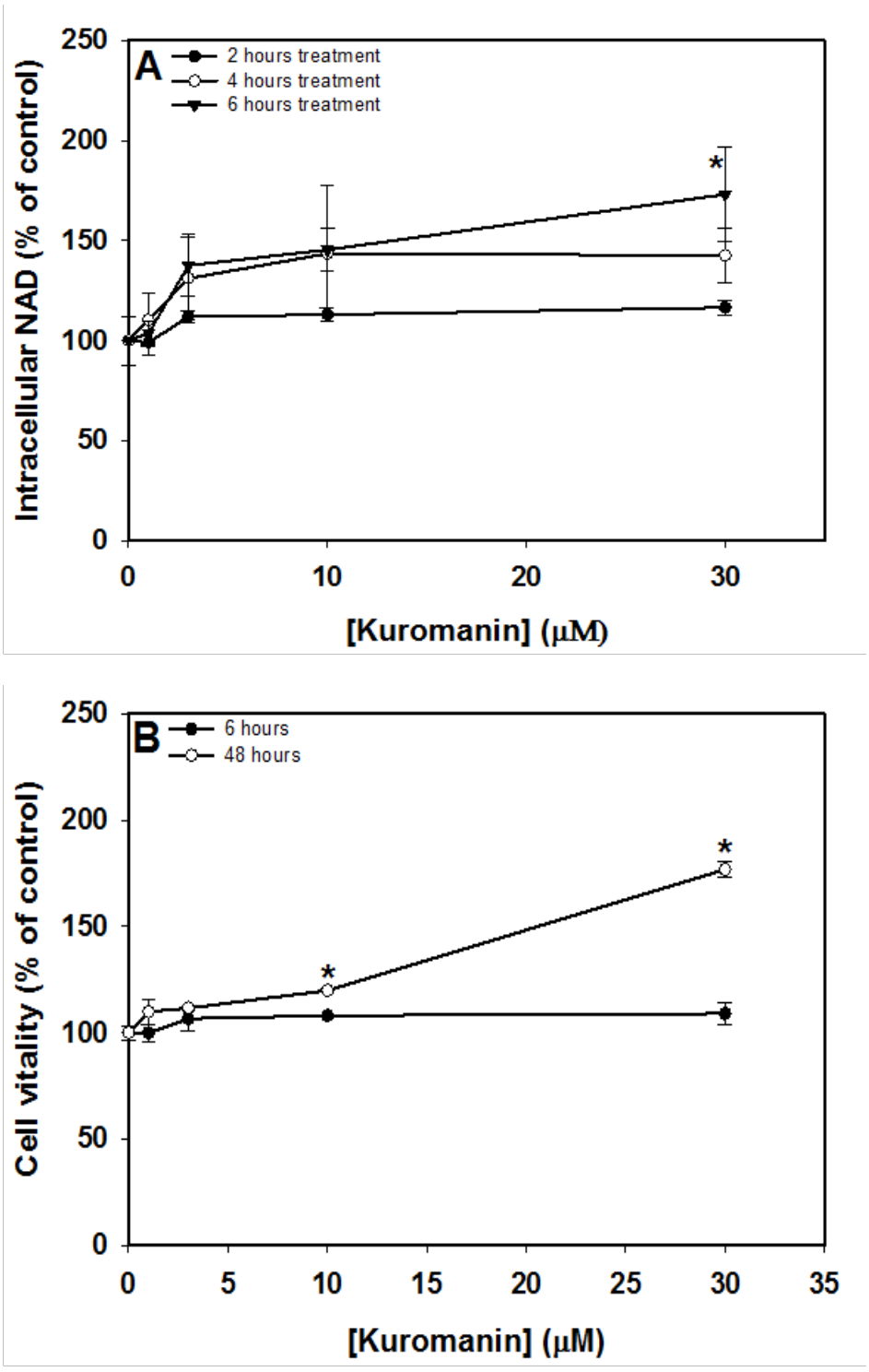

Figure 3.18 Effect of treatment with kuromanin up to 30 μM on (A) intracellular NAD levels in RAJI cells over 6 h comparing to untreated control (100% RAJI cells), and (B) the vitality (MTT assay) of RAJI cells when incubated for up to 48 h with kuromanin comparing to untreated control (100% RAJI cells). Data are means ± SEM, n = 3 (3-6 measurements per replicate).* denotes significant difference from the untreated RAJI cells ($P < 0.05$).

The effect of kuromanin on differentiating HL60 cells was also evaluated. Firstly, the results of kuromanin exposure on NBT reduction showed that it might inhibit the differentiation of HL60 in a concentration-dependent manner (Fig. 3.19). NBT reduction levels also decreased as the incubation with kuromanin was prolonged to 4 days, compared to 4 days differentiation without kuromanin. However, the mechanism of this effect was not really clear, and it might be due to an additional, unknown factor.

Secondly, treatment of the differentiating cells with kuromanin also affected NAD levels. The results showed significantly increased NAD levels in differentiating cells treated with 10 µM kuromanin after 6 h (Fig. 3.20). This increase in NAD levels was time-dependent, apparently concomitant with inhibition of CD38 activity.

Upregulation of CD38 expression during ATRA treatment was associated with a significant decrease in NAD levels to 60.41 ± 0.92% by 6 h of differentiation. However, inhibition of CD38 activity by kuromanin (Fig 3.20) was seen to stop the decrease in intracellular NAD and led to an increase in NAD levels to 120.71 ± 14.81% after 6 h differentiation with ATRA. The strong relationship between CD38 and NAD levels shown in several experiments may confirm a major role of CD38 as the main enzyme involved in the regulation of NAD levels. The findings with kuromanin are supported by CD38 knockout studies (Aksoy *et al*., 2006 b; Barbosa *et al.*, 2007), and findings in macrophages where CD38 has been genetically deleted (Iqbal and Zaidi, 2006). Overall, whether CD38 removed or inhibited, intracellular NAD levels are significantly elevated.

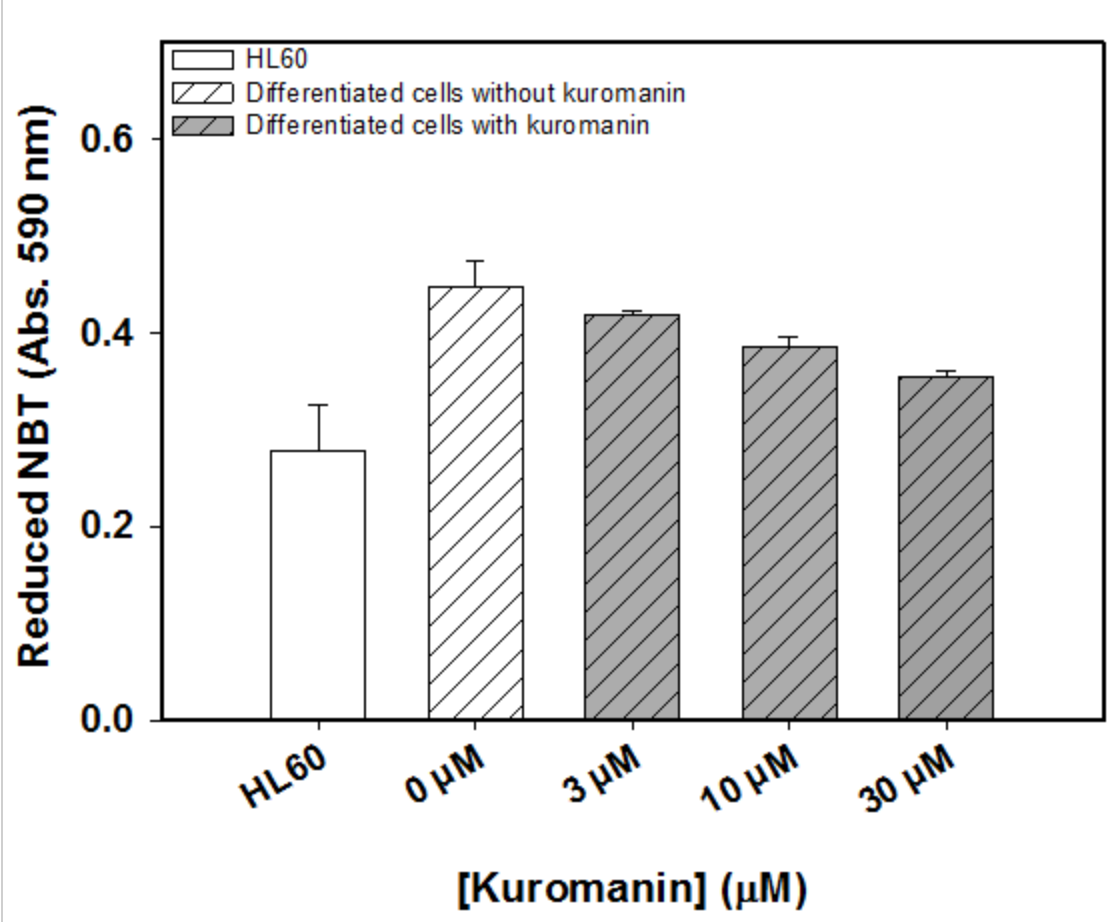

Figure 3.19 The effect of treatment with kuromanin up to 30 µM on NBT reduction by ATRA treated HL60 cells for 4 days comparing to untreated HL60 cells (control). Data are means ± SEM, n = 3 (4-6 measurements per replicate). * denotes significant difference from the control ($P < 0.05$).

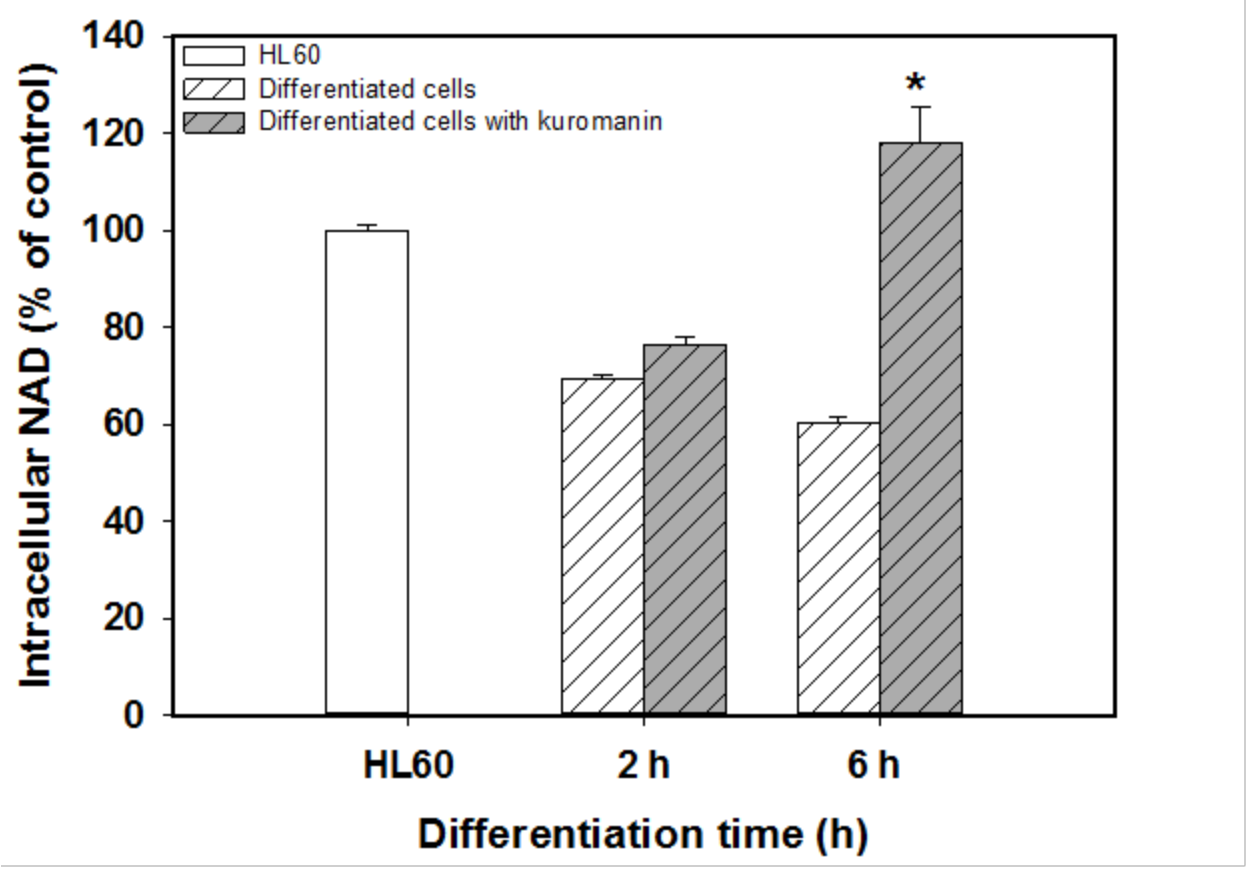

Figure 3.20 Effect of treatment with 10 µM kuromanin on intracellular NAD levels of differentiated cell up to 6 h comparing to differentiated cells without kuromanin treatment (as control). Data are means ± SEM, n = 3 (4 measurements per replicate). * denotes significant difference from the control (differentiated cells), $P < 0.05$.

To avoid the possibility of other known NAD-consuming enzymes (for example; PARP1, SIRT1) participating in the decline in NAD, in addition to the degradative role of CD38, during the differentiation process, other experiments were carried out, including treatment with SIRT1 and PARP1 inhibitors during ATRA-induced HL60 differentiation. The PARP1 inhibitor; 4-amino-1, 8-naphthalimide, has previously been shown to have a potent inhibitory effect on PARP activity in tumour cells (Schlicker *et al.,* 1999). PARP is also known as a major cellular NAD^+ consumer, in addition to CD38 (Sims *et al.,* 1981). Thus, inhibition of PARP activity is reported to increase NAD levels in brown adipose tissue and muscle (Bai *et al*., 2011). PARP inhibitors are currently in clinical development as antitumour drugs (Fong *et al.,* 2009).

On the other hand, NAD works as a substrate and regulator of NAD-dependent deacetylases such as SIRT1 which are located in the nuclei, and modulate ageing and energy metabolism in mammalian cells (Grubisha *et al*., 2005; Guarente and Picard, 2005; Pillai *et al*., 2005). Indeed, seven sirtuins (SIRT1-7) have been identified, which target histone and various nonhistone proteins in distinct subcellular locations. Both SIRT1 and SIRT2 may have a role in the development of cancer (Peck *et al.,* 2010). In addition, it has also been confirmed that Sirtinol, a SIRT1 inhibitor, can effectively induce significant growth inhibition or apoptosis *in vitro* studies (Peck *et al.,* 2010), or in *in vivo* studies such as with adult T-cell leukemia-lymphoma (ATL) patients (Kozako *et al.,* 2012). Thus, SIRT1 inhibitors have been suggested to be therapeutic agents for leukemia (Kozako *et al.,* 2012).

The results (Fig. 3.21 A, B) show that neither 4-amino-1,8-naphthalimide (PARP inhibitor), nor sirtinol (SIRT1 inhibitor) changed the intracellular levels of NAD during the differentiation compared to the control (the differentiating cells without the inhibitors). The results suggest that

there was not sufficient activity of either enzyme to impact on the intracellular levels of NAD. Interestingly, PARP activity has previously been reported to be decreased during neutrophilic differentiation of HL60 cells (Kanai *et al.,* 1982). This decline is suggested to be achieved through changes in the specific activity of PARP and increases in the NAD glycohydrolase activity (Kirsten *et al.,* 1991) and these findings strongly support the results obtained (Fig. 3.21 A). Moreover, the data (Fig. 3.21 B) on NAD levels during the differentiation and in combination with sirtinol, might suggest that sirtuin activity is not significant during the differentiation or that NAD levels might be mostly controlled by other NAD consuming enzymes, mainly CD38.

In conclusion, the decrease in NAD levels appears to be controlled by the main degrading enzyme CD38, and it is clearly independent of the actions of other NAD consuming enzymes (PARP and SIRT1) during HL60 differentiation. Moreover, the results of this part of the work have further confirmed that the endogenous activities of SIRT1 and PARP might be regulated via CD38 enzymatic activities by controlling the availability of their substrate, NAD.

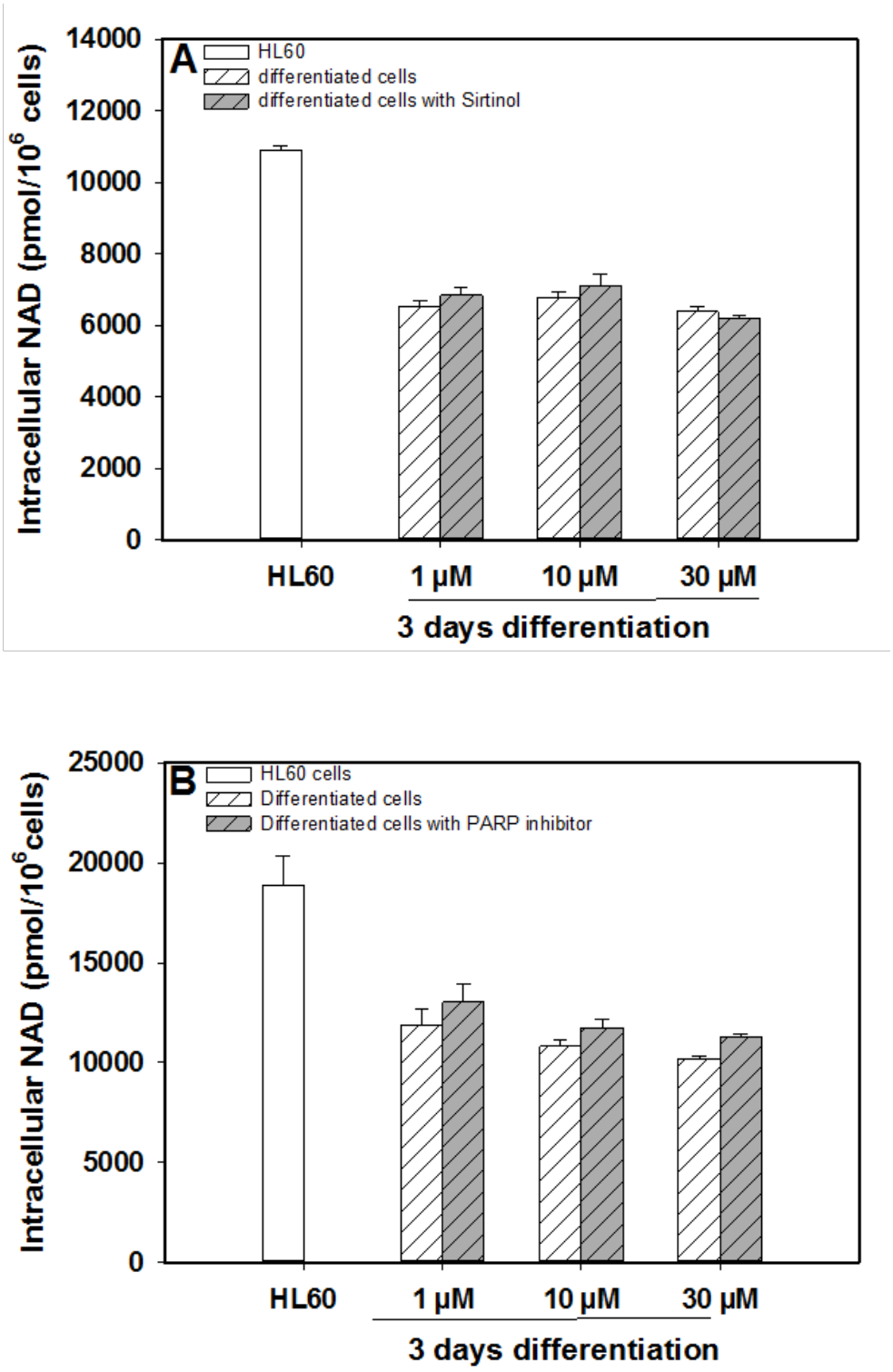

Figure 3.21 Intracellular NAD levels were investigated in differentiated cells for 3 days with ATRA after treatment with (A) PARP inhibitor (4-amino-1,8-naphthalimide) up to 30 µM or (B) sirtuin inhibitor (sirtinol) up to 30 µM. Data are means ± SEM, n = 3 (3 measurements per replicate). No significant differences in NAD levels were found between differentiated cells with or without inhibitor, $P > 0.05$.

3.3.5 Evaluation of the NAD biosynthesis enzymes during ATRA-induced HL60 differentiation

A considerable decline in NAD levels was clearly indicated in the time course of HL60 differentiation, which might be mediated mainly by the activity of CD38 and not by CD157, PARP or sirtuin. As it has been shown here that CD157 has negligible gene expression, it appears that it cannot account for the decline in NAD levels. Also inhibition of both PARP and sirtuin activities did not have any significant effect on intracellular NAD levels. Overall, the above data suggests that these enzymes might not participate in the consumption of NAD. Hence, having investigated the NAD consuming pathways, it was important to look for other mechanisms that might be involved in the decline of intracellular NAD. Thus, NAD biosynthesis enzymes were investigated in this study. The hypothesis was that changes in the level of expression of NAD biosynthesis enzymes might affect NAD levels.

It is well known that cellular NAD is synthesized either via the *de novo* pathway from tryptophan or via one of two possible recycling pathways: from nicotinic acid or nicotinamide; vitamin PP, or niacin (Magni *et al.*, 2004), and via the nicotinamide riboside pathway (Bieganowski and Brenner, 2004). Thus, mRNA levels of some NAD-biosynthesis enzymes were investigated from both the *de novo* (Fig. 3.22) and salvage pathways (Fig. 3.23 A, B).

Expression of IDO (a *de novo* pathway enzyme) was found to be upregulated early, at 12 h of differentiation ($p > 0.05$), with a clear decline later on. An increase in IDO mRNA levels then was observed at 72 h of differentiation with a continuous increase ($P < 0.05$) up to 120 h (Fig. 3.22). It has been demonstrated that the expression of the tryptophan-catabolizing enzyme (IDO) in neutrophils (as occurs during influenza infection), in addition to impairing host defense

against secondary bacterial infections, also enhances neutrophil apoptosis *in vivo* (Van der Sluijs *et al.*, 2011). This might suggest further functions for IDO in addition to its role in NAD biosynthesis.

The expression of the salvage pathway enzymes NMNAT and NAMPT was also investigated during the differentiation. Significantly increased NMNAT mRNA was observed (Fig. 3.23 A) at 120 h of differentiation, in addition to increases at 18 h and 72 h. NAMPT expression was also investigated during the time course; there was no significant change over time (Figure 3.23 B).

The results indicate an increase in NAD-biosynthesis enzymes, especially IDO, during differentiation. Taken together, the data suggest that differentiating HL60 strongly depend on the NAD *de novo* pathway to resynthesize intracellular NAD and to maintain the NAD pool.

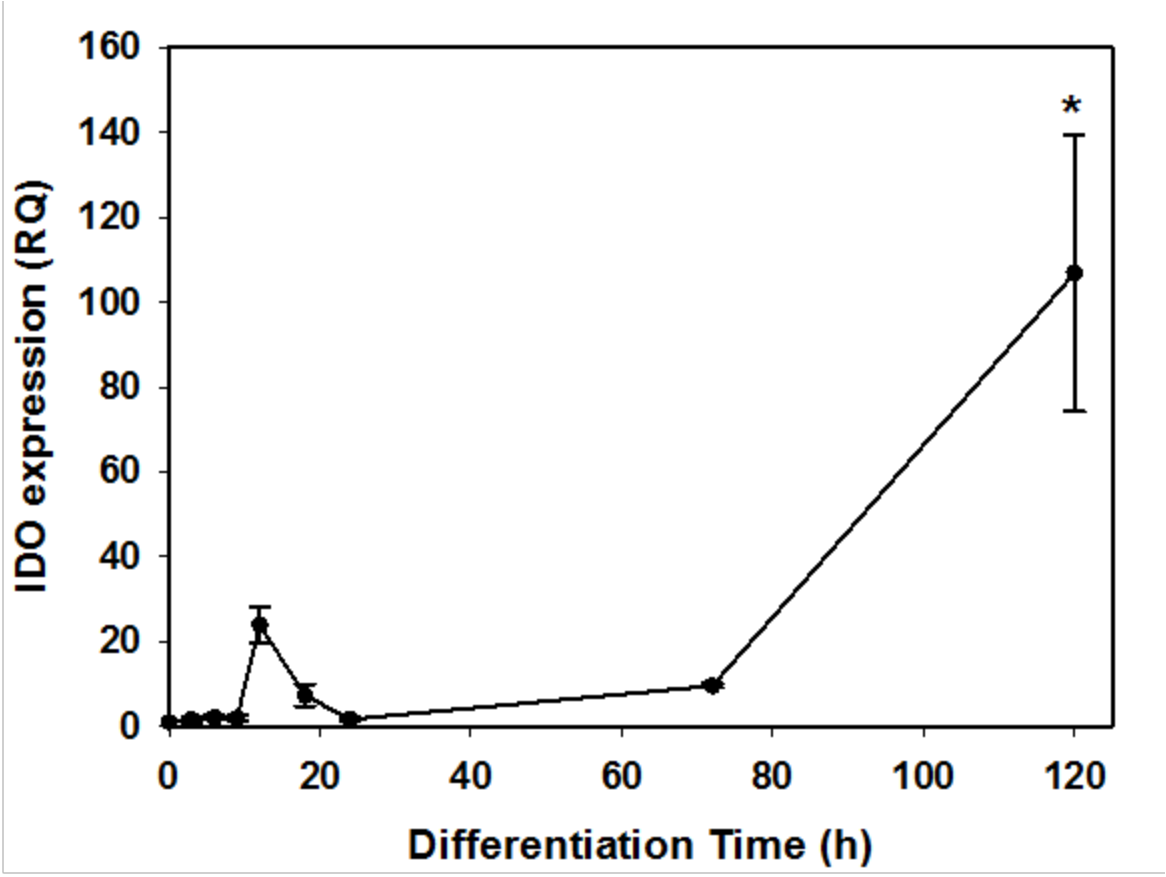

Figure 3.22 Time course of ATRA-induced differentiation of HL60 cells over 5 days showing the increase in IDO expression comparing to untreated HL60 cells (as control). Data are means ± SEM, n = 3 (3-6 measurements per replicate). * denotes significant difference from the control ($P < 0.05$).

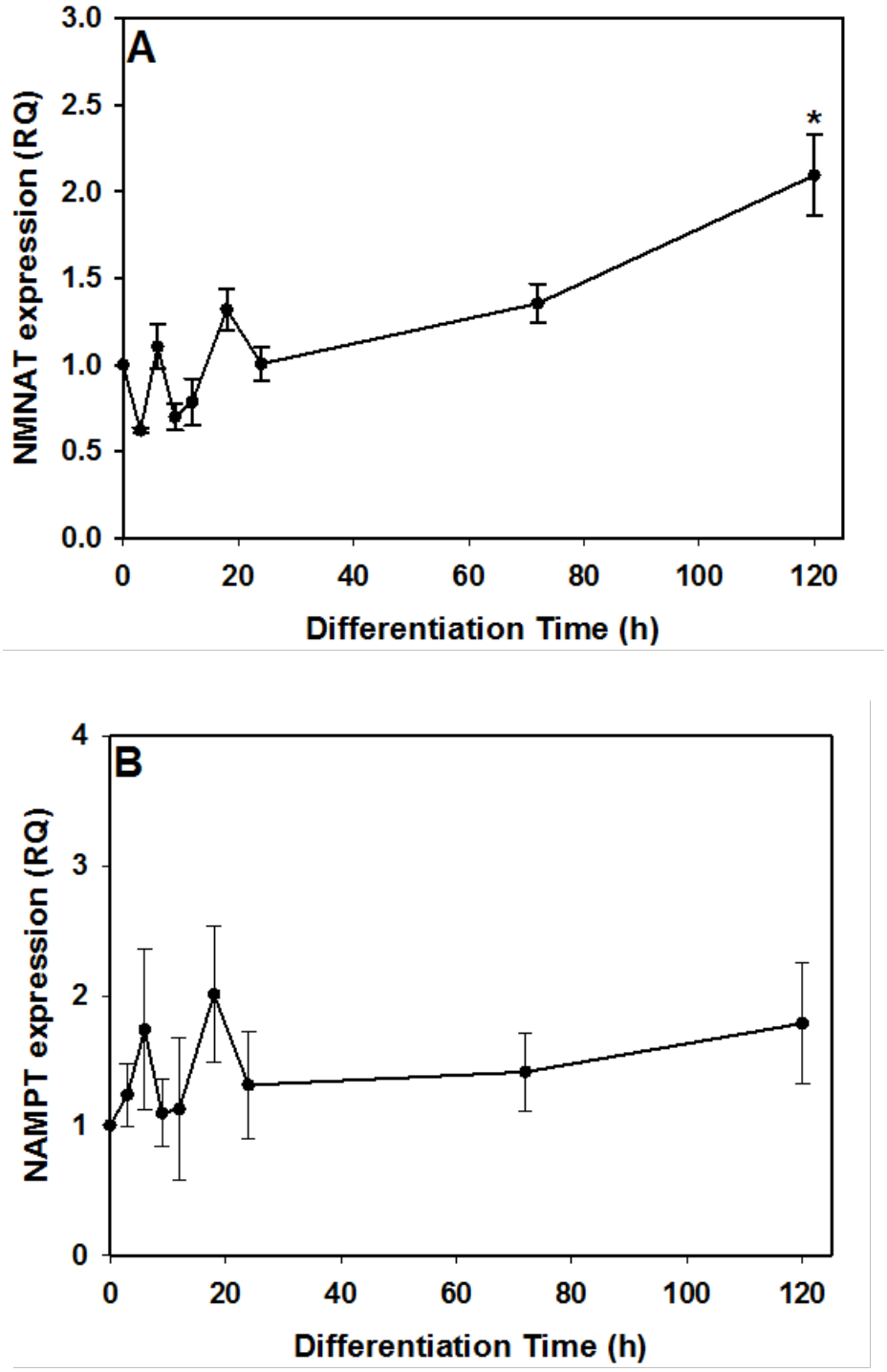

Figure 3.23 Time courses of ATRA-induced differentiation of HL60 cells over 5 days showing (A) NMNAT expression (B) NAMPT expression and were compared to untreated HL60 cells (as control). Data are means ± SEM, n = 3 (3-4 measurements per replicate). * denotes significant difference from the control ($P < 0.05$).

3.3.6 CD38 and cell proliferation

It is well known that induction of granulocytic differentiation in HL60 cells by ATRA is followed by cell death via apoptosis (Mehta *et al.,* 1996). Hence, a reduction in cell proliferation was evident after 24 h of culture with ATRA and was most pronounced after 3 and 5 days of differentiation (Fig. 3.4). However, the finding of less cell proliferation was not expected in cells expressing CD38, since, as previously mentioned (Chapter 1), $CD38^+$ CLL cells proliferate more in comparison to $CD38^-$ CLL cells. However, one possible explanation was the presence of CD31, as an effective proliferation factor, known as a CD38 non- substrate ligand. The CD38/ CD31 interaction has a role in CLL progression via the induction of a proliferation effect (Deaglio *et al.,* 1998; 2000; 2005). Therefore, the hypothesis was to test whether creating environments similar to those of leukemia (CLL), by culturing $CD38^+$ cells (differentiated cells) with human solid tumour cell lines expressing CD31 such as MCF-7 (breast carcinoma; Tang *et al.,* 1993), would induce a proliferation in differentiating cells that are expressing CD38, but not CD31.

There was a significant decrease in cell vitality in the 3 day- differentiated cells as assayed using MTT (Fig. 3.24). However, a reversed effect on cell proliferation was interestingly shown after co-culturing the differentiated cells ($CD38^+$) with MCF-7 cells ($CD31^+$) for 1 day. This suggests that an interaction between CD38 and CD31 signalling might have occurred. CD38/ CD31 interactions and their effects have been previously reported; Gao *a*nd colleagues (2007) stated that CD38 expression induced by ATRA increases adhesion of differentiated HL60 cells to vascular endothelial cells ($CD31^+$), that results from a protein-protein interaction between CD31 and CD38 molecules.

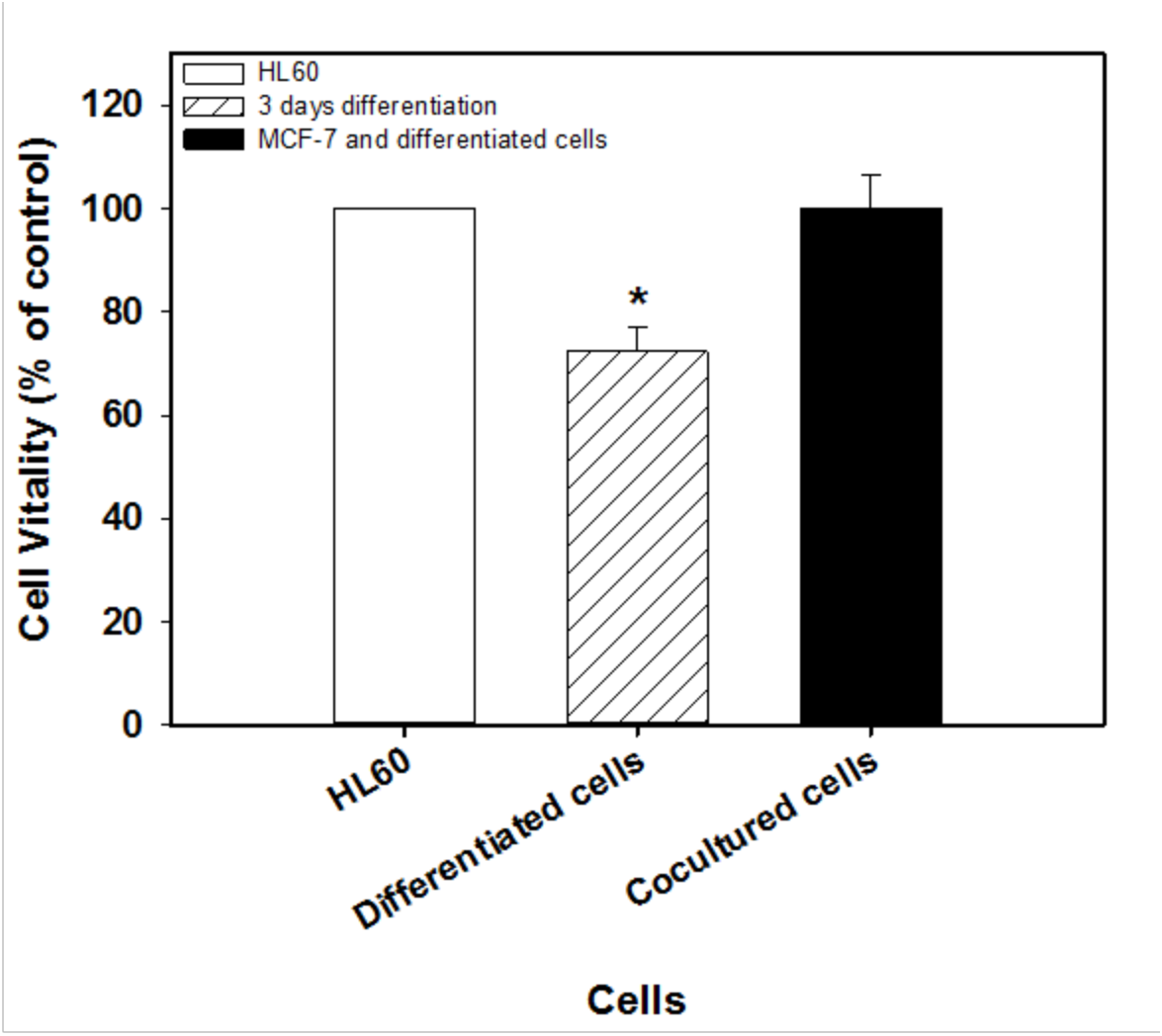

Figure 3.24 The effects of 1 day culture of differentiated cells (3 days) with MCF-7 cells on cell proliferation (MTT assay) as compared to the differentiating cells for 3 days (as control). Data are means ± SEM, n = 3 (8 measurements per replicate). * denotes significant difference from the control ($P < 0.05$).

It is worth mentioning that important evidence for the effect of CD38/CD31 interaction on cell proliferation can also be confirmed in HL60 cells. The undifferentiated HL60 cells have a high proliferation capacity and low CD38 levels, but express significant levels of CD31 (Gallay *et al.*, 2007). Moreover, no observed regulation of CD31 antigen was reported when HL60 cells were stimulated to granulocytes by ATRA (Trayner *et al.,* 1998). That explains the low proliferation capacity of the $CD38^+$ cells (the differentiated cells) compared to the leukemia cell line (HL60). Thus, cell proliferation increased especially when $CD38^+$ cells interacted with CD31. This also suggests the effective role of CD38/CD31 interaction on cell proliferation in $CD38^+$ leukemia patients.

3.4 Discussion

The role of CD38 as a modulator of NAD levels has not been completely elucidated. Therefore, in the present work, the effect of CD38 expression on NAD levels was investigated in the human leukaemia cell line (HL60) as a relevant model which can differentiate to neutrophil-like cells. A novel key finding of the present study is that HL60 cells are $CD38^-$ and have high levels of NAD, whereas the differentiating cells were $CD38^+$ and have a low content of NAD, which correlates with CD38 expression. These results suggest that CD38 may be a main NAD degrading enzyme that is expressed during HL60 differentiation. The expression of CD38 in the cells was demonstrated using real time PCR coupled with reverse transcription, western blotting and flow cytometer. These findings might help with the understanding of the mechanisms that regulates NAD levels, and the consequences of this degradation on different cell functions in health and disease. This is because NAD has important roles in energy homeostasis, signal transduction and ageing by serving as a substrate for a network of enzymes. Based on the current

results, it was further hypothesized that in $CD38^+$ leukemia cells NAD levels might also be decreased compared to $CD38^-$ leukemia cells. In reviewing the literature, no data was found on the association between CD38 and NAD levels in leukemia. Thus, CD38 enzymatic function speculated to have an important role, in addition to its receptor function, in leukemia. It was hypothesized that CD38 behaviour as a receptor is independent of its enzymatic function (Lund, 2006; Congleton *et al.,* 2011). However, there might be a connection between CD38 as a receptor and as an enzyme to achieve its functions in processes such as cell proliferation, apoptosis, differentiation and activation in disease as in leukemia patients, where CD38 is known to be a distinct prognostic marker (Malavasi *et al*., 2008). The upregulation of CD38 expression might affect intracellular NAD levels and several consequences on cell physiology might occur. Hence, poor prognosis might be a result of a complex mechanism derived from the effect of CD38 enzymatic function, in addition to its receptor functions.

The present studies, employing a range of techniques, show that differentiating HL60 cells possess CD38 which is located extracellularly in the plasma membrane as well as intracellularly in the nucleus. Interestingly, CD38 expression can significantly degrade intracellular NAD during HL60 differentiation, since the results confirmed that CD38 was not just expressed on the plasma membrane. The findings of this study, as well as those of previous reports, have further confirmed the presence of intracellular CD38 expression where intracellular NAD, its main substrate, is present (Trubiani *et al.,* 2008; Zhao *et al.,* 2012). The presence of intracellular CD38 was demonstrated by western blotting (a weak 45 kDa band for CD38 at 24 h; Fig. 3.12 A) and cyclase activity associated with the nuclear extract (activity shown on day 1; Fig. 3.12 B). Also, FACS data for intracellular CD38 shows unexpected, high protein formation levels starting at least by 10 h of differentiation. Indeed, CD38 antibody showed high reactivity with extracellular

CD38 positive cells before permeabilization with less reactivity to detect the intracellular CD38 after permeabilization. This might be due to the presence of CD38 as type II and type III (opposite orientations) in the cell membrane. These two types were confirmed to be present in differentiating HL60 cells (Zhao *et al.,* 2012), which might explain the high levels of extracellular CD38 detected, since this antibody might also detect the intracellular CD38 at the time of its expression from the cytosol to the cell surface.

Furthermore, the other NAD-consuming enzymes (CD157, PARP, and SIRT) showed a negative contribution to NAD degradation during the differentiation. Since there was a virtually undetectable level of CD157 mRNA expression, this suggests that this enzyme cannot account for the large decline in NAD levels. Moreover CD157 cyclase activity has been reported to be one hundred-fold lower than that of CD38 when murine BST-1 has been expressed in yeast (Hussain *et al.,* 1998). Additionally, low activities of PARP (Kanai *et al.,* 1982) and SIRT have also been suggested during HL60 differentiation. This was confirmed by the lack of change in intracellular NAD levels following the addition of inhibitors of PARP and SIRT. Interestingly, sirtuin activity is strongly controlled by NAD availability that is, in turn, regulated by the main consuming enzyme; CD38 (Aksoy *et al.,* 2006b). Importantly, for enzyme inhibition, concentrations of 1-30 μM of the sirtuin inhibitor (sirtinol) and PARP inhibitor (4-amino-, 1, 8-naphthalimide) were applied during HL60 differentiation. It is worth noting, that this range of concentrations has previously been shown to inhibit both enzymes (Hegan *et al.,* 2010; Fernandes *et al.,* 2012). The current results during HL60 differentiation, also suggest that CD38 might be limiting the availability of NAD to other NAD-consuming enzymes. Furthermore, they reflect the restricted role of other NAD-consuming enzymes in the degradation of NAD during the differentiation.

The strongest evidence that clearly confirms the essential role of CD38 in degrading NAD levels during the differentiation comes from the observed effects of kuromanin. The effect of inhibition by kuromanin on CD38 cyclase activity occurred at micromolar concentrations. Kuromanin efficiently elevated intracellular NAD levels compared to those in untreated cells. The mechanism of this inhibition is suggested to be through interaction of the inhibitor with the active site of CD38, which affects the binding of CD38 with NAD^+ (Kellenberger *et al.*, 2011). In addition to increasing NAD levels, treatment with kuromanin also suppressed the differentiation of HL60 to neutrophil-like cells as assessed by the NBT assay. This might be through the inhibition of CD38 activity, which is involved in the mechanism of HL60 differentiation. The recent data strongly confirm the major CD38 role in degrading NAD, because CD38, and no other NAD-consuming enzymes (PARP, sirtuin and CD157), is mainly expressed over time during the differentiation. Inhibition of CD38 activity might serve as a pharmacological target for multiple disease conditions, especially in CLL. Indeed, in CLL, studies have developed from CD38 as a marker to CD38 as a disease modifier and a therapeutic target (Deaglio *et al.*, 2008). The effects of kuromanin might also need to be investigated in other leukaemia cells expressing CD38 *in vivo* and *in vitro*. Following these investigations, kuromanin may represent a possible therapeutic agent to target CD38 in leukaemia.

As it was confirmed that NAD appeared to be consumed via the activity of CD38 during the differentiation, resynthesis of NAD would be necessary to maintain the functions of a wide variety of NAD-dependent enzymes in cells. It was found that during HL60 differentiation NMNAT expression showed a significant increase, but the rate-limiting enzyme (NAMPT) showed no significant change in expression. Hence, this pathway is unlikely to be able to compensate for the decrease in NAD levels through CD38 activity. An apparent elevation in IDO

expression was also recorded. However, IDO activity might also not be able to compensate for the decline in NAD levels, since it has been previously estimated that only 1/60 of NAD synthesis comes from tryptophan degradation via IDO (Bender, 1992). Thus, IDO expression might be linked to other functions; for instance, IDO serves more than one role in the immune system (Mellor and Munn, 2004). Furthermore, it has been documented that overexpression of the NAD biosynthesis enzymes might not necessarily affect NAD levels as the pyridine nucleotides can be turned over at a considerable rate (Mack *et al.,* 2001; Anderson *et al.,* 2002). Thus, the change in the expression of NAD biosynthesis enzymes might have other functions rather than maintaining NAD levels. For instance, It has been mentioned that NAMPT and NMNAT have important roles in regulating the functions of NAD-dependent enzymes such as the protein deacetylase, SIRT1, and PARP1 (Zhang *et al.* 2009). It has also been found that NMNAT activity correlates with DNA synthesis during the cell cycle (Solao and Shall 1971). Moreover, it has been suggested that IDO expression has a role in controlling autoimmune diseases (Opitz *et al.,* 2007) and chronic infection (Zelante *et al.,* 2009). Importantly, it is chronically activated in many cancer patients (Schroecksnadel *et al.,* 2007). Thus, IDO expression or enzymatic activity correlates with a poor prognosis in patients with various cancers (Ino *et al.,* 2008*;* Pan *et al.,* 2008). The role of IDO in the poor prognosis in cancer is therefore an interesting area and is yet to be determined. This could be achieved by exploring whether a link exists between CD38 expression, IDO expression, low intracellular NAD levels and poor prognosis. Hence, IDO might also serve as a target in patients with various cancers, such as $CD38^{+}$ leukemia subset patients. Moreover, further investigation is needed to confirm whether NAMPT or NMNAT expression are associated with CD38 expression and low levels of NAD which are also expected to be as potential targets for therapeutic applications in leukemia.

Furthermore, in view of the results obtained in this study, it would be interesting to investigate the effect of low intracellular NAD levels on cADPR production. cADPR is a key messenger in the mobilization of intracellular Ca^{2+} stores, and is involved in a variety of cellular processes, including fertilization, cell proliferation, and differentiation (Lee, 2004; Guse, 2005). Thus, the observed decline in intracellular NAD levels might either suggest a high turnover of intracellular NAD levels to produce high levels of this secondary messenger, or alternatively that low levels of the messenger might be formed because of a low availability of its precursor, NAD. However, it has been found that CD38, in addition to inducing cell proliferation, also increases intracellular Ca^{2+} levels (Zocchi *et al.,* 1998), so, when CD38 is expressed, a consequential accumulation of cADPR might occur. Importantly, the ability of cADPR to increase cell proliferation has been observed in several human cell lines (Bruzzone *et al.,* 2003; Kim *et al.,* 2008; Yue *et al.,* 2009). Moreover, CD38-mediated cADPR production has been implicated in several diseases (Chapter 1), and the current finding may have attractive functional implications in $CD38^{+}$ leukemia patients. One of the possible implications is that the decrease in NAD levels concomitant with CD38 expression might be accompanied by a peak in cADPR production that might play a causal role in mediating leukemia proliferation and poor prognosis. However, the effect of CD38 expression in degrading NAD levels suggests that there is still much work to be done to understand this interesting relationship.

It is worth noting that the extracellular location of CD38 and the intracellular location of the substrate NAD and its product cADPR have raised an unresolved issue known as the 'topological paradox', since it was hard to understand how the product, cADPR, could exert its calcium-mobilizing activity intracellularly if it were produced extracellularly (De Flora *et al.,* 2000). However, there are two mechanisms that have been suggested to resolve the CD38 topological

paradox, depending on the membrane orientation of CD38. The first mechanism for NAD and CD38 product trafficking has been suggested by De Flora's group (De Flora *et al.,* 2004). It is based on the observation that CD38 is expressed as a type II protein on the cell surface. These findings suggest that a connexin-43 (CX43) channel is present in the plasma membrane to transport the cytosolic substrates, NAD and NADP (Bilington *et al.,* 2008a), and to make them available to the extracellular CD38 (Zocchi *et al.,* 1999). Ultimately, both the products, cADPR and NAADP, are transported back into the cytosol via a nucleoside transporter (NuT) to act on their targets by affecting Ca^{2+} release from the intracellular stores (Bruzzone *et al.,* 2001; Lee, 2012). It has also been suggested that cADPR is transported through CD38 itself by a channel mechanism (Franco *et al.,* 1998). Importantly, type III CD38 serves as a simple solution to the topological paradox (De Flora *et al.,* 2000), and represents the second proposed mechanism. Indeed, CD38 with type III orientation should be more suitable than the type II isoform for performing intracellular signalling functions, since its substrate NAD location and the sites of CD38 action mediated by cADPR and NAADP, are all cytosolic. Altogether, these two signalling mechanisms are consistent with the wide range of functions that are regulated by this enzyme activity (Zhao *et al.,* 2012). Interestingly, it has been suggested that both type II and type III orientations may possibly be in the same cell (Lee, 2012). For instance, both types of CD38 are found on the cell surface of HL60 on the first day of ATRA-induced differentiation as well as in other cells, such as human primary monocytes and the U937 monocytic cell line after activation by IFN-γ (Zhao *et al.*, 2012). In view of the results of this study, type III CD38, which has been shown in differentiating HL60 cells, supports the main role of CD38 in degrading intracellular NAD. Moreover, the presence of two signalling mechanisms in the differentiating cells might require a rapid NAD degradation by CD38 both extracellularly and intracellularly. In

summary, these findings further support the current investigations which confirmed a high drop in intracellular NAD levels in cells expressing high levels of CD38. In addition, in the context of leukaemia conditions, the presence of CD38 in two orientations might suggest a complex mechanism associated with CD38 signalling that is involved in cell proliferation and poor prognosis.

In conclusion, the main aim in this particular study was to provide new evidence for the main role of CD38 as the major NAD regulatory enzyme in the cells. An elevated level of this efficient enzyme on the surface or in the cytosol of some cells might have an impact on different NAD-dependent pathways. However, the three main processes which might be affected are (a) the NAD-dependent glycolysis pathway, which directly affects cellular energy since the NAD^+:NADH ratio is a direct measure of the energy status of a cell, and (b) the formation of cyclic ADP-ribose, a Ca^{2+}-mobilizing messenger, which is known to play a role in the control of gene expression and apoptotic cell death (Zupo *et al.,* 1994; Hardingham *et al.,* 1997). In this context, Yalcintepe *et al.,* (2005) postulated that NAD may function as a signal that regulates nuclear calcium homeostasis and gene expression. Finally, (c) increasing CD38 cyclase activity not only decreases the intracellular NAD levels, but it also limits the substrate availability for other ectoenzymes such as ADP-ribosyl transferases and the intracellular enzymes such as PARP and sirtuin. These enzymes mediate important roles in modified cellular functions such as genomic stability, apoptosis, cell signalling and stress tolerance (Malavasi *et al.,* 2010). Finally, further studies are needed to explore whether CD38-mediated NAD degradation might provide solutions that increase understanding of the reasons as to why patients with CLL and high CD38 expression have a progressive stage of this disease and a lower survival rate (Deaglio *et al.,*

2008). CD38 enzymatic function might also serve as a possible target in leukemia therapy, in addition to its receptor function.

CHAPTER 4

EFFECT OF LOWERED NAD LEVELS ON CELL PHYSIOLOGY

4.1 Introduction

NAD(H) and its phosphorylated form, NADP(H), play key roles in major aspects of energy metabolism (Berger *et al.*, 2004; Ying, 2006). NAD mediates glycolysis by acting as a coenzyme for some key glycolytic enzymes (such as GAPDH). It also modulates other important energy metabolism-related reactions in cytosol, such as the lactate dehydrogenase catalyzed lactate-pyruvate conversions. Furthermore, NAD(P)(H) is an essential co-enzyme in some of the most fundamental reaction pathways, such as the TCA cycle and the pentose phosphate pathway (Ziegler, 2000). In addition to NAD having major roles in energy metabolism, it can also affect cellular antioxidant capacity through its phosphorylated form, NADP, the precursor for synthesizing the major reducing molecule NADPH (Stryer, 1995). The latter carries out several cell protective functions (Pollak *et al.*, 2007). Importantly, the role of NAD has been extended from simply being an oxidoreductase coenzyme to acting as a precursor for a wide range of products produced by other enzymes. These include ADP-ribosyl cyclase/NAD glycohydrolase (CD38), NAD-dependent protein deacetylases (sirtuins), poly (ADP-ribose) polymerases (PARP), and ADP-ribosyl transferases (ARTs). Altogether, NAD provides a direct link between the cellular redox status and the control of DNA repair (via PARP; Kim *et al.*, 2005), post-translational protein modification (via ARTs; Koch-Nolte *et al.*, 2008), gene expression (via sirtuins; Michan and Sinclair, 2007) and Ca^{2+}-signalling (via CD38/CD157; Malavasi *et al.*, 2008). Several studies have also confirmed that NAD works as a modulator of protein activities due to nucleotide availability (Ying, 2006; 2008). The NAD^+:NADH ratio is an important regulator of mitochondrial permeability transition (MPT; Zoratti and Szabo, 1995), and may indirectly affect mitochondrial function by modulating calcium homeostasis, which is known to profoundly affect mitochondrial activities (Nicholls *et al.*, 1999). NAD regulates calcium

homeostasis through the formation of Ca^{2+}-mobilizing messengers, for example cADPR, which is known to play a role in the control of gene expression and also apoptosis (Zupo *et al.,* 1994; Hardingham *et al.,* 1997).

As such, changes in NAD levels or the NAD^+:NADH ratio, which lead to changes in metabolism, have been implicated directly and indirectly in the mechanisms of several age-associated diseases such as diabetes, cancers and neurodegenerative diseases e.g. Parkinson's disease (Soriano *et al.,* 2001; Zhang *et al.,* 2002; Greenamyre *et al.,* 2001; Lin and Guarente 2003). Thus, NAD has major roles in multiple physiological processes via a number of pathways, and there has been much interest in the NAD homeostasis pathways as potential pharmacological targets for a wide variety of diseases. However, studies have not fully examined the effect of low NAD levels on cell physiology, particularly in HL60 cells, during treatment with ATRA and under conditions of upregulation of CD38 expression. Therefore, the aim of this study was to extend the studies of Chapter 3, and to examine the effect of low NAD levels on the NAD^+:NADH ratio and the levels of major antioxidants such as glutathione. In addition to examine the effect of low intracellular NAD in differentiated cells on lipid peroxidation status and glycolysis. From this study it might be possible to understand the reason for metabolic dysfunction and a resistence to apoptosis cell death or find a mechanism that explains the reason for the poor prognosis in $CD38^+$ leukemia subset patients.

4.2 Materials and methods

4.2.1 Materials

Reduced glutathione (GSH), glutathione reductase, dithionitrobenzoate (DTNB), thiobarbituric acid (TBA), 1,1,3,3-tetraethoxypropane, lactate dehydrogenase (LDH), glycine, glucose, and PBS were all purchased from Sigma (Poole, UK). NAD,NADH, and NADPH were all from Melford Laboratories (Ipswich, UK). Hydrazine hydrate liquid and lactate were a kind gift from Mr. Nick Crocker (University of Plymoth, UK) and came from Sigma (Poole, UK).

4.2.2 Measurement of the NAD^+: NADH ratio

The NAD^+: NADH ratio was estimated by measuring both the NAD^+ and the NADH concentration for each sample by using the NAD cycling assay as described in Chapter 2, Section 2.9.2.1. Briefly, the control cells and HL60 treated with ATRA for 1, 3 and 5 days were harvested and both NAD^+ and NADH were extracted from each sample as detailed in Chapter 2. After the extraction, NAD^+ and NADH levels were estimated by comparison with NAD^+ and NADH standards. Also nucleotide levels were normalized to the cell concentration for each sample. The NAD^+:NADH ratio was calculated by dividing intracellular NAD^+ levels by the NADH levels in the same sample.

4.2.3 Determination of total glutathione by the enzymatic recycling assay

This assay was used to measure total intracellular glutathione levels (GSH and GSSG). In this assay, GSH reacts with the DTNB to produce 5-thio-2-nitrobenzoate (TNB) and a mixed disulphide (GSSTNB). The latter produce GSH again in the presence of glutathione reductase

(GR) and NADPH. A similar reaction may form two molecules of GSH by reducing GSSG in the presence of both GR and NADPH (Jones, 2002), as shown in Figure 4.1.

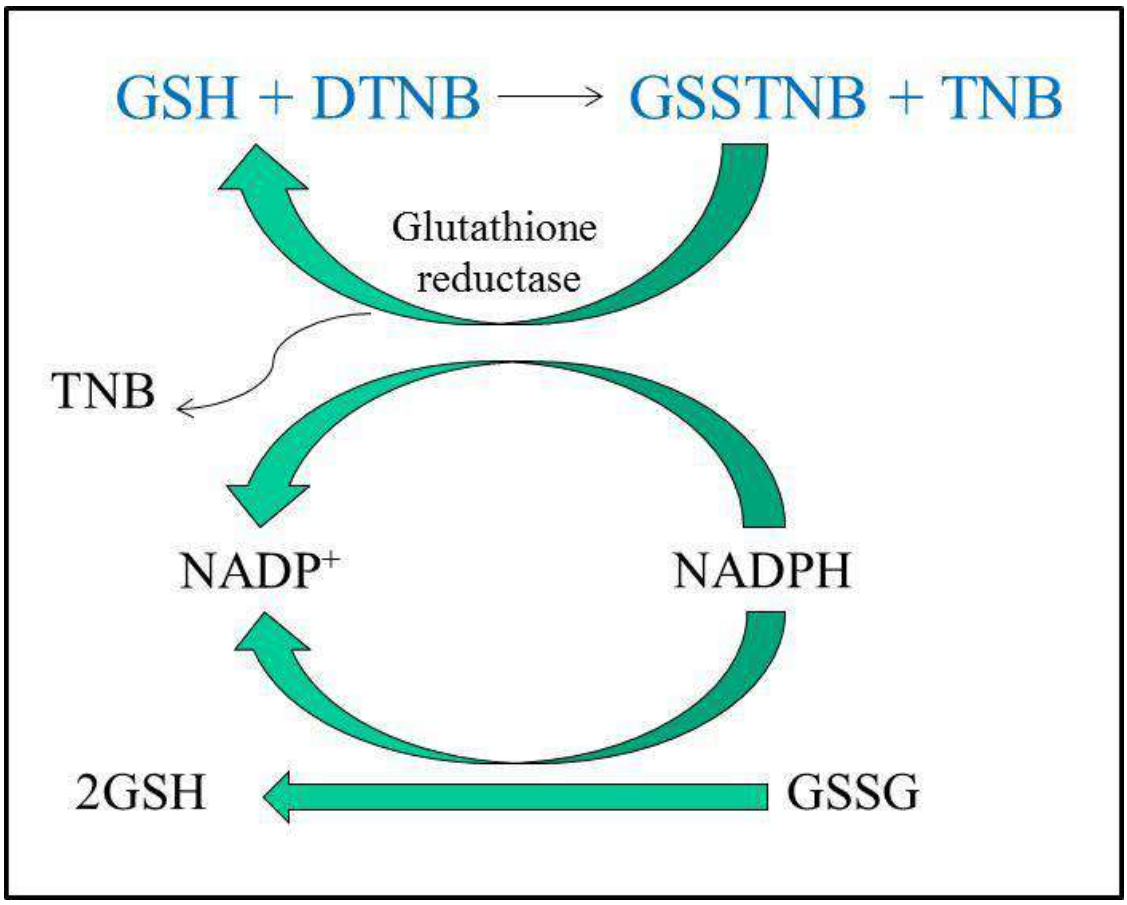

Figure 4.1 Principle of the total glutathione assay. GSH produce GSSTNB in the presence of DTNB. GSSG or the mix (GSSTNB) converted again to GSH in the presence of glutathione reductase (GR) and NADPH.

The total glutathione (GSH and GSSG) assay was performed as described by Adams *et al.* (1983). The control or ATRA-treated HL60 cells (1×10^6 cells ml^{-1}) were collected and washed twice with PBS. After collection, cells were lysed in the assay buffer (100 mM potassium

phosphate, pH 7.5, containing 5 mM potassium EDTA) by three cycles of freeze-thawing followed by centrifugation at 7000 × *g* for 5 min. Sample lysate (40 µl) or GSH standard (after being mixed with an equal volume from fresh buffered DTNB (10 mM in assay buffer)) were added to 210 µl of assay buffer containing 0.15 U glutathione reductase. The reaction was started by adding 60 µl of freshly prepared 1 mM NADPH, and the absorbance at 412 nm was read at room temperature for 10 min. Total glutathione results are expressed as nmol per 10^6 cells.

4.2.4 Thiobarbituric Acid Reactive Substance assay

Lipid peroxidation is used as an indicator of oxidative stress in cells and tissues. Lipid peroxides are unstable and decompose to form a complex series of compounds including reactive carbonyl compounds. Polyunsaturated fatty acid peroxides generate malondialdehyde (MDA) and 4-hydroxyalkenals (HAE) (Esterbaue *et al.,* 1991). The thiobarbituric acid reactive substances (TBARS) assay measures lipid hydroperoxides and aldehydes, such as MDA, in the cell culture medium and cell lysate. MDA combines with thiobarbituric acid (TBA) in a 1:2 ratio to form a coloured complex that is measured at 532 nm. TBARS are expressed as MDA equivalents (Dubuisson *et al.,* 2000).

The measurement of MDA was performed according to the protocol reported by Ohkawa *et al.* (1979). Briefly, untreated HL60 cells (the control) and cells treated with ATRA (5-10 × 10^6 cells ml^{-1}) were collected in 15 ml tubes, followed by low-speed centrifugation (200 × g) for 5 min. The cell pellets were re-suspended in 0.2 ml ice-cold PBS and sonicated for 15 s at low power sonication (4 W output, Microson TM Ultrasonic Cell Disruptor, USA) on ice. Aliquots (100 µl) of the cell lysate were assayed for MDA according to the following protocol: Ice-cold 10% TCA (200 µl) was added to 100 µl of each sonicated sample to precipitate proteins and the sample

centrifuged at 7000 × g for 5 minutes at 4 °C, followed by addition of 200 µl of 4.6 mM (0.67%) thiobarbituric acid (TBA) to an equal volume of each supernatant. The color was developed by incubating at 100 °C for 30 min and the reaction was stopped by cooling on ice for 5 min. Three hundred microlitres from each sample was transferred to a 96-well plate and the absorbance at 532 nm was measured with reference to a reagent blank. The lipid peroxide levels were expressed in terms of pmol of malondialdehyde per 10^6 cells of each sample and calculated from a standard curve (Fig. 4.2) made with various concentrations of 1,1,3,3-tetraethoxypropane (0-100 µM).

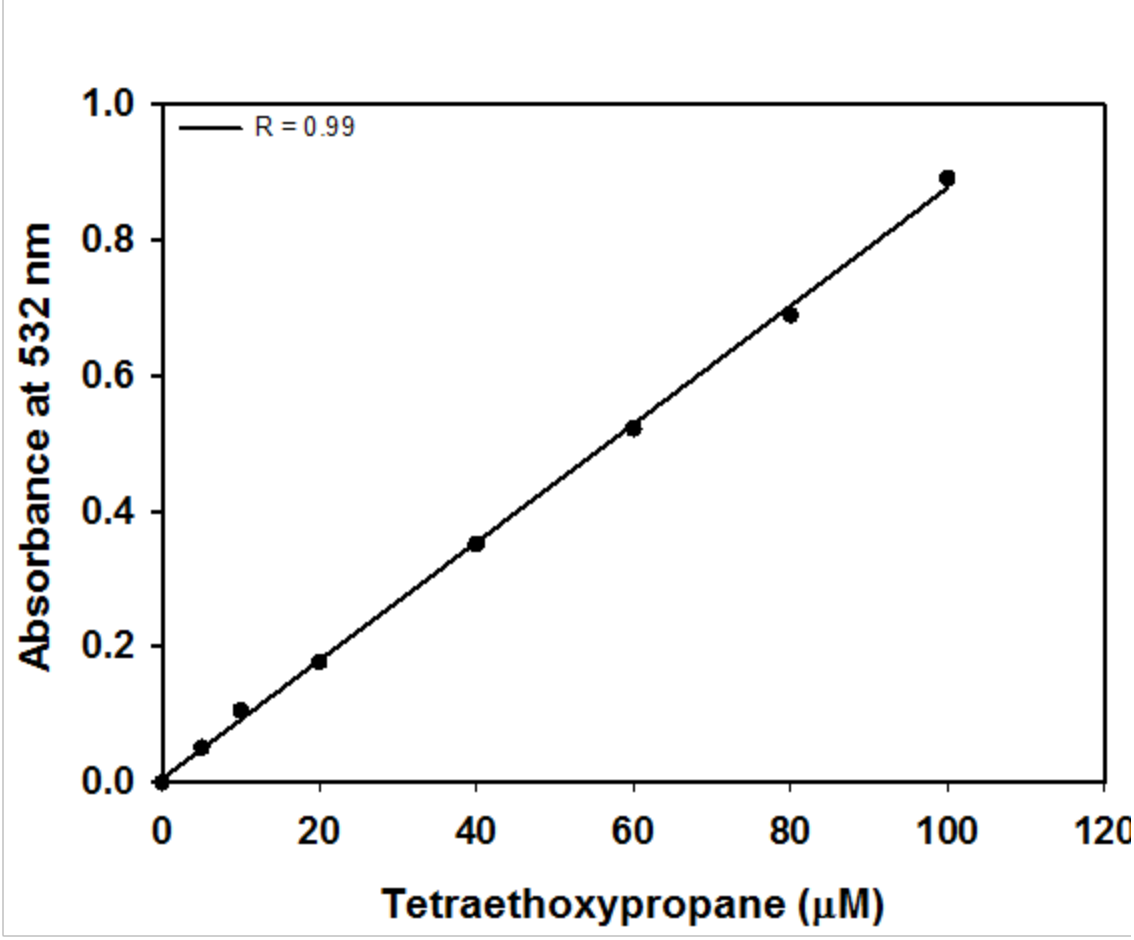

Figure 4.2 Standard curve of (0-100µM) 1,1,3,3-tetraethoxypropane, was used to estimate of TBARS levels for each sample. Change in absorbance is recorded at 532 nm.

4.2.5 Lactate assay

Lactate accumulation in the medium was used to assess the rate of glycolysis during HL60 cell differentiation with ATRA for 1-5 days (Fig. 4.3). Two hundred and fifty microlitres of the assay mixture (containing 500 mM glycine, 400 mM hydrazine, 20 mM NAD^+ and 16.6 U/ml of lactate dehydrogenase) was mixed with 50 µl from the sample (medium) or lactate standard solution (0.1-1 mM) and incubated at 37 °C for 30 min to complete the reaction. The absorbance at 340 nm was measured in a plate reader (VersaMax, Molecular Devices, Sunny Vale, CA).

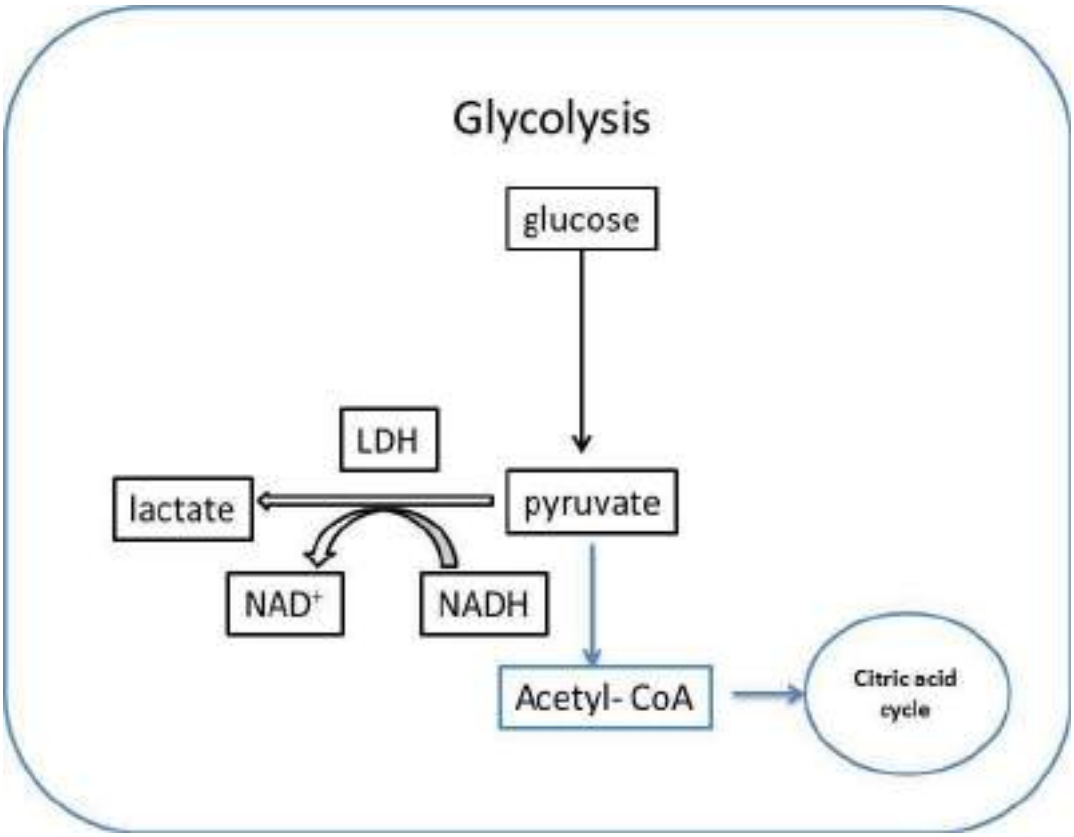

Figure 4.3 Simple diagram showing lactate production from glycolysis as product of lactic fermentation.

4.2.6 Glucose challenge

Cells treated with either 1 µM ATRA, 100 µM NAD for 1 day, or untreated cells (control) were harvested by centrifugation (200 × g) for 5 min, resuspended in fresh medium and treated with 25 mM glucose for 1 h at 37 $^{\circ}$C. Incubated cell cultures catabolized glucose through glycolysis converting it into products including lactate. Following incubation, cells were separated as pellets, and the supernatant (containing the generated lactate) was removed for the analysis of lactate content using a previously described lactate assay (Section 4.2.5).

4.2.7 Statistical analysis

Statistical analysis of the data was assessed using Fisher's one way analysis of variance (Statview 5.0.1; Abacus concepts, USA) or Student's t-test as appropriate. Data are expressed as means ± SEM for three separate experiments in triplicate. A difference of $P < 0.05$ was considered statistically significant.

4.3 Results

4.3.1 NAD^+:NADH ratio during HL60 differentiation

As has been previously shown (Chapter 3), CD38 expression during HL60 differentiation leads to a decrease in intracellular NAD^+ levels in a time dependent manner. So, in this Chapter, it was questioned whether this NAD degradation could cause a further effect on cell metabolism, as NAD(H) is a major coenzyme in glycolysis.

Firstly, both oxidized and reduced nucleotides, NAD^+ (Fig. 4.4 A) and NADH (Fig. 4.4 B) were investigated during the time course of HL60 differentiation. NAD^+ levels significantly decreased throughout differentiation and a similar decline in NADH levels could be seen on the 3^{rd} and 5^{th} days of differentiation compared to each appropriate control.

As the results showed an apparent drop both in the oxidized and reduced forms, the NAD^+:NADH ratio, as one of the important metabolic indicators, was therefore assessed during ATRA-induced HL60 differentiation (Fig. 4.4 C), to further investigate the consequences of CD38 expression on the nucleotide levels and on their dependent processes. Notably, there was no marked change in the NAD^+:NADH ratio after 1 and 3 days of differentiation, i.e. the ratio remained relatively stable during early differentiation.

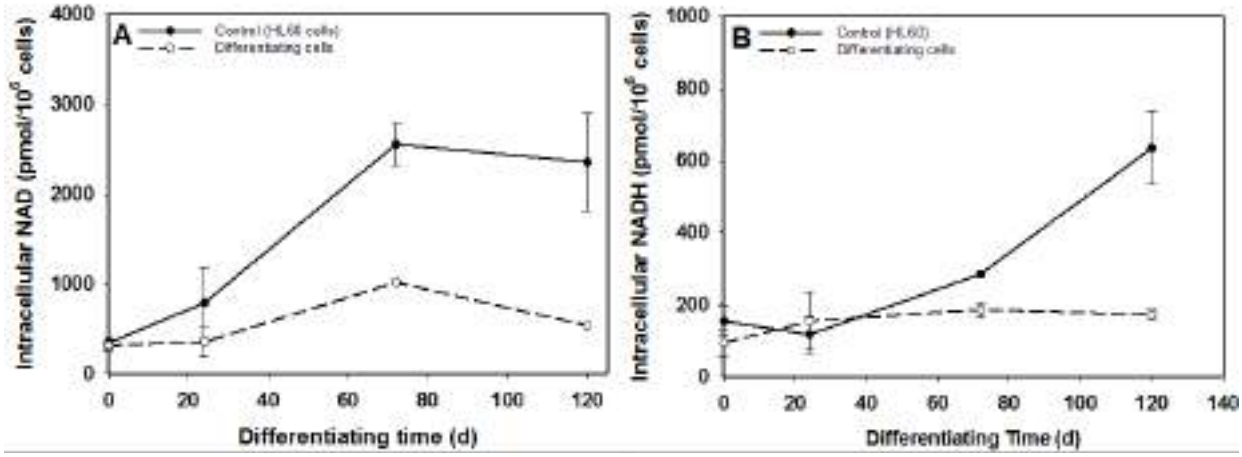

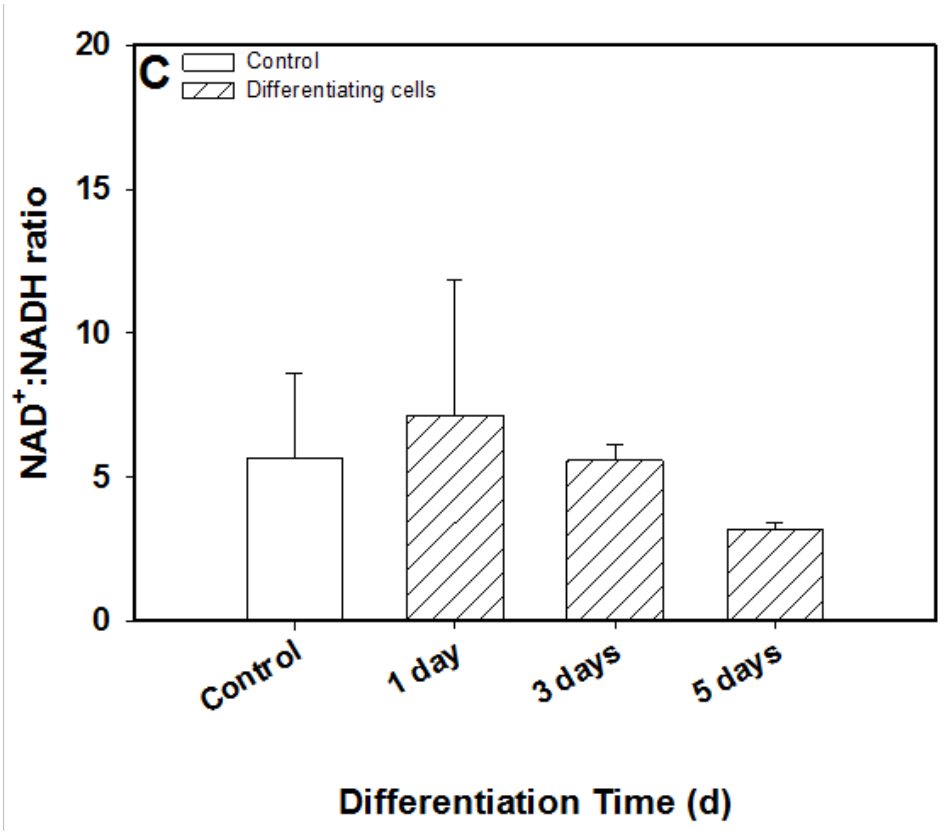

Figure 4.4 Time course of ATRA induced differentiation of HL60 cells over 5 days comparing to HL60 (as control), showing (A) intracellular NAD levels (B) intracellular NADH levels (C) the NAD^+: NADH ratio. Data are means ± SEM, n = 2 (3-6 measurements per replicate).

4.3.2 Effect of low intracellular NAD levels on lactate levels before and after glucose application and during cell differentiation

To assess the effect of lowered NAD levels on cell physiology lactate production (the product of lactic fermentation) levels in the medium was measured, as it was expected that lactate levels might be reduced when NAD levels dropped due to the effect of lower levels of NAD on glycolysis. The data revealed that HL60 cells treated with ATRA showed a negligible, but significant decrease in lactate accumulation on days 1-3 after induction of HL60 differentiation compared to the control. However, the lactate levels after the 4^{th} day of differentiation were not different from the control (HL60), whereas they increased at day 5 of differentiation in comparison to the control as shown in Figure 4.5. These results suggest that lowered NAD levels might have an effect on glycolysis activity.

The lactate production during cell differentiation was further investigated after supplying the glucose (25 mM) to the cells. In this test and after 1 day of HL60 differentiation, cells were treated for 1 h with 25 mM glucose. Glucose was used to assess the glycolytic activity and to investigate whether glycolysis can potentially use the glucose to produce lactate even at the lowered NAD levels.

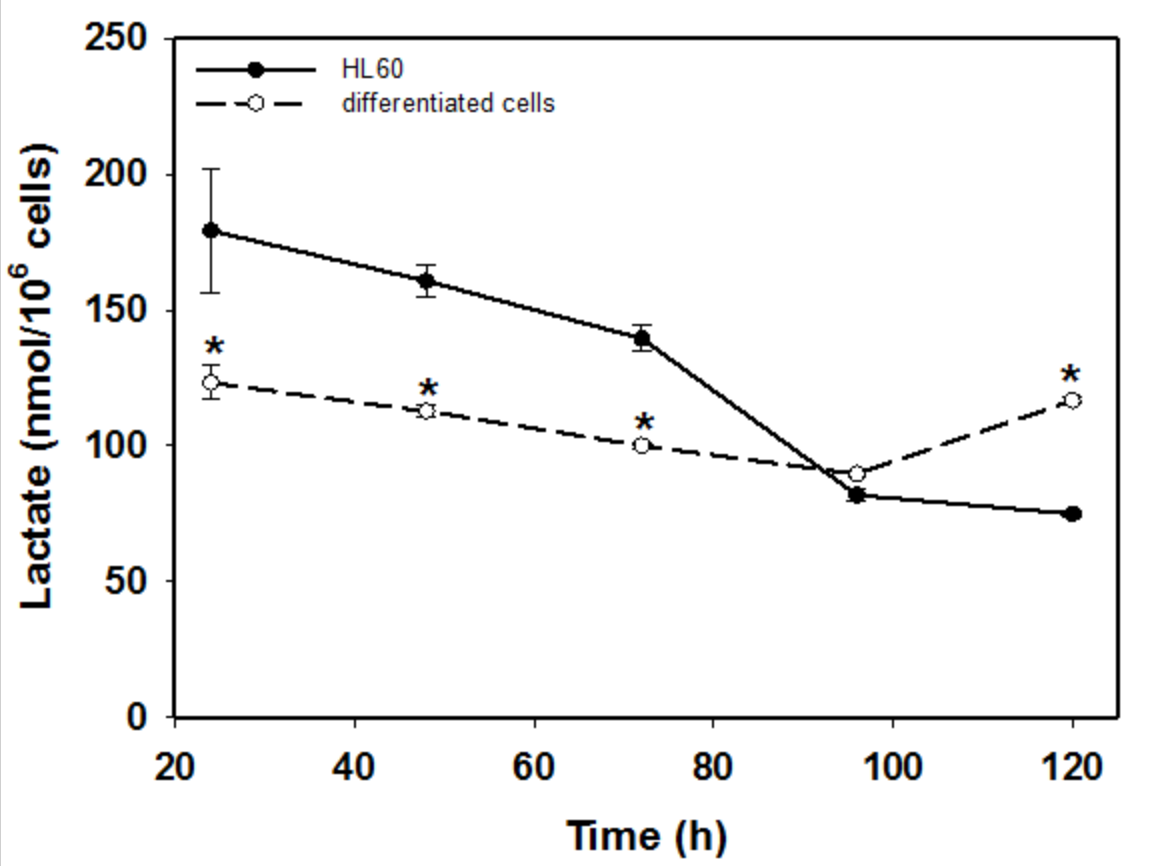

Figure 4.5 Lactate production expressed as nmol/10^6 cells during the time course of ATRA-induced differentiation of HL60 cells over 5 days compared to untreated HL60 cells (control). Data are means ± SEM, n = 4 (3 measurements per replicate). * denotes a significant difference from the appropriate control, $P < 0.05$.

The results (Fig. 4.6) show that the production of lactate was not increased in spite of the presence of 25 mM glucose when compared to the control incubated without glucose (differentiated cells). Treatment with glucose was also performed in HL60 cells with no significant change being recorded. However, this is not the case when the differentiating cells were treated with 100 μM NAD^+ for 1 day (to replenish the intracellular NAD, during the differentiation with ATRA; see Chapter 5), before they were treated with or without 25 mM glucose. The results (Fig. 4.6) show that lactate levels in the medium were relatively high after NAD^+ application compared to the untreated differentiated HL60 cells and were similar to lactate levels in undifferentiated HL60 cells. A similar elevation in lactate levels was also seen in differentiated cells that treated with glucose following the incubation with NAD^+ for 1 day (Fig. 4.6). However, after treatment with glucose and/or NAD^+ no changes in lactate levels were seen in HL60 cells, possibly because these cells already had high NAD levels compared to the differentiated cells. These data reveal the effect of low NAD levels on cell metabolism particularly glycolysis, as reflected by lactate levels.

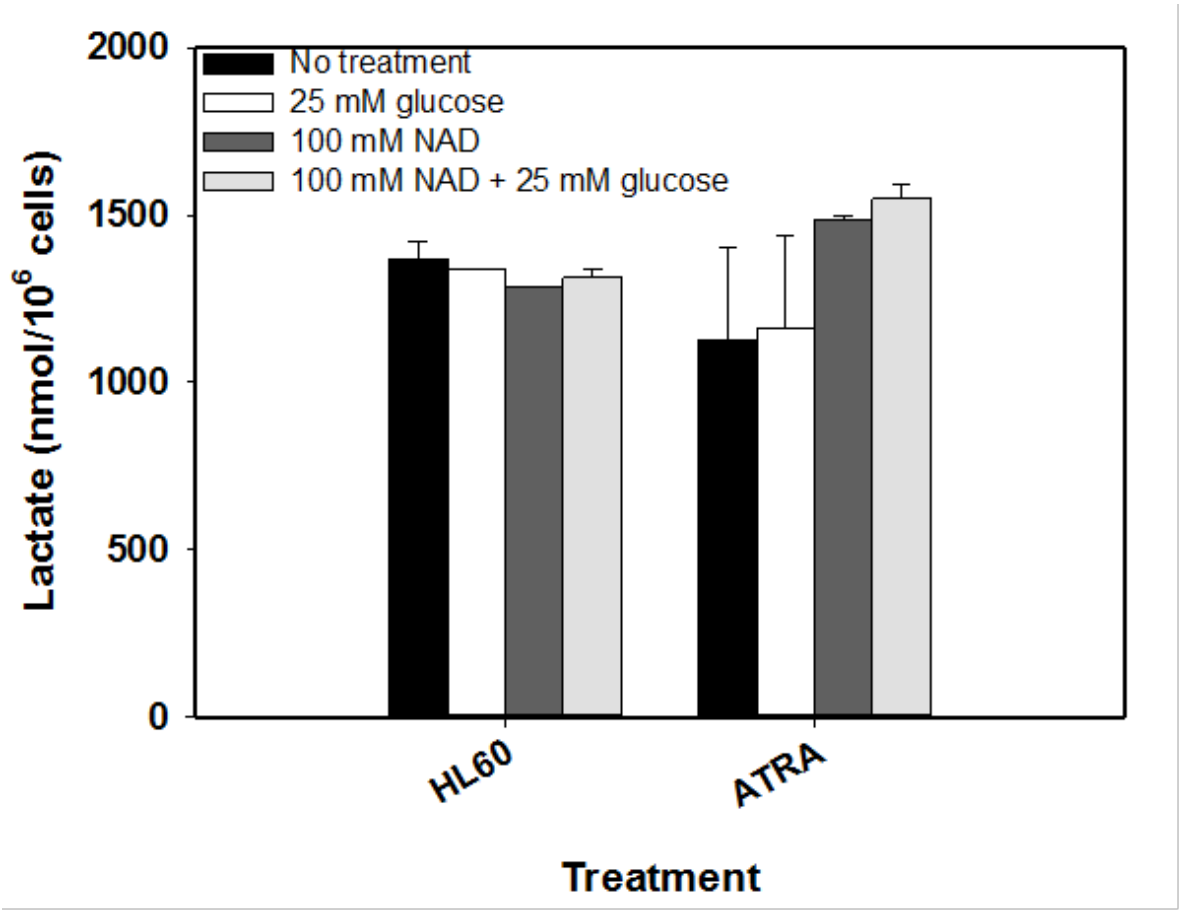

Figure 4.6 Lactate production expressed as nmol/10^6 cells after incubation of HL60 cells or 1 day-differentiated cells (either treated or not treated with 100 µM NAD) for 1 h with 25 mM glucose and compared to appropriate untreated control. Data are means ± SEM, n = 3 (5 measurements per replicate), $p > 0.05$.

4.3.3 TBARS production during ATRA-induced HL60 differentiation

To further determine the consequences of the decline in intracellular NAD levels on cell physiology, intracellular reactive oxygen species (ROS) were assessed during ATRA-induced HL60 differentiation. Lipid peroxidation was evaluated by measuring TBARS production (Fig. 4.2). Lipid peroxidation in ATRA-treated HL60 cells, as well as untreated cells, was evaluated after 1, 3 and 5 days incubation. TBARS levels increased significantly in differentiating cells in a time-dependent manner (Fig. 4.7) compared to the appropriate control, reaching highest levels on day 5.

Taken together, these data suggest that an imbalance in the oxidant/antioxidant status might have occurred, as high lipid peroxidation levels might reflect low antioxidant levels which might be a consequence of NAD depletion.

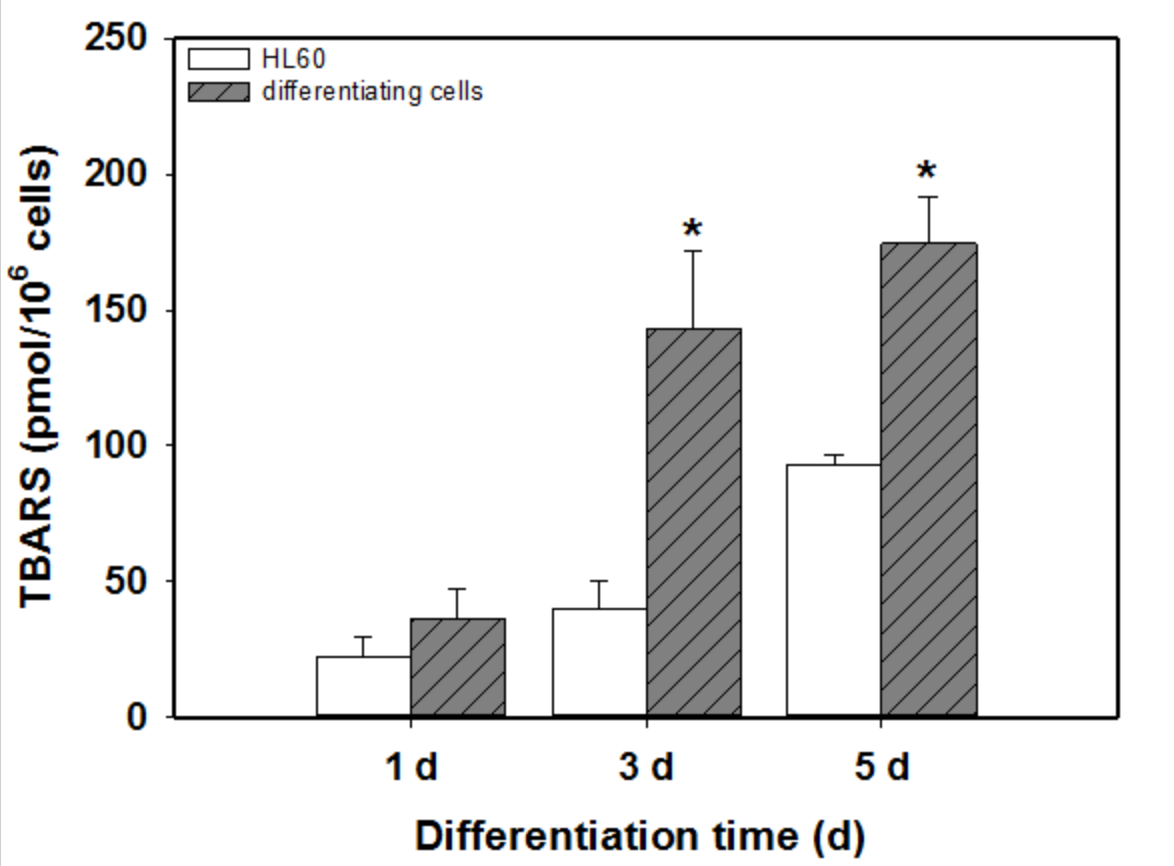

Figure 4.7 Lipid peroxidation as evaluated by TBARS levels during the time course of HL60 differentiation over 5 days comparing to untreated HL60 cells (control). Data are means ± SEM, n = 3 (3 measurements per replicate). * denotes a significant difference from each appropriate control, $P < 0.05$.

4.3.4 Total glutathione levels

ATRA-induced HL60 differentiation seems to be accompanied by an increase in oxidative stress (as measured by TBARS levels) that may be due to the effect of CD38 expression and the significant drop in NAD levels. To further investigate this, a key cellular antioxidant system was also investigated by measuring total glutathione (GSH) levels during cell differentiation (Fig. 4.8).

A significant elevation in glutathione levels (oxidized GSSG and reduced GSH) after one day of differentiation (Figure 4.8) was observed, with less increase after three days of differentiation compared to the control. However, glutathione levels returned to control levels by the 5^{th} day of differentiation.

The significant increase in glutathione levels after one day of differentiation suggests the involvement of glutathione during the differentiation as an antioxidant. However, glutathione levels were not further increased during the 3^{rd} and 5^{th} days of differentiation. These observations suggest a link between NAD depletion and glutathione levels; they also suggest that NAD depletion-mediated by CD38 might disturb the balance in the oxidant/antioxidant state during the differentiation.

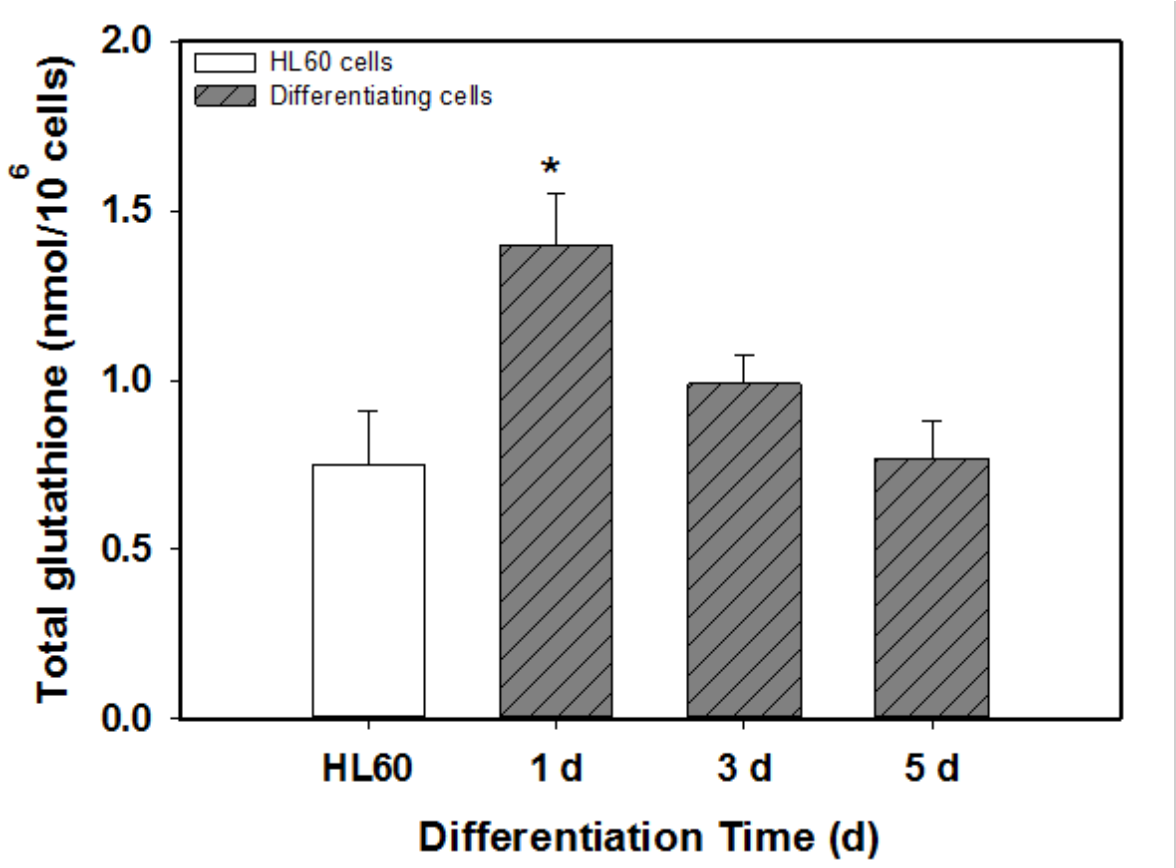

Figure 4.8 Time course of ATRA-induced HL60 differentiation over 5 days showing the increase in total glutathione levels after day 1 of differentiation but not after 3 and 5 days comparing to untreated HL60 cells (control). Data are means ± SEM, n = 4 (4 measurements per replicate). * denotes a significant difference from the control (HL60), $P < 0.05$.

4.4 Discussion

As mentioned in Chapter 1, one of the interesting events during HL60 differentiation is the regulation of CD38 activity which could affect NAD levels over time. Although the pyridine nucleotides, NAD^+ and NADH, have been shown to be important for glycolysis and its regulation (Tilton *et al.,* 1991) and as vital cofactors for numerous enzymes, no previous studies or explanations are available for the effects of the apparent depletion of NAD levels on the cell metabolism, including lactate accumulation, NAD^+: NADH ratio, antioxidant status represented by glutathione levels and TBARS levels (as a lipid peroxidation marker) during HL60 differentiation. Low NAD levels might affect cell physiology particulary in cells expressing CD38 (for instance in leukemia).

In this Chapter, cell metabolism was first investigated by measuring the NAD^+:NADH ratio during HL60 differentiation using ATRA. In this study, levels of both nucleotides (NAD^+, NADH) were significantly decreased. Surprisingly, despite the significant decreases in NAD^+ and NADH levels during the differentiation process, there were limited changes in the NAD^+:NADH ratio during early differentiation. The NAD^+:NADH ratio has been suggested to be relatively constant in order for normal physiological processes to proceed (Barron *et al.,* 2000); NAD is a coenzyme for over 700 oxidoreductases, such as glyceraldehyde-3-phosphate dehydrogenase and the pyruvate dehydrogenase complex that catalyze numerous biochemical reactions in cells (Matthew *et al.,* 2000). For instance, in cancer cells the NAD^+:NADH ratio is suggested to be constant, because the high glycolytic rate generates excessive pyruvate and NADH, which are converted to lactate and NAD^+ by the action of lactate dehydrogenase (LDH), thereby maintaining the stability of the NAD^+:NADH ratio (Sun *et al.*, 2012). Ultimately, the

NAD^+:NADH ratio plays an important role in regulating the intracellular redox state (Droge, 2002). The NAD^+/NADH redox state also influences the production of ROS, since ROS production by the respiratory chain increases as the NAD^+/NADH redox pair becomes more reduced (Starkov and Fiskum, 2003). Thus, in the current study, the negligible change in the ratio might also be linked with ROS generation during cell differentiation. Interestingly, in the current study, the data for NAD^+:NADH ratio, is within the range of previously reported ratios: 3-10 in mammals (Swierczynski *et al.,* 2001) and 0.03-4 in several cell lines derived from mice (Gaikwad *et al.*, 2001; Sanni *et al*., 2001).

The second factor related to the effects of lowered NAD levels during HL60 differentiation on glycolysis is lactate accumulation. Studies on HL60 differentiation using ATRA, in this Chapter, indicated that there was a relative decrease in lactate production during the early days of differentiation compared to undifferentiated HL60 cells and that this was correlated with the drop in NAD levels which might suggest a small effect on glycolysis at this stage. This decrease in lactate accumulation was also previously shown during HL60 differentiation with DMSO (Wu *et al.,* 1991). Interestingly the presence of additional glucose failed to increase the glycolysis rate as shown by low lactate production. However, the same results were not obtained with NAD^+ application. These results suggest that the change in lactate accumulation might be linked to the change in NAD levels during the differentiation, but that it might be independent of changes in glucose levels. The lowered lactate production during early differentiation might be caused (a) by glycolysis dysfunction as a result of the lowered NAD levels, and (b) by ongoing metabolism of pyruvate via the Krebs' cycle and oxidative phosphorylation. However, the increase in lactate production during the last days of differentiation might be because when HL60 cells differentiate to neutrophil-like cells they lose mitochondrial function and hence rely on increased glycolysis

(lactic fermentation), like neutrophils, which rely mainly on glycolysis for the generation of ATP (van Raam *et al.*, 2008).

However, it is also worth mentioning that HL60 cells show relatively high lactate production compared to the differentiatied cells. This might suggest that lactic fermentation is a dominant pathway for energy production in HL60 cells (Boyunaga *et al.*, 2011). It is well known that a variety of cancer cells show high rates of lactate production from glucose, and an enhanced rate of lactic fermentation, despite the presence of oxygen and functional mitochondria; this is known as the Warbug effect (Warburg, 1956; Baggetto, 1992). This shift in cell metabolism ensures the propagation and survival of cancer cells, and allows them to obtain ATP at a faster rate through a simpler process (Tennant *et al*., 2009), without requiring oxidative metabolism (Boyunaga *et al.*, 2011). The enhancement of glycolytic activity is also thought to provide sufficient pyruvate, which might work as an antioxidant in cancer cells (Brand and Hermfisse, 1997). Lactic fermentation might also be preferred in leukemia cells. If so, one might expect that in $CD38^+$ leukemia, in addition to a high demand for NAD as the substrate for CD38, there will be a requirement for high levels of NAD to maintain the high rate of lactic fermentation. Low NAD levels might cause poor physiological consequences (such as a resistance to apoptotic cell death) and that might explain the reason for poor consequences in $CD38^+$ leukemia patients.

The remaining metabolic indicators used to evaluate the consequences of low NAD levels on redox state and cell physiology in cells expressing CD38, were TBARS (an indicator of lipid peroxidation) and total glutathione (as a key antioxidant). The results confirmed that when CD38 expression was increased following ATRA treatment, lipid peroxidation was also enhanced, suggesting a link between CD38 expression mediating a lowering in NAD levels and the increase

in lipid peroxidation. One possible explanation for this is that CD38 might mediate intracellular $O_2^{\bullet-}$ production via cADPR/Ca^{2+}-mediated activation of NAD(P)H oxidase (NOX4). The latter has been reported to be a major source of ROS in the vasculature (Mohazzab *et al.*, 1994; Xu *et al.*, 2012). Interestingly, the production of ROS was markedly reduced in embryonic fibroblasts from $CD38^{-/-}$ mice (Ge *et al.*, 2010). This strongly suggests a connection between CD38 and ROS production; undifferentiated HL60 cells, which are $CD38^-$, have lower TBARS levels than the differentiated ($CD38^+$) cells. Hence, in common with differentiated HL60 cells, high ROS levels might be also expected in $CD38^+$ leukemia compared to $CD38^-$ leukemia. Interestingly, a relative increase in the oxidative stress state has been observed in CD38 positive CLL patients compared to CD38 negative patients (Ortin *et al.*, 2012). These data suggest a possible reason for the observed resistance to apoptotic cell death and the induction of cell proliferation in cells expressing CD38, since high ROS might contribute to a resistance to apoptotic cell death and consequently poor prognosis in leukemia.

In addition to evaluating the oxidative state, the antioxidant level was also evaluated by measuring glutathione, which is the major non-enzymatic component of intracellular antioxidant defenses, and is present both in a reduced, biologically active form (GSH), and in an oxidized form, namely glutathione disulphide; GSSG (Circu and Aw, 2010). During HL60 differentiation, the results showed a negligible increase in total glutathione levels in the first 24 h with decreased levels in the periods afterwards. Decreased glutathione levels might reflect depletion of the non-enzymatic antioxidant reserve, due to overproduction of ROS (consistent with the TBARS results). GSH works as a vital intracellular scavenger of ROS, protecting the cells against toxic free radicals (Wu *et al.*, 2004). Another possible explanation is that a decline in NAD levels might affect glutathione levels, i.e. that glutathione might be NAD-dependent. However, the

early increase in glutathione levels might suggest low ROS production. Interestingly, it has been demonstrated that GSH levels are dynamic during HL60 differentiation when stimulated by several inducing agents (Krance *et al.,* 2010). Finally, a measurable change in the redox status during ATRA-induced HL60 differentiation was seen. These changes might be linked to the elevation in CD38 activity and a reduction in NAD levels.

The indicated declines in NAD^+ levels that are mediated by CD38 activities might have a further consequence on $NADP^+$ levels, since the biosynthesis of $NADP^+$ requires the phosphorylation of NAD^+ in a reaction catalysed by NADK (ATP:NAD 2-phosphotransferase) as shown in Figure 4.9 (Pollak *et al.*, 2007). Hence, a decline in $NADP^+$ might be occurring due to the drop in NAD^+ levels. If so, one might expect further consequences on NADP-dependent processes, for instance NADPH synthesis. The latter is synthesised through $NADP^+$-specific dehydrogenases, including glucose-6-phosphate dehydrogenase (G-6-P), isocitrate dehydrogenase (IDP), malic enzyme (ME) and aldehyde dehydrogenase (ALDH), (Fig. 4.9). Alternatively, NADPH can also be generated through phosphorylation of NADH via NAD kinase (Pollak *et al.,* 2007). It is worth noting that the phosphorylated nucleotide, NADPH, has been shown to be crucial in maintaining an effective defense against oxidant-mediated damage. It has been shown to be essential in the function of catalase and the maintenance of reduced glutathione, both of which have important roles in the antioxidant defense as previously confirmed in the erythrocytes (Gaetani *et al.,* 1989). $NADP^+$ is also involved in signal transduction as a precursor of the messenger molecule, NAADP. Hence, a decline in NAD might have an effect on $NADP^+$ levels and cause a disturbance in the antioxidant defense system, or it might also affect other NADP-dependent processes.

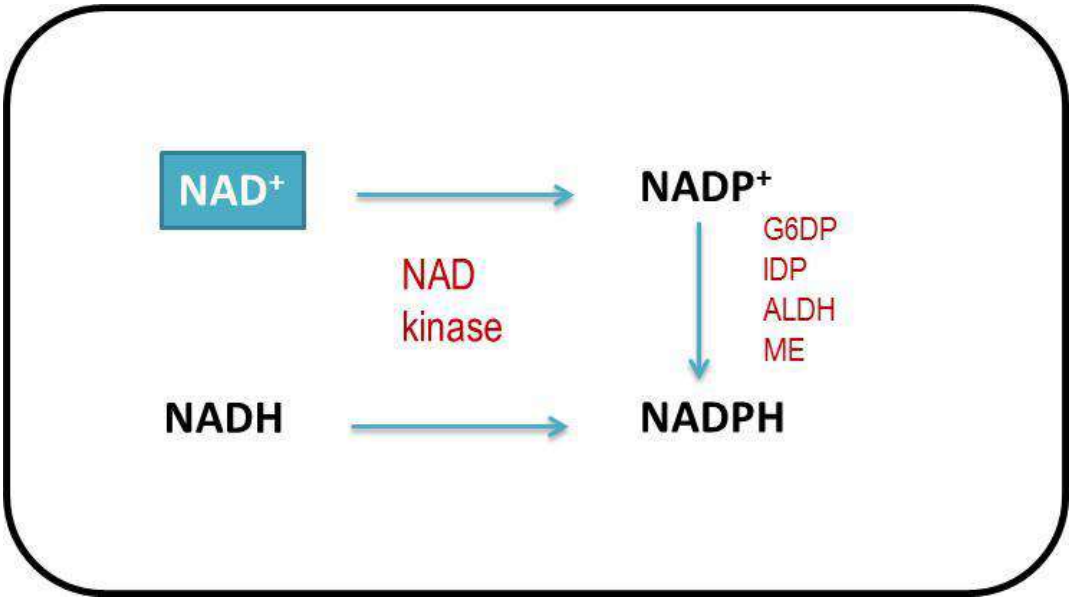

Figure 4.9 Simple diagram representing generation of $NADP^+$ from NAD and NADPH from $NADP^+$. Adapted from Pollak *et al*. (2007).

Studies on glutathione levels in leukemia are generally partial and contradictory. An elevation of glutathione levels in CLL patients was reported to cause cell survival and also to protect the cells from drug-induced cytotoxicity (Zhang *et al.*, 2012). However, a decrease in cellular glutathione was also indicated in CLL patients along with an increase in TBARS levels (Trachootham *et al.*, 2008; Ortin *et al.*, 2012). Interestingly, disabling this protective mechanism significantly sensitizes CLL cells to drug treatment (Zhang *et al.*, 2012). This seems to be because under mild oxidative stress, protein glutathionylation was shown to regulate the functions of multiple proteins (Ghezzi, 2005). For instance, it has been found that glutathionylation of the antiapoptotic protein MCL1, a novel substrate of glutathionylation, regulates its stability and protects it from being cleaved by caspase-3, and thus promotes cell survival (Trachootham *et al.*, 2008). However, removal of glutathionylation by a glutathione-depleting agent, such as PEITC, rendered MCL1 susceptible to rapid proteolytic cleavage, leading to leukemia cell death